Katholieke Universiteit Leuven
Group Biomedical Sciences
Faculty of Medicine
Department of Microbiology and Immunology
Rega Institute for Medical Research
Laboratory of Bacteriology

Characterization of *Staphylococcus aureus* type I signal peptidase SpsB, in view of its potential use as a novel antibiotic target

Smitha Rao C.V.

Jury:

Promoter: Prof. Dr. Jozef Anné
Chair: Prof. Dr. Ghislain Opdenakker
Secretary: Prof. Dr. Johan Van Eldere
Jury members: Prof. Dr. Anastasios Economou, Dr. Anil Koul, Prof. Dr. Johan Van Eldere, Prof. Dr. Piet Herdewijn

Leuven, 09.06.2010

Doctoral thesis in Medical Sciences

Acknowledgements

It is my privilege to have had Prof. Dr. Jozef Anné as my promotor. I thank him for giving me a free hand in working here, while at the same time making timely comments/suggestions during the course of this work.

I would like to thank Prof. Dr. Johan Van Eldere, Prof. Dr. Piet Herdwijn and Prof. Dr. Ghislain Opdenakker for critically examining and evaluating my work during the course of the doctoral study. I would also like to thank Prof. Dr. Anastasios Economou and Dr. Anil Koul for their valuable suggestions.

The financial support from Interfacultaire Raad voor Ontwikkelingssamenwerking (IRO) of K.U.Leuven is gratefully acknowledged.

I would like to express my gratitude to ing. Hugo Klaassen, Dr. Patrick Chaltin and Dr. Arnaud Marchand from CISTIM Leuven Vzw, Leuven. Many thanks to Prof. Dr. Yves Engelborghs and Dr. Sangeeta Nath, Laboratory of Biomolecular Dynamics, K.U.Leuven for their valuable inputs and stimulating discussions.

Thanks to all my colleagues from the Lab of Bacteriology. Nick, thanks for your support and discussions that instilled my interest on signal peptidases. Lieve and Kenneth, thanks for all the help and critical reading of the thesis manuscript. Leen, Philip, Veerle, Dorein, Evileen, Kristof, Liesbeth V, Liesbeth M, Sophie, Sofie, Kristof, Elke, Eef, Ilya, Wesley, Els, Katrijn, Barbara, Emmy- "*van harte dank aan jullie voor de hulp, goede samenwerking en voor de gezellige tijd bij jullie in het Bacteriologie labo*". Thanks also to José and Sonja for keeping the kitchen well stocked, I never had to worry about having enough sterile tips, glasswares, media and so on. Bárbara and Souliem, thanks for the great time in the lab- "*muchas gracias*". To those of you from different parts of the world - Elsita, Julio, Grisel, Bayan, Canan and Titilola, it was nice working with you in spite of the short duration of your stays. Thanks are also due to David for the discussions/suggestions on my work and for sharing your views on religion, culture, food and everything else under the sun from an American (or an atypical American?) perspective.

I am grateful to my parents who have been constant sources of inspiration and support all along. Thanks also to my siblings Shwetha and Guruprasad for the confidence they put in me. Thanks to my parents-in-law, relatives and friends. Special thanks to Santosh for taking time off to help me with my manuscript.

I am deeply indebted to my husband, Badrinath for helping me in every possible way during this period. I thank him for supporting my pre-doctoral work and for standing by me when I proposed to continue studying, for giving me an ear when I talked to him about my experiments (with happiness or disappointment; can't remember the in between) and for providing suggestions. Last but not the least, I thank my little daughter, Alpana, who has been my stress buster (of course not just that). I would look forward to her curious question "finished your offu (office)?" when I returned home and the joy in her expression when she said "mama offu nee" (no office for mom). Thank you, little one, for your incredible understanding.

Smitha

Table of Contents

List of publications

In international peer reviewed journals

Rao C.V.S, Bockstael K, Nath S, Engelborghs Y, Anné J and Geukens N (2009). Enzymatic investigation of the *Staphylococcus aureus* type I signal peptidase SpsB – implications for the search for novel antibiotics. *FEBS J.* **276**: 3222-3234.

Bockstael K, Geukens N, **Rao C.V.S**, Herdewijn P, Anné J and Van Aerschot A (2009). An easy and fast method for the evaluation of *Staphylococcus epidermidis* type I signal peptidase inhibitors. *J Microbiol Methods.* **78**: 231-237.

Geukens N, **Rao C.V.S**, Mellado R.P, Frederix F, Reekmans G, De Keersmaeker S, Vrancken K, Bonroy K, Van Mellaert L, Lammertyn E, and Anné J (2006). Surface Plasmon Resonance-based interaction studies reveal competition of *Streptomyces lividans* of type I signal peptidases for binding preproteins. *Microbiology.* **152**: 1441-1450.

Rao C.V.S, Rao R and Agrawal R (2003). Enhanced production of Verbenol a high value food flavourant by an intergeneric fusant strain of *Aspergillus niger* and *Penicillium digitatum*. *Biotechnol Appl Biochem.* **37**: 145-147.

Agrawal R, **Rao C.V.S**, Gayathri C.N and Premnath R (2003). Intraspecific auxotrophic hybridization in *Aspergillus niger* and *Penicillium digitatum* by protoplast fusion for strain improvement in Verbenol production. *Asian J Microbiol Biotechnol Environ Sci.* **5**: 79-86.

Communications on international conferences (only available as abstract)

Rao C.V.S, Bockstael K, Anné J and Geukens N (2008). The type I signal peptidase as a tool for screening of potential anti-staphylococcal drug candidates. Society for General Microbiology (SGM) conference, March 31st- April 3rd, Edinburgh, UK.

Rao C.V.S, Bockstael K, Nath S, Engelborghs Y, Anné J and Geukens N (2009). Biochemical characterization of the *Staphylococcus aureus* type I signal peptidase SpsB. Federation of European Microbiological Societies (FEMS) conference, June 28th- July 2nd, Gothenburg, Sweden.

Rao C.V.S, Klaassen H, Segers K, Marchand A, Chaltin P and Anné J (2010). High-throughput screening of inhibitors of the type I signal peptidase SpsB for medicinal intervention against the *Staphylococcus aureus* superbug. Screening Europe conference, February 11th and 12th, Barcelona, Spain.

Communications on national conferences (only available as abstract)

Segers K, **Rao C.V.S**, Economou A, Klassen H, Chaltin P, Anné J (2010). Bacterial Sec-dependent protein translocation as a target for novel antibiotics. FlandersBio, Benelux Venture 50, May 11th, Ghent, Belgium.

Gayathri C.N, **Rao C.V.S** and Agrawal R (2000). Formation of Intergeneric stable recombinant from *Aspergillus niger* and *Penicillium digitatum* by protoplast fusion. 14th Indian Convention of Food Scientists and Technologists.

Rao C.V.S, Gayathri C.N and Agrawal R (2002). Biotransformation of alpha pinene to Verbenol by intraspecific fusant strain of *Penicillium digitatum*. 15th Indian Convention of Food Scientists and Technologists.

Thesis

Rao C.V.S (2006) Substrate specificity analysis of the *Streptomyces lividans* signal peptiases and functional analysis of a signal peptidase-like protein. Promotor: Prof. Dr. Jozef Anné. Pre-doctoral Certificate of Medical Sciences, KULeuven, Leuven, Belgium.

List of abbreviations

agr	accessory gene regulator
bp	basepair(s)
CBB	Coomassie Brilliant Blue
Dabcyl	4-(4-dimethylaminophenylazo) benzoic acid
DMF	*N,N*-dimethylformamide
DMSO	dimethyl sulphoxide
DNA	deoxyribonucleic acid
dNTP	deoxynucleotide-5'-triphosphate
EDANS	5-(2-aminoethyl)aminonaphthalene-1-sulfonic acid
ER-type	endoplasmic reticulum-type
ESI-MS	electrospray ionization mass spectrometry
FRET	Fluorescence resonance energy transfer
HTS	High-throughput screening
IC_{50}	half maximal (50 %) inhibitory concentration
IPTG	isopropyl-β-thiogalactopyranoside
IsaA	immunodominant staphylococcal antigenA
kb	kilo basepair(s)
kDa	kilo Dalton
LB	Lysogeny broth or Luria-Bertani broth
Lep	Leader peptidase
MCS	multiple cloning site
MIC	minimum inhibitory concentration
MRSA	methicillin-resistant *Staphylococcus aureus*
MW	molecular weight
NBT/BCIP	nitroblue tetrazolium chloride/5-bromo-4-chloro-3-indolylphosphate
Ni^{2+}-NTA	nickel nitrilo-tri-acetic acid
OD_x	Optical density at wavelength x nm
PCC	protein conducting channel
PCR	polymerase chain reaction
PMF	proton-motive force

pre-IsaA	immunodominant staphylococcal antigenA preprotein
P-type	prokaryotic-type
PVDF	polyvinylidene fluoride
RFU	relative fluorescence unit(s)
RNA	ribonucleic acid
RP-HPLC	reversed-phase high performance liquid chromatography
SCC	Staphylococcal cassette chromosome
SceD peptide	fluorogenic synthetic decapeptide based on *S. epidermidis* SceD protein signal peptide
SDS	sodium dodecylsulphate
SDS-PAA	sodium dodecylsulphate polyacrylamide
SDS-PAGE	sodium dodecylsulphate polyacrylamide gel electrophoresis
Sip or SPase	signal peptidase
SpsB	signal peptidase from *Staphylococcus*
SRP	signal recognition particle
Tat	twin-arginine translocation
Tris	tris(hydroxymethyl)aminomethane
tr-SpsB	N-terminally truncated (active) SpsB derivative
tr-mut-SpsB	N-terminally truncated active site mutant of SpsB
sc-SpsB	self-cleavage product of SpsB
v/v	volume to volume ratio

Names and IUPAC abbreviations of amino acids

3-letter code	*1-letter code*	*Name*
aa	X	any amino acid
Ala	A	alanine
Arg	R	arginine
Asn	N	asparagine
Asp	D	aspartic acid
Cys	C	cysteine
Gln	Q	glutamine
Glu	E	glutamic acid
Gly	G	glycine
His	H	histidine
Ile	I	isoleucine
Leu	L	leucine
Lys	K	lysine
Met	M	methionine
Phe	F	phenylalanine
Pro	P	proline
Ser	S	serine
Thr	T	threonine
Trp	W	tryptophan
Tyr	Y	tyrosine
Val	V	valine

Summary

Type I signal peptidases (SPasesI) play an indispensable role in the export of secretory proteins by cleaving off the N-terminal extensions called signal peptides from proteins that are translocated across biological membranes. The bacterial SPasesI are also regarded as attractive antibiotic targets due to their essentiality, relative accessibility and their unique and conserved catalytic mechanism. Of the two genes encoding homologues of type I signal peptidase in *Staphylococcus aureus*, *spsA* and *spsB,* we focused on the latter that encodes the catalytically active and essential type I signal peptidase, SpsB. The aim of this work is the biochemical investigation of the enzyme SpsB, development of *in vitro* screening systems and finally high-throughput screening of compounds in the search for new inhibitors.

In the first stage, we demonstrated the *in vitro* activities of the full length SpsB and N-terminally truncated derivative of SpsB (tr-SpsB) on a native preprotein substrate, immunodominant staphylococcal antigen A precursor (pre-IsaA). The ability of the truncated SpsB to cleave the preprotein substrate implies that the transmembrane segment is not essential for SPase activity. The specific enzymatic activities of the full-length and the tr-SpsB were determined using a FRET assay involving an internally quenched synthetic decapeptide designated as SceD peptide. The k_{cat}/K_M value of the full-length SpsB was 1850 $M^{-1}s^{-1}$, approximately 30-fold higher in comparison with tr-SpsB. This shows that the transmembrane segment residues, although not essential, are required for optimum activity of the enzyme.

In the second stage, we analyzed the *in vitro* behaviour of the full-length SpsB. The pH-rate profile for SpsB revealed an optimum pH of approximately 8. The apparent pK_a values for the free enzyme were determined to be approximately 6.6 and 8.7 with possibly another pK_a around 11.8. In common with the other SPasesI characterized so far, SpsB undergoes intermolecular self-cleavage, following the (-3,-1) rule for signal peptidase recognition and cleavage. The self-cleavage of SpsB resulted in an N-terminally truncated product with the catalytic Ser as the penultimate residue but was inactive in the FRET assay. By comparing the amino acid sequences and activities of the self-cleavage product of SpsB and tr-SpsB, we suggest that 9 amino acid residues immediately

preceding the catalytic Ser, that are lacking in the self-cleavage product, are essential for SpsB activity.

In the third stage, we demonstrated *in vitro* inhibition of SpsB in the FRET assay as well as in the preprotein processing assay, using known SPase inhibitors. The FRET assay was standardized in a 96-well format, evaluated by screening compounds and assessed for quality and reproducibility. The preprotein assay served as a secondary assay to test potential inhibitors.

In the final stage, the FRET assay was adapted in a 384-well format and transferred to a high-throughput screening facility. Approximately 27,000 diverse small molecule candidates were screened in the FRET assay against SpsB. Although, the quality of the screen reflected the robustness of the assay (with an average Z' value of 0.73), no potent inhibitors were obtained. Further analysis led to finding a weak inhibitor (code JRD2189) of SpsB with IC_{50}=51 μM in the FRET assay. The compound was also active against *E. coli* LepB but could not inhibit preprotein processing.

In short, we have analyzed the properties of SpsB and developed *in vitro* systems to facilitate the search for new classes of antibiotics against *S. aureus*.

Samenvatting

Type I signaalpeptidases (SPasesI) spelen een essentiële rol in eiwitsecretie aangezien deze enzymen verantwoordelijk zijn voor de afsplitsing van de N-terminale signaalpeptiden van secretorische eiwitten na hun transport over een biologische membraan. Bacteriële SPasesI worden beschouwd als een interessant antibacterieel doelwit omwille van hun essentieel karakter, omdat ze relatief gemakkelijk toegankelijk zijn voor kleine moleculen en hun katalytisch mechanisme uniek en geconserveerd is. In dit proefschrift hebben we SpsB, één van de twee SPaseI-homologen die aanwezig zijn in *Staphylococcus aureus,* bestudeerd. In tegenstelling tot SpsA is SpsB katalytisch actief en van essentieel belang voor *S. aureus*. Het doel van dit proefschrift was een biochemische karakterisering van SpsB en de ontwikkeling van *in vitro* screeningtesten, om finaal via high-throughput screening SpsB-remmers te identificeren.

In het eerste deel van dit proefschrift hebben we aangetoond dat zowel het volledige (fl-SpsB) als een N-terminaal ingekorte vorm (tr-SpsB) van SpsB *in vitro*-activiteit vertonen ten opzichte van het natieve preproteïne-substraat, immunodominant staphylococcus antigen A precursor (pre-IsaA). Het vermogen van de ingekorte vorm van SpsB om het preproteïne-substraat te klieven impliceert dat het transmembranair domein niet essentieel is voor de activiteit van SpsB. De specifieke enzymatische activiteit van fl-SpsB en tr-SpsB werd bepaald d.m.v. Fluorescentie Resonantie Energie-Transfer (FRET), met een gemerkt synthetisch decapeptide, het SceD peptide. De k_{cat}/K_M-waarde van fl-SpsB was 1850 $M^{-1}s^{-1}$, ongeveer 30 keer hoger dan de k_{cat}/K_M-waarde die voor tr-SpsB werd verkregen. Dit toont aan dat aminozuren in het transmembranair domein van SpsB niet essentieel, maar toch belangrijk zijn voor optimale enzymatische activiteit.

In het tweede deel van dit proefschrift hebben we fl-SpsB verder *in vitro* biochemisch gekarakteriseerd. Het pH-profiel van de SpsB-activiteit vertoonde een optimum bij pH 8. De schijnbare pK_a-waarden voor het vrije enzym waren ongeveer 6.6 en 8.7, met mogelijk een tweede pK_a rond 11.8. Net zoals de andere SPasesI die tot nog toe zijn gekarakteriseerd, ondergaat ook SpsB intermoleculaire zelfsplitsing volgens de (-3,-1)-regel voor signaalpeptidase-herkenning en -splitsing. Zelfsplitsing van SpsB resulteert in een N-terminaal ingekorte vorm (sc-SpsB) met het katalytische Ser als het voorlaatste aminozuur. Deze zelfgesplitste proteinevorm bleek geen SPase-activiteit te vertonen in

de FRET-test. Door de aminozuursequenties en de activiteit van het zelfsplitsing product en tr-SpsB te vergelijken, lijkt het ons aannemelijk dat de 9 aminozuren die het katalytische Ser voorafgaan (en die ontbreken in het zelfsplitsingsproduct) essentieel zijn voor SpsB-activiteit.

In het derde deel van dit proefschrift hebben we gekende SPase-remmers gebruikt om de *in vitro*-remming van SpsB aan te tonen, en dit zowel d.m.v. de FRET-test als d.m.v. een test waarbij de splitsing van een preproteïne door SpsB kan worden gevolgd. De FRET-test werd gestandardiseerd in een 96-well-formaat en geëvalueerd voor de screening van kleine moleculen door de kwaliteit en de reproduceerbaarheid van de test na te gaan. De test waarbij de splitsing van een preproteïne door SpsB wordt gevolgd, werd als een bijkomende test gebruikt om potentiële SpsB-remmers te bestuderen.

In het laatste deel van dit proefschrift werd de FRET-test aangepast naar een 384-well-formaat om gebruikt te kunnen worden voor high-throughput screening. Ongeveer 27000 kleine moleculen werden zo getest tegen SpsB. Ondanks de robuustheid en de hoge kwaliteit van de test (met een gemiddelde Z'-waarde van 0.73) werden geen sterke SpsB-remmers gevonden. Na verdere analyse werd een zwakke remmer (code JRD2189) geïdentificeerd met een IC_{50} van 51 μM in de FRET-test. Dit molecule was ook actief tegen *E. coli* LepB, maar was niet in staat om de splitsing van een preproteïne door SPaseI te remmen.

We kunnen dus concluderen dat we in dit werk SpsB biochemisch hebben gekarakteriseerd en *in vitro*-testen hebben ontwikkeld voor het identificeren van een nieuwe klasse van antibiotica gericht tegen *S. aureus*.

Chapter 1: Introduction

1.1 The need for new drugs

Bacterial and parasitic diseases are the second leading cause of death worldwide. The treatment of bacterial infections has become increasingly challenging as antibiotics that have been saving millions of lives are losing effect. This is mainly due to their overuse or misuse contributing to the emergence of multiple drug-resistant strains. Of major concern is multidrug resistance in (i) common respiratory pathogens including *Streptococcus pneumoniae*, *Mycobacterium tuberculosis* (ii) Gram-negative bacilli (eg: *Pseudomonas aeruginosa*, *Acinetobacter baumannii* and *Klebsiella pneumoniae*) and (iii) *Staphylococcus aureus*. In addition, an increase in the use of indwelling and prosthetic devices has added biofilms (communities of sophisticated matrix-encased, surface-attached bacteria that exhibit a distinct phenotype) in which bacteria are less sensitive to antibiotics, to the already existing problem. On the other hand, the number of different antibiotics available to treat infections is dwindling and there are only a handful of new antibiotics in the drug development pipeline (Devasahayam *et al.*, 2010). Therefore, there is an urgent need for new drugs preferably with new modes of action to potentially avoid cross-resistance (Payne, 2008). Of late, there has been an increase in interest in identifying and characterizing non-conventional antibiotic targets including the components of the bacterial protein secretion pathway such as SecA, a protein translocation ATPase and the type I signal peptidases (SPasesI), which are key enzymes in preprotein processing (Stephens & Shapiro, 1997). This work focuses on the latter component of the secretion machinery.

1.2 An overview of bacterial protein secretion

In bacteria, approximately 25-30 % of the proteins synthesized are destined to function at the cell envelope or outside. These proteins are transported from their site of synthesis (cytoplasm at the ribosomes) across the cytoplasmic membrane in three steps: targeting, translocation and release/maturation. The majority of proteins destined for transmembrane transport are synthesized as precursors or preproteins with a small amino-terminal extension called the signal peptide, which apart from other functions, serves primarily as a zip code for sorting and targeting (von Heijne, 1998). The process of targeting and translocation is accomplished by the general secretion pathway (Sec

pathway) which is essential and universal in bacteria or the twin-arginine translocation (Tat pathway) that also exists in several bacteria (Natale *et al.*, 2008). Both pathways consist of separate targeting components and in each case, a membrane-embedded pore through which the preprotein is translocated (the translocon), is present. A major difference between the two pathways is that, while the former translocates unfolded proteins, the latter serves in transporting folded proteins across the membrane. During or shortly after translocation of the preproteins, the hydrophobic signal peptides are cleaved off by enzymes, called the signal peptidases, ensuring their release from the membrane (Paetzel *et al.*, 2002b). In a major role, the type I signal peptidase (also known as leader peptidase and abbreviated as SPaseI or Lep or Sip), a membrane-bound serine endopeptidase, processes non-lipoproteins thereby enabling them to reach their final destination. In a minor role, SPase II or the lipoprotein signal peptidase (Lsp) processes lipid-modified lipoprotein precursors. The type IV SPase (SPase IV) specializes in the cleavage of type IV preprepilin and prepilin like proteins. Unlike SPaseI, neither of the latter enzymes are essential for cell viability (Paetzel *et al.*, 2002b). In Gram-positive bacteria fully translocated proteins are exported to the cell wall or the surrounding medium. In Gram-negative bacteria, these proteins are released into the periplasm, integrated into or transported across the outer membrane or finally exported to the cell wall or the outside medium. Bacteria also possess additional dedicated protein secretion systems designated type I to type VII secretion systems (or T1S to T7S) (Bitter *et al.*, 2009; Economou *et al.*, 2006; Thanassi & Hultgren, 2000). These systems mainly function in the translocation and secretion of proteins across the double hydrophobic membrane barriers as in Gram-negative bacteria. Some of the additional systems also involve the Sec or Tat machinery for transport across the cytoplasmic membrane, for example as in the case of T2S, T4S and T5S.

1.2.1 Signal peptides

Signal peptides have an average length of 20 amino acid residues (generally longer in those from Gram-positive bacteria) and strikingly show no conservation of sequence. However, three distinct regions can be recognized

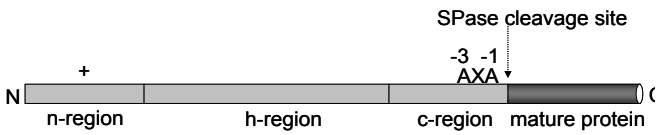

Figure 1.1: Schematic representation of the tripartite structure of a signal peptide showing the SPase recognition sequence and cleavage site.

which are a positively charged amino-terminal (n-region), a hydrophobic core (h-region) and a polar carboxyl terminal (c-region) (von Heijne, 1990) (Figure 1.1). The h-region is the largest part of the signal peptide and is formed by a stretch of hydrophobic residues that seem to adopt an α-helical conformation and often has a helix-breaking Gly or Pro in the middle of the region that might facilitate signal peptide insertion into the membrane (de Vrije *et al.*, 1990). The n-region is composed of a positively charged stretch of polar residues which appears to interact with the negatively charged phospholipids in the membrane and determines the orientation of the signal peptide thereby obeying the "positive-inside rule" (Dalbey, 1990; von Heijne, 1992). The c-region usually has a helix-breaking Pro or a Gly residue at position -4 to -6 relative to the SPase cleavage site and ends with small, neutral residues (most commonly Ala) at positions -1,-3 which has been referred to as the "Ala-X-Ala" SPase recognition sequence. The c-region faces the extracytoplasmic side of the membrane after translocation and must have a β-stranded conformation in order to be recognized by the SPase (van Roosmalen *et al.*, 2004). The non-lipoprotein signal peptides share the same generic structure but the Tat signal peptides differ from the Sec signal peptides in certain aspects, notably in the presence of two invariant arginines, the eponymous twin-arginine motif at the interface of the n- and h- regions (Natale *et al.*, 2008). Besides the non-lipoprotein signal peptides, which are processed by SPasesI, there are two other types of signal peptides namely lipoprotein and prepilin signal peptides. Lipoprotein signal peptides also have the n-, h- and c- regions but in addition possess the lipobox at the c-region that has information for lipid modification at the +1 cysteine residue. After lipid modification of the +1 cysteine the signal peptide is cleaved from the preprotein by SPasesII. Preprepilin signal peptides are present in type IV prepilins and prepilin-like precursors that form a part of the type II secretion system. These signal peptides are characterized by a short basic region without any hydrophobic domain and are processed by type IV prepilin SPases (Paetzel *et al.*, 2002b).

A comparative analysis of 107 experimentally determined *E. coli* SPase substrates (Choo *et al.*, 2008) revealed a high conservation of amino acid residues at positions P3 (-3) and P1 (-1). In particular, position P1 is dominated by small, hydrophobic, and neutral amino acids, with Ala being the predominant residue (92 %), followed by Gly (9 %). Position P2 shows a strong preference for bigger side chains with 87 % possessed by medium- or large-sized residues at this location. Position P3 also shows a preference for hydrophobic

residues and contains mainly small amino acid residues but can also accommodate both medium and large residues. Only 50 % of the sequences analyzed contained the consensus Ala-X-Ala recognition motif, where as 18% contained Val-X-Ala recognition sequence.

Signal peptides are functionally important because they are recognized by the targeting components of the secretion machinery and passed onto the translocation machinery for transmembrane transport (van Roosmalen *et al.*, 2004). They serve as topological determinants for the preprotein in the membrane. In addition, they inhibit or retard folding of the nascent chains thus retaining the preproteins in a translocation-competent state and also avoiding the activation of potentially harmful enzymes inside the cell. The signal peptides are cleaved off by the signal peptidases and are subsequently degraded by enzymes called signal peptide peptidases (Paetzel *et al.*, 2002b).

1.2.2 The Sec and the Tat pathway

The process of protein translocation is most extensively studied in *E. coli*. Briefly, the Sec system consists of protein targeting components, a membrane-embedded, protein-conducting channel (PCC) comprising three proteins (SecY, SecE and SecG) which form the Sec translocase and a peripherally associated, ATP-driven motor protein SecA. SecD, SecF and YajC form the translocon-associated complex and YidC is involved in membrane protein integration and folding (Figure 1.2). The central components of the Sec translocation system of Gram-positive and Gram-negative bacteria show a high degree of conservation, suggesting similar functions and

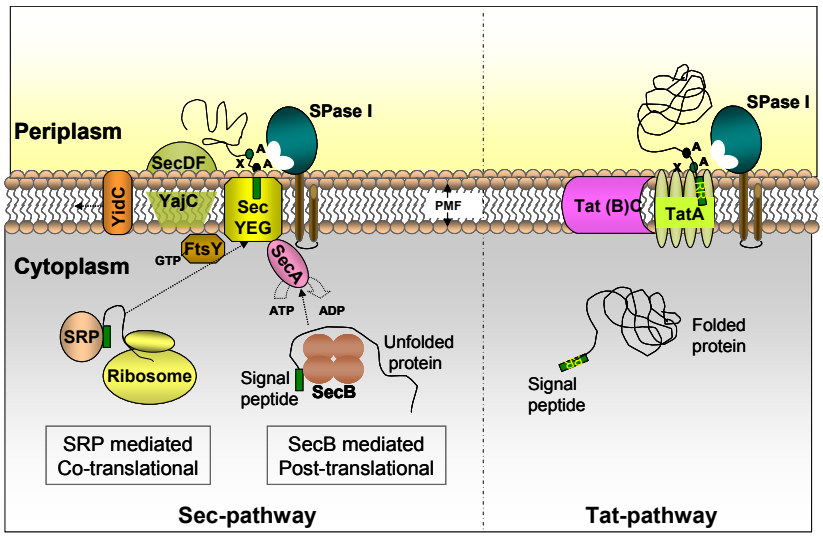

Figure 1.2: A schematic view of preprotein targeting, translocation and processing by the type I SPase resulting in the release of the mature protein.

working mechanisms. However, certain differences can be identified, for example the absence of a secretion-specific, chaperone-like SecB in Gram-positive bacteria. The targeting of secretory proteins in the Sec pathway occurs either post or co-translationally. In case of the former, the fully synthesized preprotein detaches from the ribosome and is directed to the Sec translocase guided by SecB, which maintains the translocation-competent unfolded state. In co-translational targeting the signal recognition particle (SRP) binds to the signal sequence of the secretory protein while it emerges from the ribosome and the entire ternary complex of SRP/ribosome/nascent secretory protein chain is targeted to the Sec translocase with the aid of signal recognition particle receptor (SR or FtsY). SecA accepts the unfolded proteins and threads them through the transmembrane channel (PCC) using the energy provided by ATP and the proton-motive force (PMF) (Ito & Mori, 2009; Natale *et al.*, 2008). In the Tat pathway, pretranslocational folding is necessitated by the incorporation of metallo-factors, assembly into oligomeric complexes, and presumably rapid folding kinetics (Panahandeh *et al.*, 2009). The Tat system consists of two or three membrane-integrated subunits namely TatA and TatC (especially in Gram-positive bacteria) or TatA, TatB and TatC that together form a receptor and a protein-conducting machinery for Tat substrates. TatC and TatB form a complex that is involved in recognition of Tat signal sequences and their insertion into the membrane, while TatA mediates the actual translocation event. However, it remains unclear whether TatA does so by forming the pore-like structures that it displays when purified to homogeneity (Panahandeh *et al.*, 2009). The energy for the process is derived from PMF. The Sec and the Tat pathways have not been characterized in *S. aureus*. Nevertheless, components of the two pathways have been identified based on BLAST searches with the corresponding proteins of *Bacillus subtilis* (Sibbald *et al.*, 2006).

1.3 Type I signal peptidases in bacteria

1.3.1 **Co**mmonalities and differences among SPases of Gram-positive and Gram-negative bacteria

The type I signal peptidases (EC 3.4.21.89) belong to the serine protease family S26 and are classified into the evolutionary clan of serine proteases SF, which utilize a Ser/Lys (prokaryotes) or possibly Ser/His (eukaryotes) catalytic dyad mechanism instead of the more common Ser/His/Asp triad mechanism (Paetzel *et al.*, 2000). SPasesI are further subdivided into prokaryotic (P)-type and endoplasmic reticulum (ER)-type SPases. Apart

from other differences, the ER-type SPases have a histidine residue instead of the catalytic lysine in P-type SPases. All eubacterial SPases are of the P-type with the exception of *B. subtilis*, having both the (ER)-type (SipW) and the P-type (SipS, SipT, SipU, SipV) SPases (van Roosmalen *et al.*, 2004). SPasesI from different bacterial species have five conserved regions denoted as boxes A-E as revealed by sequence alignment data (Paetzel *et al.*, 2000). Although the Gram-positive and Gram-negative bacterial SPases have the same function, they do display the following differences. (i) Gram-negative bacteria typically have only one SPaseI. For example *E. coli* has a single gene encoding SPaseI (*lepB*). This gene has been shown to be essential for cell growth and viability (Dalbey & Wickner, 1985). Gram-positive bacteria often have more than one SPaseI, of which none of the individual enzymes was found to be essential for viability. When a species contains multiple SPasesI, some seem to be more important for efficient preprotein processing than others. Therefore, they are grouped as major and minor SPases, respectively (van Roosmalen *et al.*, 2004). In such cases, the SPases have overlapping but non-identical substrate specificities and some of the SPase-encoding genes are temporally regulated. (ii) Gram-negative and Gram-positive bacterial SPases differ in membrane topology in that the former typically are anchored in the cytoplasmic membrane by at least two N-terminal transmembrane segments while the latter usually have one N-terminal domain. For example, *E. coli* LepB has two N-terminal transmembrane segments, a small cytoplasmic domain between them and a large C-terminal catalytic domain while *e.g.*, *S. aureus* SpsB is predicted to have only one. (iii) The SPases of Gram-negatives are generally larger in size than those of Gram-positives mostly due to the presence of more than one N-terminal transmembrane segment (van Roosmalen *et al.*, 2004). *E. coli* LepB and *S. aureus* SpsB contain approximately 300 and 200 amino acids, respectively. (iv) The catalytic domain of SPasesI of most Gram-positive bacteria is also significantly smaller compared to that of *E. coli* LepB, mainly due to the absence of a large β-sheet between the conserved domains D and E and a relatively small β–hairpin between domains B and C. (v) The SPases from the two groups also differ in their substrate specificities. For example, although active, none of the *B. subtilis* SPases were able to complement LepB-deficient *E. coli* cells for growth and viability (van Roosmalen *et al.*, 2004).

It should be noted that in entire text that follows the terms 'SPase(s)I' or simply 'SPase(s)' refers to the type I signal peptidase(s) only and LepB is used to refer to the SPaseI of *E. coli*.

1.3.2 Biochemical characteristics

Biochemical data of the type I SPases have been obtained largely from the Gram-negative bacterium *E. coli* followed by the Gram-positive organisms *Bacillus subtilis, Streptomyces lividans*, *Streptococcus pneumoniae* (van Roosmalen *et al.*, 2004). Based on the *in vitro* data available, the SPases of Gram-positive and Gram-negative bacteria have several properties in common which include (i) intermolecular self-cleavage of the enzyme; (ii) enhanced activity in the presence of some non-ionic detergents and phospholipids; (iii) reduced activity of the truncated SPases (devoid of the transmembrane segment) compared to the full-length SPases; (iv) high optimum pH (ranging from pH 8 to pH 11) in contrast to all other serine protease families.

In vitro SPaseI assays involving preprotein or synthetic peptide substrates have been instrumental in characterization, enabling comparison between the SPases from different bacteria (Paetzel *et al.*, 2000). One of the best SPase substrates for *E. coli* LepB is a full-length hybrid preprotein substrate, pro-OmpA nuclease A which has *S. aureus* nuclease A attached to the signal peptide of the *E. coli* outer membrane protein, OmpA (Chatterjee *et al.*, 1995). Using this substrate, the activation energy of LepB was estimated to be 10.4 ± 1.6 kcal/mol, which indicates that this SPase is catalytically equally efficient as typical serine proteases with a Ser/His/Asp triad mechanism (Suciu *et al.*, 1997). Synthetic peptide substrates in general are poor substrates, when compared to the full-length preproteins possibly due to conformational preferences for the latter which are not fulfilled by synthetic peptides (Dalbey et al., 1997). Despite this fact, a number of synthetic peptide substrates (Table 1.1) have proved indispensable for rapid screening of SPase inhibitors.

It was observed early on that the bacterial type I signal peptidases are not inhibited by the standard protease inhibitors against the four standard protease classes (serine protease, cysteine protease, aspartic protease and metalloproteases) (Black *et al.*, 1992; Kuo *et al.*, 1993; Zwizinski *et al.*, 1981) and probably belong to a new protease family. The initial evidences for the SPases utilizing an unconventional Ser/Lys dyad mechanism came

Table 1.1: Comparison of the specific enzymatic activity of SPases for different peptide substrates used in screening assays of inhibitors and a preprotein substrate (topmost).

Substrate (Reference)	***Assay***	k_{cat}/K_M $(M^{-1}s^{-1})$		
		S. aureus SpsB	*E. coli lepB*	*S. pneumoniae Spi*
∗Pro-OmpA-Nuclease A (Chatterjee *et al.*, 1995)	SDS-PAGE/ densitometry	16	$1.1x10^7$	-
Y(NO2)FSASALA↓KIK(Abz) (Zhong & Benkovic, 1998)	+FRET/ spectrofluorometry	18.4	71.1	-
K(5)-L(10)- Y(NO2)FSASALA↓KIK(Abz) (Stein *et al.*, 2000)	+FRET/ spectrofluorometry	-	$2.5x10^6$	-
KLTFGTVK(Abz)PVQA↓IAGY(NO2)EWL (Peng *et al.*, 2001b)	+FRET/ spectrofluorometry	-	-	$2.7x10^2$
A proprietary lipopeptide substrate (Ashman *et al.*, 2000)	+FRET/ spectrofluorometry	$4.6x10^4$	-	-
Decanoyl-LTPTAKA↓ASKIDD-OH (Bruton *et al.*, 2003)	+FRET/ spectrofluorometry	$2.3x10^6$	$4.2x10^5$	-

∗Fusion protein made up of signal peptide of outermembrane protein A from *E. coli* and the nuclease A from *S. aureus*.
#Fluorescence resonance energy transfer

from site-directed mutagenesis (Sung & Dalbey, 1992; Tschantz *et al.*, 1993) and chemical modification studies on *E. coli* LepB (Black *et al.*, 1992; Black, 1993; Paetzel *et al.*, 1997), *Bacillus subtilis* SipS (van Dijl *et al.*, 1995), *S. pneumoniae* Spi (Peng *et al.*, 2001a) and was finally confirmed by the crystal structure of LepB.

1.3.3 Structural data

For structure determination, a truncated derivative of *E. coli* LepB (referred to as Δ2-75 SPase) lacking residues from 2-75 corresponding to the N-terminal transmembrane regions (MW of 27.9 kDa; MW of full-length = 35.9 kDa) was designed, in order to avoid problems of instability due to self-cleavage and to improve solubility. The Δ2-75 SPase has been purified, characterized (Kuo *et al.*, 1993; Tschantz *et al.*, 1995), crystallized in its apoform (Paetzel *et al.*, 1995; Paetzel *et al.*, 2002a) and in complex with different types of inhibitors [β-lactam (Paetzel *et al.*, 1998), lipopeptide (Paetzel *et al.*, 2004), lipopeptide and a β-sultam inhibitor (Luo *et al.*, 2009)] and has also been used in nuclear magnetic resonance (NMR) studies (Musial-Siwek *et al.*, 2008b). Nevertheless, this mutant

also required the non-ionic detergent Triton X-100 for optimal activity and crystallization and the addition of SPase inhibitor greatly facilitated in obtaining high-resolution structural data. Interestingly, an NMR study was reported on the full-length SPase (Musial-Siwek *et al.*, 2008a).

1.3.3.1 3D structure of the catalytic domain of *E. coli* SPase, LepB

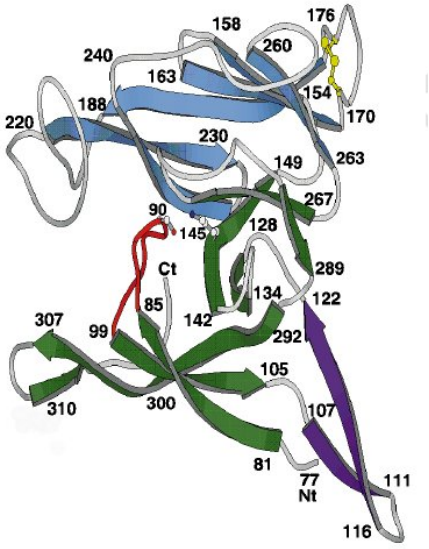

Figure 1.3: A ribbon diagram of the general fold of truncated *E. coli LepB* (Δ2-75). The conserved domain I β-sheet is in green and the domain II β-sheet is in blue. The β-hairpin extension protruding from domain I is in purple. Active site residues Ser and Lys are labelled 90 and 145 respectively [reprinted by permission from Macmillan Publishers Ltd: *Nature* (Paetzel *et al.*, 1998)], copyright (1998)].

The structure of Δ2-75 SPase (Paetzel *et al.*, 1998) has a primarily β-sheet protein fold consisting of two anti-parallel β-sheet domains (termed Domain I and II), two small 3_{10}-helices (residues 246-250 and 315-319; see Figure 1.3) and one small α-helix (residues 280-285). Domain I, termed the "catalytic core", contains the conserved regions (Boxes B-E), all of which reside near or are a part of the active site (Paetzel *et al.*, 2000). The structure has four extended loops or hairpins that are disordered (108-124, 170-176, 198-202, and 304-313). The large β-sheet Domain II (154-264) and a long extended β-ribbon (107-122) observed in *E. coli* SPase structure are insertions within Domain I. Structure-based multiple sequence alignment data of representative type I SPases reveal that Domain I is conserved throughout evolution. In contrast, Domain II is relatively smaller and the extended β-ribbon is lacking in Gram-positive bacterial SPases which is attributed to the generally smaller size of these SPases (Paetzel *et al.*, 2000). The conserved Domain I also contains a large unusually exposed hydrophobic surface, which is rarely found in soluble proteins. This hydrophobic surface runs along the β-sheet made up from three β-strands and is proposed to be involved in membrane association (Paetzel *et al.*, 1998). Notably, one of the β-strands has an essential Trp300 (Kim *et al.*, 1995) which, like other aromatic amino acids, is thought to play an important role in protein/membrane interfaces. This residue

is presumed to facilitate the insertion or association of *E. coli* SPase into the membrane (Paetzel *et al.*, 2000). Sequence alignments indicate that several conserved aromatic or hydrophobic residues exist in the proposed membrane-association domain in both Gram-positive and Gram-negative bacterial type I SPases (Paetzel *et al.*, 2000). The recent crystal structure of Δ2-75 SPase revealed the presence of pronounced solvent channels directly adjacent to the proposed hydrophobic membrane-association domain where the required detergent is likely to accumulate, stabilizing the significantly exposed hydrophobic surface area on the *E. coli* signal peptidase molecule (Luo *et al.*, 2009).

The structural motifs of the enzyme residing in the four conserved boxes could be identified in the tertiary structure (Paetzel *et al.*, 2000). Box B (residues 88-95) contains the proposed nucleophile Ser90 that resides on a well-ordered loop (see Figure 1.3; shown in red) between the first two β-strands of the periplasmic catalytic portion of *E. coli* LepB. Box B also contains Ser88 which is conserved in SPases of Gram-negative bacteria (replaced by Gly in SPases of Gram-positive bacteria) and Met91, which allows for the placement of its sulphur side-chain adjacent to the nucleophile serine, in common with that observed in the active site of other serine proteases (Paetzel *et al.*, 2000). Boxes C (residues 127-134) and D (residues 142-153) contain two antiparallel hydrogen-bonded β-strands (β-5 and β-6) of which the latter contains the proposed general base Lys145 and has main chain atoms aligned perfectly to make β-strand-type hydrogen bonds with the signal peptide substrate, also in common with other serine proteases. Box E contains the strictly conserved Gly272 explained by the fact that it sits directly adjacent to the Nζ of Lys145 and any other residue at this site would necessarily position a side chain into this region that would clash with the essential Lys145 side chain. Box E also contains a conserved Ser278, which hydrogen bonds to the Lys145 and is suggested to help position the Lys145 Nζ for its general base role with Ser90. The highly conserved Asp280 and Arg282 form a strong salt bridge and play an indirect role in catalysis by contributing to the structural stabilization of the active site.

1.3.4 Catalytic residues

The first direct evidence that the Ser90 Oγ acts as the acylating nucleophile in the SPase hydrolysis reaction came from the co-crystal structure of Δ2-75 SPase with 5*S*,6*S* β-lactam (penem) inhibitor (Paetzel *et al.*, 1998). The electron density at the active site revealed a covalent bond between the Ser90 Oγ and the carbonyl (C7) of the inhibitor.

The SPase-inhibitor co-crystal structure also showed that the Ser90 O γattacks the *si*-face of the β-lactam amide bond, a peptide-bond analogue. This indicates that SPasesI are unique and differ from all known Ser/His/Asp serine proteases and the group 2b β-lactamases, which perform a *re*-face attack. These observations further supported the earlier prediction of *si*-face attack based on the preference of SPasesI for 5S rather than the 5R stereochemistry of the penem inhibitor (Allsop *et al.*, 1997). Further, the structure revealed that Nζ of Lys145 forms a strong hydrogen bond with Ser90 Oγ and is the only titratable group in the vicinity of the active-site nucleophile. The position of Lys145 Nζ is fixed relative to Ser90 by hydrogen bonds to the conserved Ser278 Oγ and the carbonyl oxygen (O10) of the inhibitor side chain. Therefore, Lys145 is correctly positioned to act as the general base in both the acylation and deacylation step of catalysis. The side chain of Lys145 is completely buried in the inhibitor complex, making van der Waals contacts with the side-chain atoms of Tyr143, Phe133 and Met270 and the main chain-atoms of Met270, Met271, Gly272 and Ala279, all of which are contained within the catalytic core (Domain I). The hydrophobic environment surrounding the Lys145 ε–amino group is likely essential for lowering its pK_a, such that it can reside in the deprotonated state required for its role as the general base (Paetzel *et al.*, 1998). An important component of the catalytic machinery in serine proteases is the oxyanion hole that works by neutralizing the developing negative charge on the scissile carbonyl oxygen during the formation of the tetrahedral intermediates. The co-crystal structure with penem first indicated that Ser90 amide might contribute to the formation of an 'oxyanion hole' as the main-chain amide of Ser 90 forms a strong hydrogen bond with the carbonyl oxygen (O8) of the cleaved β-lactam ring. Subsequent mutagenesis data (Carlos *et al.*, 2000a) and analysis of the active site of the apoenzyme (Paetzel *et al.*, 2002a) suggested

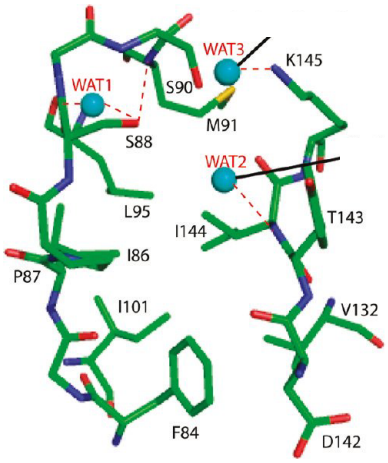

Figure 1.4: The three conserved water molecules in the active site of *E. coli* SPase. The residues near the active site and binding cleft are represented in stick and coloured by element (carbon, green; nitrogen, blue; oxygen, red). The hydrogen bonding interactions between the waters (cyan spheres) and the residues of SPase I are indicated in red dashed lines [reprinted with permission from Luo *et al.*, 2009. Copyright 2009 American Chemical Society].

that the other contributor to the oxyanion hole could be side-chain hydroxyl hydrogen (Ser88 OγH) besides the main-chain amide hydrogen (Ser90 NH). Gram-negative bacterial SPases are unusual in this respect as the oxyanion hole is typically formed by two main-chain amide hydrogens that serve as hydrogen bond donors to the developing oxyanion (Menard & Storer, 1992). However, in most SPases of Gram-positive bacterial origin Ser88 is replaced by a Gly residue and it is assumed that the main chain NH of the Gly might contribute in stabilization of the oxyanion transition state (van Roosmalen *et al.*, 2004). A comparison of the apoenzyme structure (Paetzel *et al.*, 2002a) with the previously obtained acyl-enzyme structure showed significant side-chain and main-chain differences in the binding site and active site regions, which resulted in a smaller S1 binding pocket in the apoenzyme. The apoenzyme structure also revealed three conserved water molecules near the active site designated as water 1, water 2 and water 3 (Figure 1.4). Water 1 is coordinated to Met91 backbone NH, Ser88 O and Leu95 O. Water 2 is coordinated to Ile144 NH. Water 3 is coordinated to the Nζ of Lys145 and is hypothesized to function as the deacylating (also called the "catalytic", "hydrolytic" or "nucleophilic") water in the SPaseI catalysis. A homology model of Gram-positive *Bacillus subtilis* SipS and supporting data have been used to compare the possible role of corresponding residues in catalysis, which ultimately will have to be confirmed when the crystal structure becomes available (van Roosmalen *et al.*, 2004).

1.3.5 Substrate specificity

Mapping of surface clefts on the SPase structure and modelling of a tetrapeptide (poly-Ala) into the active site led to the identification of two shallow hydrophobic pockets (designated as S1 and S3 substrate binding sites) appropriate for accommodating -1 (P1) and -3 (P3) residues of the signal peptide (Paetzel *et al.*, 2000). The model helped explain the Ala-X-Ala (or -3,-1 rule) cleavage-site specificity of signal peptidases. Furthermore, modelling of an *E. coli* periplasmic dithiol oxidase, DsbA 13-25 precursor protein into the active site of *E. coli* LepB led to defining thirteen subsites S7 to S6' within the SPase substrate-binding site (Choo *et al.*, 2008). It has been suggested that the narrow clefts at S3, S2, S1 and S1' play a direct role in high specificity of the signal peptide residues while the larger clefts at S3' and S4' could be responsible for interactions with the mature moieties (Figure 1.5). Additionally, NMR studies on the Δ2-75 SPase revealed that a small subset of eighteen residues, mostly residing in the proposed binding pockets, undergo a conformational change upon (synthetic alkaline phosphatase) signal peptide

binding, while the rest of the enzyme structure did not change substantially (Musial-Siwek *et al.*, 2008b). The residues whose conformation changes upon signal peptide binding include the catalytic residues (Ser90 and Lys145) and residues contributing to SPase cleavage fidelity and substrate specificity (Ile86 and Ile144) (Ekici *et al.*, 2007; Karla *et al.*, 2005). The NMR data suggest that residues of S1 and S3 have to reorient in order to achieve close complementation with the docked -1 and -3 signal peptide residues, consistent with an induced fit hypothesis. Despite the conformational alterations which are ideally suited for accommodating signal peptide cleavage regions with a spectrum of different sequences, the region is too small to accommodate large side chains (Musial-Siwek *et al.*, 2008b). The residues contributing to the S1 substrate binding pocket are primarily hydrophobic and include Ile86, Pro87, Ser88, Ser90, Mer91, Leu95, Ile144, Tyr143 and Lys145 (Choo *et al.*, 2008; Paetzel *et al.*, 2000). The residues perturbed in the NMR study (Musial-Siwek *et al.*, 2008b) are underlined. It must be noted that Pro87 was

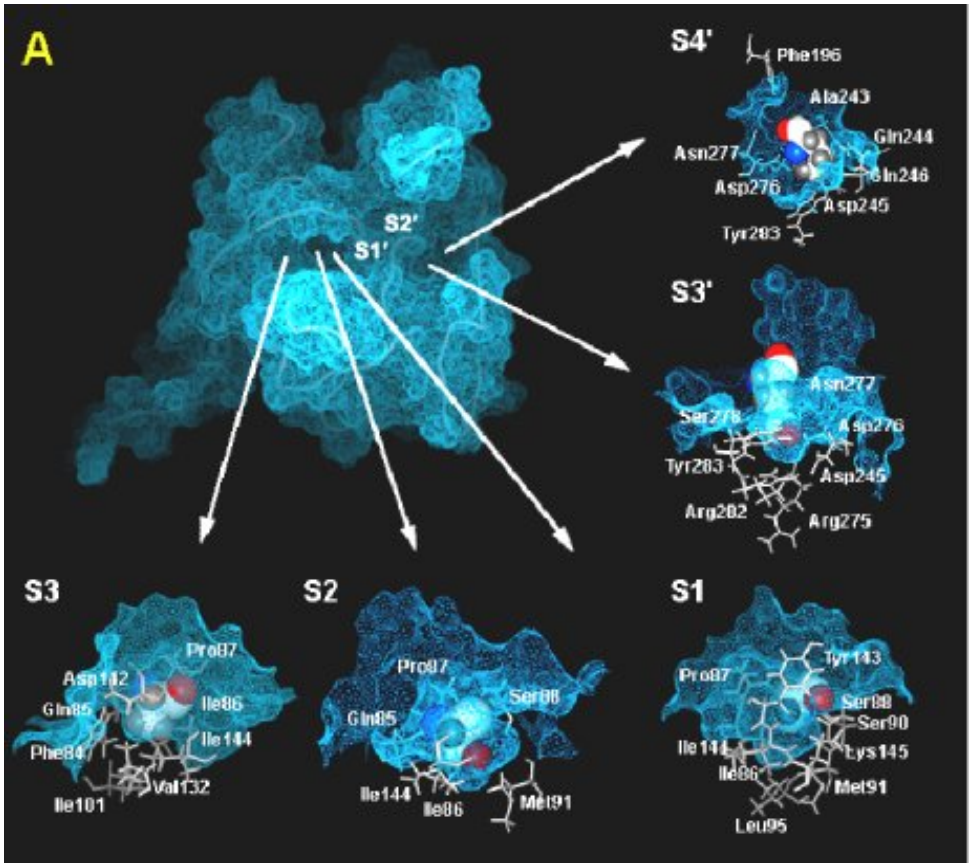

Figure 1.5: *E. coli* SPase substrate-binding site. The top view of the molecular surface of the SPase binding site (coloured blue) with Cα trace of the SPase (blue lines). The pockets accommodating signal peptide side chains are shown in detail in the surrounding views and numbered according to their position along the peptide from the S1 pocket containing the nucleophile Ser90 [reproduced from (Choo *et al.*, 2008) under CCL].

not identified by NMR since Pro residues do not have NH-CaH correlations. In addition, one other residue remained unidentified in NMR, which Musial-Siwek and co-workers (2008b), believe to be Phe84 or Tyr143. The S2 subsite, which comprises residues Gln85, Ile86, Pro87, Ser88, Met91 and Ile144, constitutes the deepest cavity within the substrate binding site and largely overlaps with S1 due to a pronounced backbone twist in the P3 to P1' binding conformation of the precursor protein. Notably, the modelling studies by Choo and co-workers (2008) showed that the P2 side chain is not solvent-exposed as believed earlier (Paetzel *et al.*, 2000), but is completely buried at this location (S2) due to the twist in the P3 to P1' binding conformation which is in agreement with recent data (Luo *et al.*, 2009). This pocket can accommodate residues with large side chains and appears to play an important role in substrate specificity of *E. coli* type I SPase. The S3 subsite, also predominantly hydrophobic in nature, is composed of non-polar atoms from residues Phe84, Gln85, Ile86, Pro87, Ile101, Val132, Ile144 and Cβ of Asp142 and is located diagonally across from the S1 site (Choo *et al.*, 2008). The S3 pocket constitutes the third deepest cavity and can accommodate a wide variety of side chains consistent with the observation that larger residues can occur at the P3 (-3) than at the P1 (-1) position of the substrate (Nielsen *et al.*, 1997). The S4 subsite consists of Phe84, Gln85, Pro87 and Asp142, which are in contact with P4 of the substrate. Collectively, the modelling data by Choo and co-workers (2008) showed that the bound precursor protein makes significant contact with *E. coli* LepB from S7 to S6'. More importantly, the side chains of P1' to P5' residues of the mature moiety are in position to make significant contacts with *E. coli* LepB, implying that both signal and mature moiety sequences play a direct role in catalysis. The NMR data also showed the involvement of three additional residues Ile80, Glu82 (residing in the S7 pocket proposed by Choo and co-workers, 2008) and Gly109 that suggests interaction of the SPase with the C-terminus of the hydrophobic core region of the peptide.

In addition, an analysis of the side chain orientation in the P3-P1' segment of the preprotein in the active site region the SPase showed the pattern ↓↓↓· (where ↓ represents a side chain oriented towards the binding site and · represents a side chain oriented away or across the binding site) supporting the stringent selectivity criteria in the P3, P2 and P1 regions and the observed variability in P1' (Choo *et al.*, 2008).

1.3.6 Proposed mechanism of catalysis

A mechanism of catalysis for preprotein cleavage by *E. coli* LepB was proposed based on the crystal structure, modelling and other biochemical data (Paetzel *et al.*, 2000) and is in agreement with currently available data. First, the signal peptide binds to the SPase with the P1 to P4 residues in an extended β-conformation, forming hydrogen bonds with the β-strand containing Lys145 (Fig. 1.6). The residues P1 and P3 of the substrate reside in the hydrophobic S1 and S3 substrate-binding pockets. Upon binding of the preprotein substrate, the neutral Lys145 ε-amino group, oriented by the O^{γ} Ser278 abstracts a proton from the side-chain hydroxyl of Ser90, activating the Ser90 O^{γ} for nucleophilic attack on the carbonyl (*si*-face) of the scissile peptide bond (*i.e.* the SPase cleavage site). A tetrahedral intermediate is formed which is electrostatically stabilized by hydrogen bonds to the oxyanion hole, formed by the Ser90 main-chain amide and the Ser88 side-chain hydroxyl group. Next, the ammonium group from the side chain of Lys145 would then donate a proton to the leaving group amide (*i.e.* the N-terminus of the mature protein).

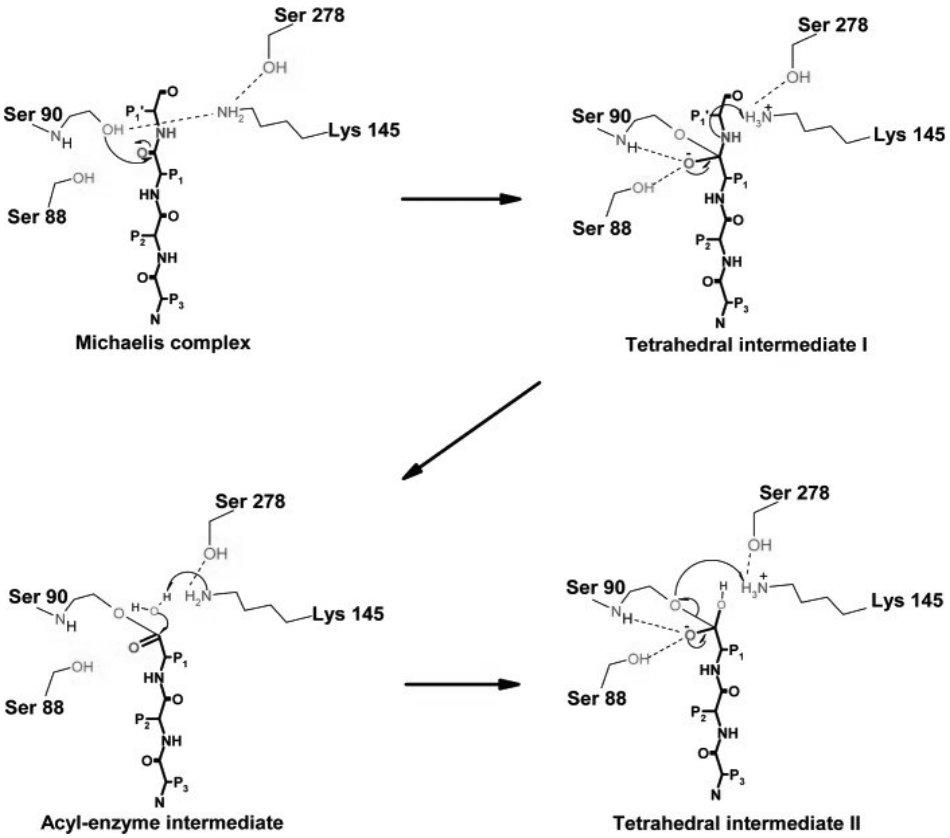

Figure 1.6: Proposed catalytic mechanism of bacterial SPasesI. The reaction proceeds through an oxyanion tetrahedral intermediate followed by the loss of the mature domain of the substrate, resulting in an acyl-signal peptide enzyme intermediate. The acyl-enzyme intermediate is attacked by a water molecule, releasing the cleaved signal peptide and the free enzyme [reprinted with permission from Paetzel *et al.*, 2002b. Copyright 2002 American Chemical Society].

This releases the mature protein from the SPase and a signal peptide-bound acyl-enzyme intermediate is formed. The deacylating water then loses its proton to the Lys145 general base and the hydroxyl group attacks the ester carbonyl to produce another tetrahedral intermediate. This then breaks down to release the signal peptide, regenerating the SPase active site.

1.4 The type I signal peptidases as drug targets

Type I signal peptidases were proposed as novel antibiotic targets (Black & Bruton, 1998; Paetzel *et al.*, 2000) as they fulfill certain basic criteria. Firstly, SPasesI are ubiquitous in all bacteria with the exception of *Mycoplasma genitalium* (Dalbey *et al.*, 1997; Fraser *et al.*, 1995). However, it is interesting to note that in the related organism *M. pneumoniae*, SPaseI-like activity has been demonstrated despite the absence of a gene encoding SPaseI (Catrein *et al.*, 2005). Secondly, SPaseI activity is essential for cell viability (Dalbey & Wickner, 1985; Date, 1983) as inhibition of SPaseI activity leads to accumulation of secretory proteins in the cell membrane and eventual cell death (Koshland *et al.*, 1982). Temperature-sensitive *E. coli* strains IT89/IT41 (Inada *et al.*, 1989) with an amber mutation in the *lepB* gene (Cregg *et al.*, 1996), show accumulation of preproteins and reduced growth rate at the nonpermissive temperature of 42 °C. These temperature-sensitive mutant strains have been used to confirm the essential function of SPases from several bacteria including human pathogens such as *Staphylocccus aureus* (Cregg *et al.*, 1996), *S. epidermidis* (Bockstael *et al.*, 2009b), *Streptococcus pneumoniae* (Zhang *et al.*, 1997), *Salmonella* Typhimurium (van Dijl *et al.*, 1990), *Legionella pneumophila* (Lammertyn *et al.*, 2004), *Rickettsia rickettsii and R. typhi* (Rahman *et al.*, 2003). Thirdly, targeting the bacterial SPasesI is likely to limit toxicity to humans due to the differences in structure, localisation and possibly catalytic mechanism from that of the eukaryotic SPases. The bacterial SPases are believed to be monomeric, located at the cytoplasmic membrane surface with their active site on the outer leaflet making it relatively accessible to potential inhibitors and operate by a Ser-Lys catalytic dyad mechanism. The eukaryotic SPases are multimeric, and have their active-site region located in the mitochondrial inner-membrane space (mitochondrial Imp1 and Imp2 SPases) or in the ER lumen (ER signal peptidase complex). In the latter case, Lys is not used as a general base (Paetzel *et al.*, 2002b). Further, the *si*-face attack of the substrate scissile amide carbonyl by the SPasesI, rather than the *re*-face observed in all serine-dependent hydrolases, also enables selective

inhibition. Additionally, targeting the SPases debilitates certain bacterial defences, increases susceptibility to antibiotics and potentially facilitates clearance by the human immune system. For instance, in the food-borne pathogen *Listeria monocytogenes*, deletion of one of the three SPase-encoding genes, *sipZ*, impaired secretion of the virulence factors such as listeriolysin O and phospholipase C and rendered it almost avirulent (Bonnemain *et al.*, 2004). A few examples of SPase I-dependent proteins important in this respect are: β-lactamases that confer resistance to β-lactam antibiotics, pertussis toxin from *Bordetella pertussis*, HMW1 adhesin of *Haemophilus influenzae*, pyelonephritis-associated pili (Pap) important for pathogenesis in uropathogenic *E. coli* strains and IgA protease from *Neisseria gonorrhoeae*.

1.5 Inhibitors of the type I SPases and their antibacterial activity

As mentioned earlier, SPasesI are resistant to general protease inhibitors. On the other hand apparently, very few SPase molecules per cell need to be fully active for *E. coli* cells to divide and grow, at least at 30 °C in a non-stressed environment (Cregg *et al.*, 1996). Therefore finding potent SPase inhibitors with effective antibacterial activities is considered a challenging task. Initial studies showed that *E. coli* LepB activity is adversely affected by high concentration of sodium chloride (> 160 mM), magnesium chloride (1 mM) and dinitrophenol (Zwizinski *et al.*, 1981) and since then, a few effective inhibitors have been identified as described below.

1.5.1 Peptide and protein inhibitors

The studies involving this type of inhibitors were the first to provide substantial basic information about the SPasesI. For example, *in vitro* inhibition of the cleavage of M13 procoat and maltose binding protein (MBP) in the presence of a synthetic leader peptide comprising of 23 residues preceding the M13 bacteriophage procoat-cleavage site demonstrated that signal peptides could competitively inhibit SPaseI and that leader peptide is indeed the primary region of substrate recognition by the signal peptidase (Wickner *et al.*, 1987). Preproteins or synthetic peptide substrates with Pro at +1 position (the first residue in the mature part of the protein) remain uncleaved and competitively inhibit the activity of *E coli* LepB *in vivo*, rendering an impaired growth to the cells (Barkocy-Gallagher & Bassford, 1992; Nilsson & von Heijne, 1992). This feature is also common with proteases in general as they are unable to cleave an X-Pro bond. However, attempts to find effective peptide inhibitors using the classical approach were not

successful until the approach was applied to lipopeptide inhibitors. Interestingly, an antimicrobial peptide derivative of flesh fruit fly resembling a natural signal sequence was found to competitively inhibit SPaseI (Kaderbhai *et al.*, 2008). The protease-resistant peptide (D)-KLKL$_6$KLK has an IC_{50} of 50 μM against LepB and MIC of 16 μM against *E. coli* with bactericidal activity also against Gram-positive pathogens (Table 1.2).

1.5.2 β-lactam type inhibitors

The β-lactam analogs, monocyclic azetidinones, were the first (but not very potent) non-peptide inhibitors reported to inhibit *E. coli* LepB in a pH- and time-dependent manner (Kuo *et al.*, 1993). 5S penem stereoisomers were the first potent irreversible inhibitors identified along with a few other weak inhibitors including clavam and clavem systems (Black & Bruton, 1998). The compound allyl (5*S*,6*S*)-6-[(*R*)-acetoxyethyl] penem-3-carboxylate (Figure 1.7) inhibits SPaseI activity of both *E. coli* LepB (IC_{50}=0.38 μM) and *S. aureus* SpsB, completely blocks the processing of β-lactamase protein by the leader peptidase of an *E. coli* ESS strain which has a leaky outer membrane (Black & Bruton, 1998) and was also used for co-crystallization of the Δ2-75 SPase (Paetzel *et al.*, 1998). The co-crystal structure revealed that the side-chain methyl group (C16) of the penem, previously reported to be essential for the effectiveness of the inhibitor, was located in the SPase substrate-binding pocket (S1), probably mimicking the P1 (-1) (Ala) side chain of the substrate. In addition the co-crystal structure also showed that the inhibitor acts via acylation of the active-site serine. Unfortunately, penem inhibitors have poor antibacterial activity against some of the clinically more relevant strains, which might be explained by low compound penetration across the bacterial wall and compound instability. Recently, the synthesis of the 5*S*-penem was described and as with the parent penem, no significant antibacterial activity was observed against *S. aureus* and *E. coli*. Interestingly moderate activity was observed against *S epidermidis* (Harris *et al.*, 2009). In addition, carbamate-derivatized penems moderately inhibited MRSA (Table 1.2).

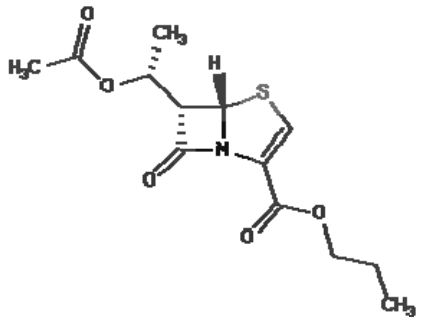

Figure 1.7: Structure of (5S,6S)-6-[(R)acetoxyeth-2-yl]-penem-3-carboxylatepropane [PDB ID: 1PN (Paetzel *et al.*, 1998)]

Furthermore, (5S)-tricyclic penems with a third heterocyclic ring fused to the C2 and C3 positions of the (5S,6S)-6-[(R)-hydroxyethyl]-penem core have an increased potency with IC_{50} values of 0.2 μM and 5 μM against *E. coli* and methicillin-resistant *Staphylococcus aureus* (MRSA) SPases, respectively (Hu *et al.*, 2003). This higher *in vitro* potency is predicted to be likely due to additional binding features, as observed by molecular modelling. In these studies, tricyclic penem was found to extend into the S3-binding pocket of the SPase. Again, the antibacterial activity of the tricyclic penems on whole cells was poor, possibly because of instability of the compound.

1.5.3 Natural and synthetic lipopeptides (arylomycins) and lipoglycopeptide inhibitors

Arylomycins A and B were identified as new biaryl-bridged lipopeptide antibiotics produced by *Streptomyces* sp. Tü 6075 (Schimana *et al.*, 2002) and classified as secondary metabolites synthesized by non-ribosomal peptide synthesis. Their antibiotic property was subsequently attributed to their ability to inhibit SPasesI. Arylomycins are lipohexapeptides with the sequence D-*N*-MeSer-D-Ala-Gly-L-*N*-MeHpg-L-Ala-L-Tyr, cyclised by a [3,3] biaryl bond between MeHpg and Tyr (in the colourless arylomycin A, or a nitro-substituted Tyr in the yellow-coloured arylomycin B series) and with a C11-15 branched fatty acid attached via an amide bond to the amino terminus (Holtzel *et al.*, 2002). Molecules belonging to the arylomycin B series have significantly higher antibacterial activities compared to arylomycins of the A series suggesting that the nitro substitution and the length of the fatty-acid side chain influences the activity (Schimana *et al.*, 2002).

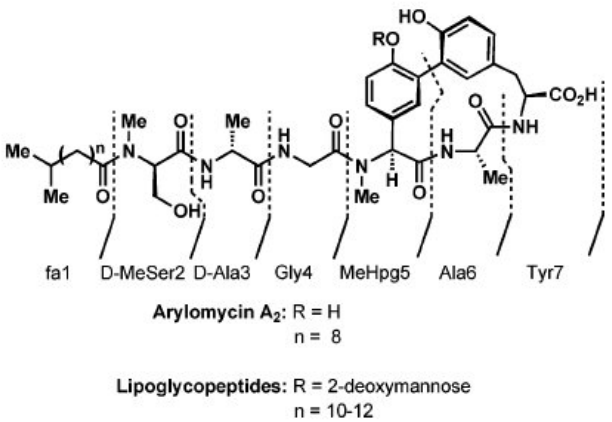

Figure 1.8: Structures of arylomycin A2 and lipoglycopeptide inhibitors of the SPasesI [reprinted with permission from Roberts *et al.*, 2007. Copyright 2007 American Chemical Society].

Arylomycin A_2 (Figure 1.8) binds non-covalently to the active site of *E. coli* SPase in a two-step binding mechanism as revealed by the co-crystal structure (Paetzel *et al.*, 2004). The structure shows the COOH-terminal biaryl-bridged end of the inhibitor pointing to

the active site and making parallel β-sheet interactions with the two β-strands lining the SPase-binding site. Further, the carboxylate oxygen atom (O45) of arylomycin A_2 positions in the active site such that it makes hydrogen bond interactions with each of the catalytic residues of LepB: the nucleophile Ser90, the general base Lys145 and the oxyanion hole Ser88. The L-Ala methyl side chain (C30) of arylomycin A_2 sits in the proposed S3-binding pocket and the D-Ala methyl side chain of the inhibitor points to a shallow pocket that might represent the S5-binding pocket of the enzyme. Interestingly, the recent structure of Δ2-75 SPase in ternary complex with arylomycin A_2 and a morpholino-β-sultam derivative (BAL0019193) revealed SPase inhibition by the two compounds at the same time via binding to non-overlapping subsites near the catalytic center (Luo *et al.*, 2009). The ternary structure provides a detailed structural information on the binding mode of arylomycin A_2, with electron density for the complete arylomycin A_2 including the 12-carbon fatty acid of arylomycin. The latter observation is in agreement with the accumulating evidence that the fatty acid chain is important for effective SPase inhibitors / synthetic substrates, as discussed later. The methylene groups of fatty acid make van der Waals interactions with part of a large hydrophobic surface with in the region of the predicted membrane-association surface of the SPase. β-Sultams are reactive sulfonyl analogues of β-lactams that inactivate serine enzymes by sulfonylation of the active-site Ser (Page, 2004). Remarkably, the β-sultam inhibitor in the ternary complex with SPase was bound non-covalently above the active site of the SPase, taking a parallel orientation relative to the biaryl ring moiety of arylomycin A_2. The β-sultam inhibitor possibly acts by displacing a water molecule that is coordinated to the catalytic Lys145, proposed to function as the deacylating water in catalysis. This mechanism of inhibition is different from the action

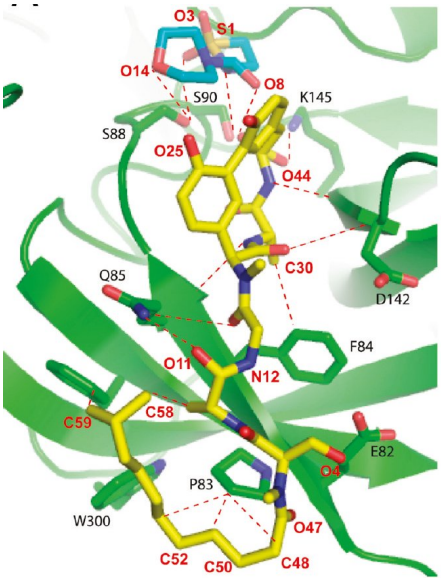

Figure 1.9: Overall binding theme of arylomycin A_2 and BAL0019193 inhibitors. SPase I is in ribbon representation (green). Inhibitor arylomycin A_2 is represented as stick and coloured by element (Carbon, yellow; nitrogen, blue; oxygen, red). Inhibitor BAL0019193 is represented as a stick and coloured by element (carbon, cyan; nitrogen, blue; oxygen, red) [reprinted with permission from Luo *et al.*, 2009. Copyright 2009 American Chemical Society].

mechanism used by β-sultams to inhibit β-lactamases and D,D-peptidases, which also use Ser/Lys catalytic activation (Luo *et al.*, 2009). The structural data showing that SPase can be inhibited by two separate inhibitors at the same time (Figure 1.9), provide excellent possibilities for rational drug design.

Lipoglycopeptides are a group of natural compounds that inhibit SPaseI, isolated from *Streptomyces* spp., (Kulanthaivel *et al.*, 2004). Also classified as secondary metabolites, these lipoglycopeptides share the core structural features of arylomycins but contain a 2-deoxymannose sugar unit in the macrocycle and have a longer (up to five carbon) fatty-acid tail (Figure 1.8). These compounds are potent inhibitors of SPases of *E. coli* and *S. pneumoniae* with modest antibacterial activity against a panel of pathogens (see Table 1.2). The compounds also block the protein secretion in whole cells as demonstrated by the inhibition of β-lactamase release from *S. aureus*. It was observed that the lipoglycopeptides as well as the β-lactam inhibitor 5*S*,6*S*-penem are more potent against the Gram-negative *E. coli* SPase than the Gram-positive *S. pneumoniae* SPase, possibly reflecting on difference in the structure of these enzymes (Kulanthaivel *et al.*, 2004). In addition, while a good correlation exists between IC_{50} and MIC values in *S. pneumoniae*, the MIC values were much higher (with respect to the IC_{50}) in *E. coli* and *H. influenzae*, possibly due to the additional outer membrane barrier that is present in Gram-negative bacteria.

Furthermore, the synthesis of arylomycin A_2 was reported along with the effect imparted by the three main modifications: N-methylation, glycosylation and lipidation (common to arylomycins and the related lipoglycopeptides) on biological activity (Roberts *et al.*, 2007). The synthetic arylomycin A_2 was found to inhibit the polymyxin B nonapeptide-permeabilized *E. coli* strain MG 1655 at high concentrations (MIC of 128 μM) but had no effect on non-permeabilized cells. Roberts and co-workers (2007) observed that arylomycin A_2 does not inhibit *S. aureus* (up to 128 μM) but remarkably it is highly potent against *S. epidermidis* (MIC of 1 μM). Additionally, it was observed that while glycosylation appeared less critical, fatty acid chain length and N-methylation influenced biological activity but varied depending on the species. Interestingly, Roberts *et al.*, 2007, compared the biological activity of synthetic arylomycin A_2 and its derivative with a longer fatty acid chain and found that the longer fatty acid chain increased biological activity on *S. aureus*. The antibacterial activity of arylomycin A_2 was also extended to its possible use on *S.*

Table 1.2: Inhibitors of the bacterial type I signal peptidases with their *in vitro* and *in vivo* activities

	Inhibitor	*SPase*	*IC_{50}*	*Micro-organism*	*MIC*	*Reference*
Peptide						
1	(D)-KLKL$_6$KLK-NH$_2$	LepB	30 μM	*E. coli*	16 μM	(Kaderbhai *et al.*, 2008)
				*E. coli**	4.8 μM	
			*ND	*S. aureus*	8 μM	
			*ND	*H. influenzae*	>64 μM	
			*ND	*S. pneumoniae*	4.8 μM	
β-lactam type						
2	Allyl (5S,6S)-6-[(R)-acetoxyethyl] penem-3-carboxylate	LepB	0.38 μM	*E .coli*	*ND	(Black & Bruton, 1998)
3	(5S,6S)-6-[(R)-hydroxyethyl] penem core with a C3 *p*-nitrobenzyl protected carboxylic acid		*ND	*E .coli**	≥200 μg/ml	(Harris *et al.*, 2009)
			*ND	*S. aureus**	≥200 μg/ml	
			*ND	*S. epidermidis*	50 μg/ml	
4	Carbamate-derivatized penem		*ND	MRSA	100 μg/ml	
5	(5S)-tricyclic penem	LepB	0.2 μM	*E. coli*	*ND	(Hu *et al.*, 2003)
		SpsB	5 μM	*S. aureus* (MRSA)	>128 μg/ml	
Lipoglycopeptide						
6	Natural lipoglycopeptides	LepB	0.11-0.19 μM	*E. coli*	4-8 μM	(Kulanthaivel *et al.*, 2004)
		Spi	2.4-24.9 μM	*S. pneumoniae*	8-64 μM	
			*ND	*S. aureus*	32-64 μM	
			*ND	*H. influenzae*	64-64 μM	
Lipopeptide *(natural/ synthetic)*						
7	Arylomycin A$_2$		*ND	*E. coli*	>128 μM	(Roberts *et al.*, 2007)
				*E. coli**	128 μM	
		SpsB	(1 μM)	*S. aureus*	>128 μM	
		-	*ND	*S. epidermidis*	1 μM	
Lipopeptide *(rationally designed)*						
8	Decanoyl-LTPTAKAPSKIDD-OH	SpsB	0.6 μM	*S. aureus*	*ND	(Bruton *et al.*, 2003)
9	Decanoyl-LTPTANA-α-ketoamide analogs	SpsB	0.1-16 μM	*S. aureus*	*ND	
10	Decanoyl-PTANA-aldehyde	SpsB	0.09 μM	*S. aureus*	125 μg/ml	(Buzder-Lantos *et al.*, 2009)
		LepB	13.4 μM	*E. coli*	>500 μg/ml	

*ND, not determined.

epidermidis biofilms as observed by a dose-dependent reduction in cell viability (Bockstael *et al.*, 2009b).

1.5.4 Rationally designed lipopeptide inhibitors

Compounds designed on the basis of preprotein sequence data in *S. aureus*, incorporating key structural features of a signal sequence namely a membrane anchor, a helix terminus or turn motif and the AXA cassette led to the identification of highly effective synthetic substrates and inhibitors of SpsB (Bruton *et al.*, 2003). Bruton and co-workers (2003) confirmed that SpsB could be inhibited in a classical manner by either incorporation of a proline at P1' or by introducing a serine trap (α-ketoamides) at the cleavage site of a lipopeptide substrate to obtain competitive or time-dependent inhibitors, respectively (Table 1.2). A competitive inhibitor described by Bruton co-workers (2003) was used as a lead compound to optimize the minimum length required for effective inhibition and to confirm that the fatty acid chain is essential for activity (Buzder-Lantos *et al.*, 2009). Reducing the length of the core lipopeptide by eliminating amino acids from both termini and conversion of the peptide (with the C-terminal carboxylic acid) to an aldehyde resulted in an improved potency against SPases of *S. aureus* and *E. coli* (Table 1.2). On the other hand, the lipopeptide aldehyde had no significant antibacterial activity.

The amino-terminal fatty acid in the inhibitor appears to be critical for both *in vitro* and *in vivo* activity against *S. aureus* SpsB and *E. coli* LepB. A direct association between the fatty acid with the SPase was also observed in the recent crystal structure of *E. coli* LepB (Luo *et al.*, 2009). Additionally, previous attempts at developing peptide inhibitors using the classical approach were not effective, most likely due to the absence of the fatty acid. Although, the reason for this is still unclear, it is presumed that the amino-terminal fatty acid might aid in orientating the inhibitor/substrate appropriately in the binding cleft of the enzyme by mimicking the hydrophobic region of the signal peptide of preproteins. Another hypothesis is that the fatty acid in the inhibitor probably helps in partitioning into the hydrophobic part of the detergent milieu on which the signal peptidase is likely to be present as even the soluble derivatives are detergent-dependent. With regard to their potential use as drugs, however, this requirement might give them a slight disadvantage over small molecule inhibitors.

In general, a lack of correlation between signal peptidase inhibition and MICs observed for different compounds on different bacterial cells has been observed, which is unlikely due to a single factor. The possible reasons for disparities in the biochemical and whole cell assays include (a) the problem of penetration of the

compound in order to reach the target, (b) compound stability *in vivo* or modifications as a result of exposure to cellular enzymes and (c) the presence of an additional selective permeability barrier (the outer membrane) in Gram-negative bacteria which hinders accessibility to the target. In the case of lipopeptide aldehyde and arylomycin inhibitors, a high concentration of the compounds is needed to inhibit *S. aureus* in contrast to their high *in vitro* potency against SpsB. This suggests that additional factors such as those mentioned above (see a & b) also may play a role in a compounds biological activity.

1.6 *Staphylococcus aureus*

1.6.1 Microbiology

Staphylococcus aureus belongs to the genus *Staphylococci*, comprising of Gram-positive, non-spore forming, non-motile, catalase-positive, spherical bacteria of approximately 1 μM in diameter. *Staphylococci* appear as grape-like clusters when viewed under a microscope (Figure 1.10) because cell division takes place in more than one plane. *Staphylococci* are facultative anaerobes capable of generating energy by aerobic respiration and by fermentation which yields mainly lactic acid. Another feature of the genus is the cell wall peptidoglycan structure that contains pentaglycine residues in the cross-bridge in the cell wall peptidoglycan, which causes susceptibility to lysostaphin (Plata *et al.*, 2009). *S. aureus* produces coagulase, which interacts with prothrombin in the blood causing plasma to coagulate by converting fibrinogen to fibrin. Plasma coagulation is used to distinguish *S. aureus* from other members of the genus which are collectively called coagulase-negative staphylococci. On a rich medium, *S. aureus* forms medium-size "golden colonies". The golden pigmentation of the *S. aureus* colonies (also the etymological root of the name; 'aureus' meaning 'golden' in Latin) is caused by the presence of carotenoids and is reported to be a virulence factor protecting the pathogen against oxidants produced by the immune system (Plata *et al.*, 2009).

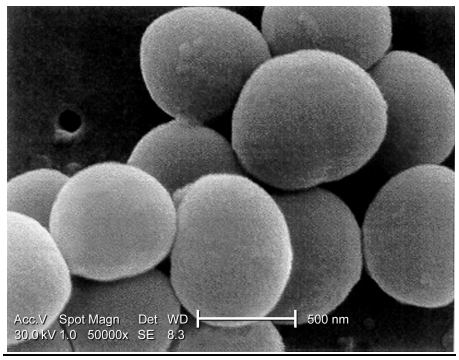

Figure 1.10: Scanning electron micrograph (SEM) showing clumps of *S. aureus* at 50,000x magnification (Source: CDC, PHIL).

1.6.2 Infections

S. aureus is both a commensal and a pathogen. It can colonize the skin and moist squamous epithelium of anterior nares of individuals. At least 20 % of the population is permanently colonized by *S. aureus*, 60 % are intermittent carriers and 20 % never carry the organism (Foster, 2004). Colonization significantly increases the risk of infection since it provides a reservoir of the pathogen from which the bacteria can be introduced when the host immune system is compromised (Kluytmans *et al.*, 1997). *S. aureus* is responsible for a plethora of medical problems (Casey *et al.*, 2007; Plata *et al.*, 2009). The most common infections are those of skin and soft tissues, including cellulitis, impetigo and soft tissue abscesses, the latter being common in diabetic patients. *S. aureus* is one of the main causes of serious hospital- and community-acquired infections. It is a common cause of surgical site infections (SSIs), bone and joint infections such as acute and vertebral osteomyelitis often acquired as a result of contamination during surgery. It is also a cause of difficult-to-treat infections of catheters and other devices due to its propensity to form biofilms (Fitzpatrick *et al.*, 2005). *S. aureus* is also the most common cause of hospital-acquired bacteraemia. A leading cause of haemodialytic bacteraemia, *S. aureus* causes significant morbidity and mortality among renal patients. It is also a major cause of endocarditis, another serious deep-seated infection. Ventilator-associated *S. aureus* pneumonia, although uncommon, is associated with high mortality rates. In addition it is also responsible for toxin-mediated diseases such as toxic shock syndrome, scalded skin syndrome and staphylococcal food-borne diseases. In short, *S. aureus* is capable of causing a wide range of serious infections with morbidity and mortality rates of up to 64 % depending on the site of infection and the susceptibility of the particular strain (Casey *et al.*, 2007). The pathogenesis of *S. aureus* reflects on its ability to evade the immune system (Foster, 2005), to produce a wide array of virulence factors/toxins, to attach firmly to prosthetic material by production of a glycocalyx and an extraordinary capability of developing antimicrobial resistance.

1.6.3 Drug resistance

S. aureus is a problematic pathogen due to its remarkable ability to develop resistance to antibiotics. Believed to be naturally susceptible to the majority of antibiotics that has ever been developed, *S. aureus* has been highly successful in acquiring resistance through horizontal transfer of genes from outside sources, chromosomal mutations and antibiotic selection (Chambers & Deleo, 2009) (Figure 1.11). Back in 1928, Sir Alexander Fleming's

chance observation of the susceptibility of *S. aureus* to a substance from a contaminating mould led to the discovery of penicillin and marked the beginning of the 'antibiotic era'. The optimism of treatment with this miracle drug was dampened only a few years after its use in clinical practice, when penicillin-resistant strains began to emerge. These strains produced a plasmid-encoded penicillinase, which hydrolyses the β-lactam ring of penicillin that is essential for its antimicrobial activity. Emergence of antibiotic resistance in *S. aureus* since then has been depicted as a series of waves (Chambers & Deleo, 2009) (Fig. 1.11). Wave 1, which started after the introduction of penicillin into clinical practice in the 1940s, continues today. The first pandemic antibiotic (penicillin)-resistant strain is from the lineage known as phage type 80/81, which disappeared after the introduction of methicillin, an antibiotic from the same class but resistant to penicillinase. A second wave of resistance (wave 2) followed shortly after the introduction of methicillin.

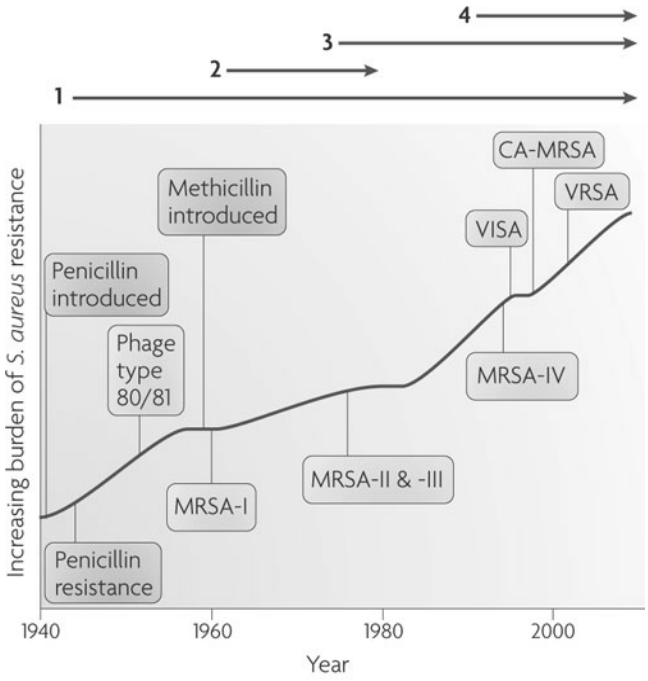

Figure 1.11: The four waves of antibiotic resistance in *S. aureus* (see text) [reprinted by permission from Macmillan Publishers Ltd: *Nature Reviews Microbiology* (Chambers & Deleo, 2009), copyright (2009)].

Methicillin-resistant *Staphylococcus aureus* (MRSA) containing a large mobile genetic element called staphylococcal cassette chromosome, *mec* I (SCC*mec*), indicated as MRSA-I in Fig. 1.11, was isolated. It carries a *mecA* gene that codes for an alternative penicillin-binding protein, PBP2a, with low affinity to the entire β-lactam class of antibiotics including penicillins, cephalosporins and carbapenems in contrast to the narrow spectrum activity of penicillinase-mediated resistance. Wave 2 lasted until the 1970s in the form of the Iberian clone. Wave 3 began in the mid to late 1970s with the emergence of new MRSA strains, containing new SCC*mec* allotypes, SCC*mec*II and SCC*mec*III (MRSA-II and MRSA-III) marking the ongoing worldwide pandemic MRSA in hospitals and healthcare facilities. The increasing burden of MRSA infections in

hospitals led to an increase in the use of vancomycin (a glycopeptide antibiotic), the drug of "last-resort" against MRSA. The increased selective pressure resulted in the emergence of vancomycin-intermediate *S. aureus* (VISA) strains that are not inhibited *in vitro* at vancomycin concentrations below 4-8 μg/ml. Wave 4 began in the mid to late 1990s and marks the emergence of MRSA strains in communities. Community-associated MRSA (CA-MRSA) strains, unrelated to hospital strains were susceptible to most antibiotics other than β-lactams and contained a new, smaller, more mobile SCC*mec* allotype, SCC*mec*IV (MRSA-IV) and various virulence factors. A small number of vancomycin-resistant *S. aureus* (VRSA) strains have been isolated (first in 2002) exclusively in healthcare settings. A recent study estimated that more people die from MRSA bacteria than from HIV in the United States (Payne, 2008) emphasizing the need for new drugs against this pathogen.

1.6.4 Novel approaches for finding new drugs

Historically, most antibiotics have come from a small subset of molecular scaffolds whose functional lifetimes have been extended by generations of synthetic tailoring (Fischbach & Walsh, 2009). The need for identifying new structural classes/scaffolds of compounds has led to two main approaches for finding antibacterials which are target-based or whole-cell-based testing of compounds in large scale. In *S. aureus*, whole genome sequence information is available for nine strains (Sibbald *et al.*, 2006) including those from two clinical strains, isolated from distinct clinical settings representing hospital- and community-acquired MRSA (Holden *et al.*, 2004). The genome sequence information continues to facilitate the identification of genes involved in virulence, drug-resistance and for survival. Several potential targets have been proposed in *S. aureus* (Garcia-Lara *et al.*, 2005; Ohlsen & Lorenz, 2007). Many novel targets have been identified and validated in *S. aureus* using molecular genetic tools (Xia *et al.*, 1999; Zhang *et al.*, 2000; Ji *et al.*, 2001; Forsyth *et al.* ,2002; Yin and Ji, 2002; Chaudhuri *et al.*, 2009). The future seems to hold some promise, as the growing challenge has led to the identification of a few interesting antibacterial drug candidates with novel mechanisms of action and a few emerging targets as well (Devasahayam *et al.*, 2010; Fischbach & Walsh, 2009).

1.7 Aim of this work

In *S. aureus* two genes designated *spsA* and *spsB* were identified encoding homologues of SPaseI of which only the latter was shown to be essential (Cregg *et al.*, 1996). SpsB

(signal peptidase from *Staphylococcus*) has also been functionally expressed in *E. coli* and is able to process *E. coli* preproteins *in vivo* (Cregg *et al.*, 1996). It was predicted that SpsA is an inactive SPase homologue as it lacks the conserved catalytic residues. The crystal structure of SpsB is not available. Nevertheless, a few substrates (for *in vitro* activity assays) and inhibitors have been described in literature. Despite its potential attractiveness as an antibiotic target no biochemical data were previously available on SpsB. The aim of this work was to characterize the enzyme SpsB in view of its potential use as a drug target, to develop and validate *in vitro* systems for screening of inhibitors and finally screen compounds in order to find SPase inhibitors. To realize this, the following steps were undertaken:

- Isolation, purification and functional analysis of *S. aureus* SpsB (Chapter 2)
- Biochemical characterization of SpsB (Chapter 3)
- Development and validation of *in vitro* inhibition assays for SpsB (Chapter 4)
- High-throughput screening of compounds against SpsB and analysis of potential hits (Chapter 5)

Chapter 2: Isolation, purification and functional analysis of *S. aureus* SpsB

In this chapter, we describe the purification of full-length and truncated SpsB derivatives of *S. aureus* and their functional characterization. In order to find out the effect of removal of the hydrophobic transmembrane segment at the N-terminus of the enzyme (the catalytic domain being located at the C-terminus), a truncated derivative of SpsB was designed and purified. Another truncated derivative, identical in sequence to the one mentioned above except for a point-mutation replacing the catalytic Ser with Ala, was purified. This truncated active-site mutant was designed for another study (crystallization trials) and was used in this work as a negative control in the activity assay described in chapter 3. A predicted native substrate of SpsB, Immunodominant staphylococcal antigen A precursor (pre-IsaA) was also isolated and purified for demonstration of *in vitro* activity of the purified SpsB.

2.1 Results

2.1.1 Cloning and purification of the full-length SpsB and the IsaA precursor

The gene encoding SpsB was amplified by PCR using primers which were designed to incorporate the following modifications: the incorporation of an *Nde*I and an *Eco*RI restriction site at the 5' and 3' end, respectively and a hexa-histidine-encoding sequence for obtaining a His-tag at the N-terminus of the produced protein to facilitate purification. The fragment of expected size and correct sequence of *spsB* was cloned after the T7 promoter in the pET-3a plasmid. The full-length SpsB (predicted MW=22.5 kDa, including the hexa-his tag) was purified from *E. coli* BL21(DE3)pLysS harbouring the plasmid pET-fl-SpsB and analyzed by SDS-PAGE. The purification of the full-length SpsB normally yielded samples of sufficient purity (>95 %) and concentration (~30-40 μM) for functional characterization (Figure 2.1a). The gene encoding pre-IsaA was amplified by PCR using oligos that were also designed to incorporate *Nco*I and *Eco*RI restriction sites and sequences encoding a hexa-histidine tag and a c-Myc tag at the N- and C-terminal end of the expressed protein, respectively. The c-Myc tag was included to facilitate immunodetection of the protein. The gene, after confirming the correct sequence, was cloned in pET-23d and expressed in *E. coli* BL21(DE3)pLysS. Pre-IsaA

(predicted MW=26.2 kDa, including hexa-his and c-Myc tag) was purified, refolded and used in the *in vitro* assay after analysis by SDS-PAGE (Figure 2.1b).

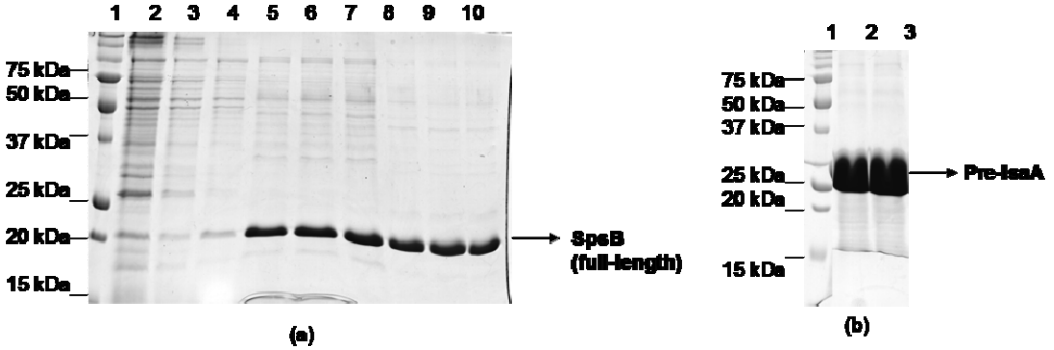

Figure 2.1: **Purified SpsB and IsaA on gel.** The N-terminally hexa-his-tagged proteins were overproduced in *E. coli*, purified by Ni^{2+} affinity chromatography and analyzed by SDS-PAGE followed by CBB staining. (a) SpsB purified under native conditions. Lane 1, molecular weight marker; Lane 2, flow through; Lanes 3 & 4, column wash with buffer containing 10 and 20 mM imidazole respectively; Lanes 5 to 7, elution fractions in buffer containing 100 mM imidazole; Lanes 8 to 10, elution fractions in buffer containing 250 mM imidazole. (b) Pre-IsaA purified under denaturing conditions. Lane 1, molecular weight marker; Lanes 2 and 3, sample in elution buffer (pH 4.5).

2.1.2 Design, cloning and purification of N-terminally truncated SpsB

Topology prediction for SpsB (sequence source: http://cmr.jcvi.org/tigr-scripts/CMR/CmrHomePage.cgi) by TMHMM (Krogh *et al.*, 2001) and Porter server (Pollastri & McLysaght, 2005) indicated the presence of a single N-terminal transmembrane segment important for membrane anchoring (Fig. 2.2). A truncated derivative, which we designated as tr-SpsB, was designed to obtain a soluble derivative of SpsB devoid of the transmembrane segment (box A) but retaining the amino acids in the conserved box B region, located in its vicinity (Fig. 3.9, chapter 3). Similarly, a second truncated derivative designated as tr-mut-SpsB with an identical sequence except for the catalytic Ser being replaced by an Ala was obtained by a double-PCR approach (designed by Geukens N, unpublished data).

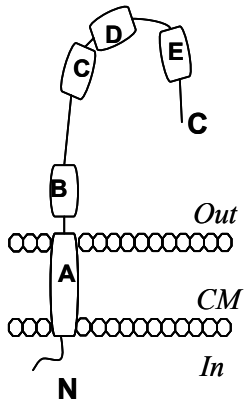

Figure 2.2: A schematic representation of membrane topology of SpsB showing the conserved boxes.

N-terminally hexa-his-tagged tr-SpsB and tr-mut-SpsB (predicted MW=18.2 kDa) were

found to be in the soluble fraction upon production in *E. coli* BL21 (DE3)pLysS harbouring the respective plasmids and could be purified under native conditions from the cytoplasmic fraction by Ni^{2+} affinity chromatography. The yield of the truncated active form was low compared to the truncated mutant and also required an additional step of cation exchange chromatography prior to its use in the *in vitro* assays while the yield of the truncated mutant was much higher (Figure 2.3). The huge difference in the yield between tr-SpsB and tr-mut-SpsB is surprising as the two proteins are identical except for a Ser residue replaced by an Ala in the latter.

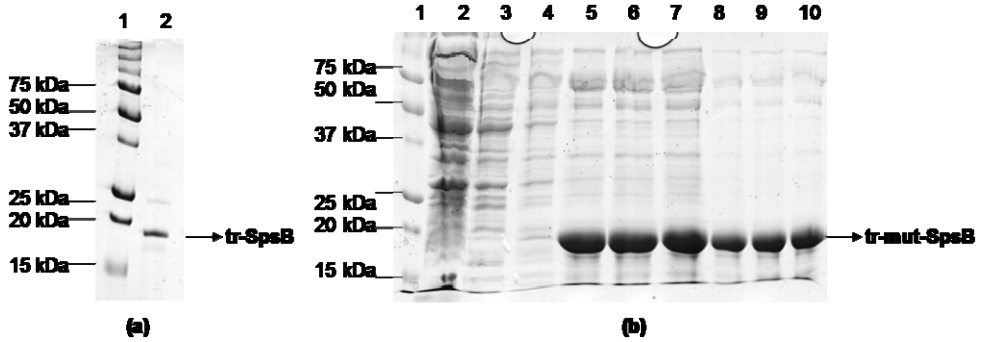

Figure 2.3: Purified truncated SpsB derivatives on gel. tr-SpsB was purified from the cytoplasmic fraction of *E. coli* harbouring pET-tr-SpsB, by nickel affinity chromatography followed by cation exchange. Purified protein was separated on SDS/PAA gel followed by CBB staining. (a) Lane 1, molecular weight marker; lane 2, purified tr-SpsB (b) tr-mut-SpsB was purified from *E. coli* harbouring pET-tr-SpsB, by nickel affinity chromatography and the purified fractions were analysed as described above. Lane 1, molecular weight marker; Lane 2, flow through; Lanes 3 & 4, column wash with buffer containing 10 and 20 mM imidazole respectively; Lanes 5 to 7, elution fractions in buffer containing 100 mM imidazole; Lanes 8 to 10, elution fractions in buffer containing 250 mM imidazole.

2.1.3 *In vitro* preprotein processing by SpsB

The choice of the preprotein substrate was made after a preliminary analysis of secreted proteins indicated in the genomic sequence data of *S. aureus*. The criteria for selection of the substrate were a good prediction on the presence and the location of the signal peptide cleavage site as indicated by SignalP 3.0 server (Bendtsen *et al.*, 2004) and a non-indication as a general protease. The latter is not desirable because it could degrade the signal peptidase itself. Pre-IsaA was selected as the substrate for this assay. IsaA was first identified as one of the four proteins expressed *in vivo* during sepsis caused by methicillin-resistant *S. aureus* (Lorenz *et al.*, 2000). It is a lytic transglycosylase and has been reported to be important for the virulence of *S. aureus* along with another paralogue SceD (Stapleton *et al.*, 2007), which is also a substrate of the signal peptidase SpsB.

The *in vitro* assay was carried out in the presence of a protease inhibitor cocktail and the reactions were stopped at different time intervals ranging from 0 to 15 h. Analysis of the assay products by means of immunodetection of pre-IsaA/IsaA, revealed the presence of two bands (Figure 2.4) in the sample containing the preprotein substrate and SpsB. The upper band corresponds to the unprocessed preprotein and the lower one to the mature protein (predicted MW=22.5 kDa). As seen in Figure 2.4, the substrate remained unprocessed in the absence of the enzyme. The amount of preprotein processed increased over time (Figure 2.4a). After 15 hours (900 min), unprocessed protein remained and the addition of fresh SpsB followed by incubation for 3 hours did not result in any significant improvement in processing. Similar observations of incomplete processing have been made previously with *in vitro* assays involving the signal peptidases and preproteins (Geukens *et al.*, 2004; Peng *et al.*, 2001a; Talarico *et al.*, 1993; van Roosmalen *et al.*, 2001) and it has been suggested that the remaining preprotein is probably in an unprocessable state. The specificity of the preprotein cleavage by SpsB was confirmed by N-terminal sequence analysis of the mature protein obtained. The substrate was cleaved at the predicted site (Figure 3.2, chapter 3), following the (-1,-3) or

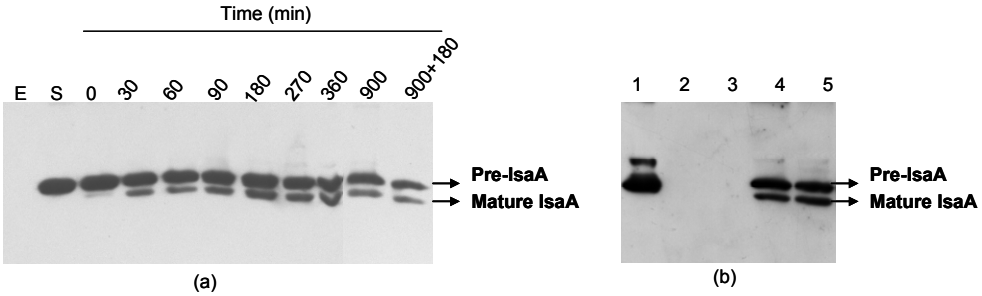

Figure 2.4: Preprotein processing by SpsB (full-length) (a) as function of time (b) in comparison with the tr-SpsB. (a) pre-IsaA (10 mM) was incubated with the full-length SpsB (2 μM) at 37° C in the assay buffer for different time periods. The proteins were separated on 12.5 % (w/v) SDS-PAA gels and analyzed by Western blotting and chemiluminescent detection (a) Lane 1, SpsB (control); Lane 2, pre-IsaA (control); Lane 3, SpsB and pre-IsaA at time=0; Lanes 4 to 10, pre-IsaA processing by SpsB with increase in time ; Lane 11, 900 min incubation followed by addition of fresh SpsB (2 μM final) and a further incubation for 3 h. (b) The assay was set up as described above except that the final concentration of SpsB was 1 μM and incubation time was fixed to 15 h. Lane 1, pre-IsaA (control); Lane 2, SpsB full-length (control); Lane 3, SpsB truncated (control); Lane 4, pre-IsaA processed by SpsB full-length; Lane 5, pre-IsaA processed by truncated SpsB.

"Ala-X-Ala" rule (Nielsen *et al.*, 1997). Additionally, the substrate was also processed by the truncated SpsB (tr-SpsB) lacking the transmembrane segment residues but containing the active-site Ser. A comparison of preprotein processing by the two enzymes is shown (Fig 2.4b).

2.2 Discussion

In this chapter, we describe the purification of SpsB and a native preprotein substrate, pre-IsaA, and demonstrate the *in vitro* processing of the substrate by the SPase as the first step in its functional characterization. SpsB has been purified earlier for use in *in vitro* assays involving synthetic peptide substrates (for references, see table 1.1). We also demonstrated the activity of a truncated derivative of SpsB lacking the hydrophobic residues in the predicted transmembrane region. This indicates that the residues in the transmembrane segment are not essential for the cleavage fidelity of SpsB as it also cleaves the preprotein. Retention of activity and cleavage fidelity has also been observed in truncated versions of *E. coli* LepB and *B. subtilis* SipS (Carlos *et al.*, 2000b). Truncated derivatives of SpsB are interesting candidates for crystal structure determination as this process can be tedious and time-consuming in case of membrane proteins. Although several membrane proteins have been crystallized, no crystal structure is currently available for the full-length SpsB or for any other bacterial SPaseI. The problem of *in vitro* self-cleavage is another factor contributing to the challenge of structure determination of SPaseI by X-ray crystallography. In this respect, the truncated active-site mutant of SpsB would be an interesting candidate for crystallization as in theory this mutant protein would be more stable than the native full-length SpsB. Pity enough, no crystals could be obtained with this truncated mutant of SpsB (Prof. R. Loris, VUB, personal communication). However, crystallization is beyond the focus of this doctoral work and the truncated active site mutant was intended to serve as a control in the *in vitro* assay (see chapter 3).

Secretomic analysis of sequenced *S. aureus* strains revealed that 58 proteins from a total ~2,600 encoded in the genome contain a potential SpsB recognition and cleavage site, of which 33 have been identified (Sibbald *et al.*, 2006). These proteins seem to be largely comprised of enzymes such as proteases and other factors such as fibrinogen- and IgG-binding proteins that are required for residing in the human host. Among the predicted substrates of SpsB are many known extracellular staphylococcal virulence factors such as exotoxins, enterotoxins (SEM, SEN and SEO), haemolysins, TSST-1, leukotoxins (LukD and LukE) and a secretory antigen SsaA homologue (Sibbald *et al.*, 2006). Furthermore, it has been shown that SpsB plays a role in the *agr* quorum-sensing system which is important for biofilm formation and virulence (Kavanaugh *et al.*, 2007). It is also interesting to note that biofilm-associated proteins (Baps), a family of surface proteins

involved in biofilm formation, are substrates of SpsB (Lasa & Penades, 2006). In essence, SpsB is an essential enzyme in *S. aureus* and also plays a major role in processing proteins necessary for biofilm growth, virulence, damaging the host tissues (toxins), conferring antibiotic resistance (β-lactamase) and quorum sensing, enhancing the significance of discovering SPase inhibitors.

The genome of *S. aureus* also contains a second gene (*spsA*) encoding a homologue of SPasesI immediately upstream of the *spsB* gene. The two genes are separated by a short spacing of 15 bases between the 3' end of *spsA* and the 5' end of *spsB* implying either cotranscription of the two genes or the presence of a cryptic promoter for *spsB*

Table 2.1: Comparison of the residues in the conserved boxes in *E. coli* LepB, *S. aureus* SpsB and SpsA.

SPase	Box B	Box D	Box E
Consensus	SMxPTL	YxKRxxGxPGD	GDNxxxSxDSR
LepB	SGSMMPTL	YIKRAVGLPGD	GDNRDNSADSR
SpsB	GESMDPTL	YVKRVIGVPGD	GDNREVSKDSR
SpsA	NNDMSPTL	YTSRIIAKPGQ	NDHDNNQHDSR

The identical residues in the boxes are highlighted in blue. The residues present in the place of catalytic Ser and Lys in SpsA are underlined.

transcription within the 3'-terminal coding region of *spsA* (Cregg *et al.*, 1996). SpsA and SpsB are proteins of 174 and 191 residues with predicted molecular weights of approximately 20.1 and 21.6 kDa respectively. SpsA has a sequence that is similar to known SPases but as seen in Table 2.1, it lacks the catalytic Ser or Lys required for SPaseI activity. It has also been shown that SpsB, but not SpsA, is responsible for the removal of the N-terminal leader of AgrD, the precursor of AIP (auto-inducing peptide) which controls the *agr*-quorum sensing system (Kavanaugh *et al.*, 2007). Thus, as of now, the role of SpsA (if any) in protein secretion is not known. Apparently inactive SPase homologues missing one of the catalytic residues (Ser or Lys) are also present in *S. epidermidis* (Sip1), *S. carnosus* (SipA), *Streptococcus mutans*, *Streptococcus pyrogenes*, and *Borrelia burgdorferi*. However, there are no data available on the role of these proteins either.

2.3 Experimental procedures

2.3.1 Bacterial strains, growth conditions and plasmids

E. coli strains TG1 (Sambrook *et al.*, 1989) and BL21(DE3)pLysS (Studier & Moffatt, 1986) used for genetic manipulations and protein expression, respectively, were grown at

37 °C in Luria-Bertani (LB) medium, supplemented with ampicillin (50 μg ml^{-1}) or chloramphenicol (25 μg ml^{-1}), where applicable. The plasmids used in this study are listed in table 2.2.

2.3.2 General molecular genetic techniques

DNA manipulations in *E. coli* were carried out as described in Sambrook *et al.*, 1989. Plasmid DNA isolation and PCR clean-up were carried out using commercial kits (Promega) according to the manufacturer's instructions.

2.3.3 Cloning of *spsB* (wild-type and derivatives) and *isaA*

The gene encoding SpsB was amplified by PCR from *S. aureus* ATCC 65388 genomic DNA as template using the oligos fl-SpsB5 and fl-SpsB3 for the full-length and oligos tr-SpsB5 and fl-SpsB3 for the truncated derivative, respectively. The oligonucleotides were designed based on the *spsB* gene sequence (http://cmr.jcvi.org/tigr-scripts/CMR/CmrHomePage.cgi). The oligonucleotide sequences are given in table 2.3 and as indicated, a hexa-histidine-encoding sequence was included at the 5' end. The resulting PCR-amplified DNA fragments were first cloned in pGEM-T Easy (Promega) and subsequently cloned as *Nde*I/*Eco*RI fragments into the pET-3a (Novagen) expression plasmid which was also cut with the same restriction enzymes.

The gene *isaA* was amplified from *S. aureus* genomic DNA using oligos pIsaA5 and IsaA3Myc, the sequence of which is given in table 2.3. The forward primer pIsaA5 contained a hexa-histidine-encoding sequence and the reverse primer IsaA3Myc contained a c-Myc-encoding sequence. PCR-amplified DNA was cloned in pGEM-T Easy and subsequently cloned as a *Nco*I/*Eco*RI fragment into the corresponding sites of pET-23d (Novagen).

2.3.4 Expression and purification of full-length SpsB

Expression of the protein was carried out essentially as previously described (Studier & Moffatt, 1986). *E. coli* BL21(DE3)pLysS cells harbouring pET-fl-SpsB were grown in 600 ml LB medium at 37 °C until the optical density at 600 nm (OD_{600}) reached 0.6. Isopropyl-β-D-thiogalactopyranoside (IPTG) was then added to a final concentration of 1 mM. Three hours later, the cells were pelleted by centrifugation (10 min, 4,000 x g, 4 °C).

For purification of full-length SpsB, the cells were resuspended in 20 ml of 50 mM Tris-HCl pH 8, containing 20 % sucrose and lysed by three passages through a French pressure cell at 15,000 psi. After removal of the cell debris by centrifugation (10 min, 12,000 x g, 4 °C), the cell lysate was subjected to ultracentrifugation at 100,000 x g for 2 h. The pellet was resuspended in 5 ml of buffer A (50 mM NaH_2PO_4, 300 mM NaCl, pH 8.0) containing 10 mM imidazole and 0.5 % Triton X-100. The sample was transferred onto a column loaded with Nickel-Nitrilo-tri-acetic acid (Ni^{2+}-NTA) sepharose and pre-equilibrated with buffer A containing 10 mM imidazole. The column was placed on ice on a rotary shaker (45 rpm) for 1h. The column was washed twice with buffer A containing 10 and 20 mM imidazole, respectively, in the presence of 0.05 % Triton X-100. Samples were eluted in two steps, first with buffer A containing 100 mM imidazole and then with buffer A containing 250 mM imidazole in the presence of 0.05 % Triton X-100. For analysis of purity, 4 µl of 6 x SDS-PAGE loading buffer was added to 20 µl of different elution fractions and incubated at 37 °C for 10 min followed by loading on 12.5 % SDS-PAA gels. After separation of the proteins (30 mA/minigel), the gel was stained with Coomassie Brilliant Blue (CBB).

2.3.5 Expression and purification of the truncated SpsB

For production of the truncated SpsB derivatives, *E. coli* BL21(DE3)pLysS was transformed with the plasmids pET-tr-mut-SpsB (Geukens N, unpublished) or pET-tr-SpsB. The cell pellets obtained after centrifugation (10 min, 4,000 x g, 4 °C) from 600 ml culture of *E. coli* BL21(DE3)pLysS harbouring the respective plasmids were resuspended in 10 ml of buffer A with 10 mM imidazole and passed through a French pressure cell at 15,000 psi, thrice. After centrifugation (10 min; 12,000 x g), the clarified sample was subjected to Ni^{2+}-affinity chromatography as described for the full-length SpsB. In case of tr-SpsB, the eluted fractions were pooled and subjected to buffer exchange on a PD-10 desalting column (GE Healthcare). The sample eluted in 50 mM HEPES buffer, pH 7.4 was further purified by cation exchange chromatography using a HiTrap SP FF column on the AKTAprime™ plus HPLC system (GE Healthcare) as described by the manufacturer. The fractions containing tr-SpsB were passed through a PD-10 desalting column and eluted in 50 mM Tris-HCl, pH 8. The purified protein was observed on CBB-stained SDS-PAA gel.

2.3.6 Expression and purification of preprotein immunodominant staphylococcal antigen A (pre-IsaA)

Pre-IsaA (with a hexa-his-tag at the N-terminus and a c-Myc-tag at the C-terminus) was expressed in *E. coli* BL21(DE3)pLysS cells harbouring pET-IsaA. IPTG induction was carried out as described above. Additionally, sodium azide (1 mM final concentration) was added to prevent the translocation of the preprotein and subsequent cleavage of the signal peptide. Pre-IsaA was purified under denaturing conditions (8 M urea) on a Ni^{2+}-NTA column as recommended by the manufacturer (The QIA*expressionist*™, Qiagen). Removal of urea and subsequent protein renaturation was carried out using PD-10 columns. The sample was eluted from the column in buffer containing 50 mM Tris-HCl, pH 8 and 0.5 % Triton X-100. The purified protein was then analyzed by SDS-PAGE and Western blotting.

2.3.7 *In vitro* activity assay for SpsB using the preprotein pre-IsaA

The concentrations of the purified proteins were determined by a protein assay (Bio-Rad) based on the Bradford method. The enzyme SpsB (pre-treated with a protease inhibitor cocktail tablet (Complete, mini, EDTA-free, Roche Diagnostics) and pre-IsaA were added to the assay buffer (50 mM Tris-HCl, pH 8 with 0.5 % Triton X-100) to get final concentrations of 2 and 10 μM, respectively. Reaction mixtures (total volume of 20 μl) were incubated at 37 °C for different periods of time ranging from 0 to 15 h. The reactions were stopped by addition of 4 μl of 6 x SDS-PAGE sample loading buffer. The proteins were separated by SDS-PAGE using 12.5 % (w/v) PAA-resolving gels and subsequently transferred to a nitrocellulose membrane (Macherey Nagel). For immunodetection, anti-cMyc (DiaMed) and anti-mouse IgG (whole-molecule)-alkaline phosphatase antibodies produced in rabbit (Sigma) were used. Chemiluminescent detection was carried out using 'Western Star™' kit (Tropix) as described by the manufacturer.

2.3.8 N-terminal sequencing

The proteins were separated by SDS-PAGE using 12.5 % SDS-PAA gels followed by electroblotting onto a polyvinylidene difluoride (PVDF) membrane. The bands were visualized by staining with Coomassie blue R-250 and destaining with 100 % methanol. The protein of interest (IsaA, in this case) was excised from the membrane and the N-terminal amino acid sequence was determined by automated Edman degradation.

Table 2.2: Plasmids used in the work

Plasmid	Description	Source
pGEM-T Easy	3'-T overhang suited for cloning PCR products; *lac*Z; Ampicillin resistance (*bla*)	Promega
pET-3a	T7 promoter ; MCS; Ampicillin resistance (*bla*)	Novagen
pET-23d	T7 promoter ; MCS ; Ampicillin resistance (*bla*)	Novagen
pET-fl-SpsB	pET-3a derivative containing hexa-his-encoding sequence (5'-end) and *spsB* between *Nde*I and *Eco*RI	This work
pET-tr-SpsB	pET-3a derivative containing hexa-his-encoding sequence and 5'-end truncated *spsB* between *Nde*I and *Eco*RI	This work
pET-tr-mut-SpsB	Identical to pET-tr-SpsB except for a single nucleotide difference to encode an active-site mutant (catalytic Ser →Ala) of tr-SpsB	Geukens N, (unpublished)
pET-pIsaA	pET-23d derivative containing hexa-his- (5'-end) and c-myc- (3'-end) encoding sequence with *pre-IsaA* (Immunodominant staphylococcal antigen A precursor) gene between *Nco*I and *Eco*RI.	This work

Table 2.3: Oligonucleotides used in this work

Oligonucleotide	Sequence	Restriction site
fl-SpsB5	5'-TACATATG*CACCATCACCATCACCAT*AAAAAAGAATTATTGGAATGGATTATTTC-3'	*Nde*I
fl-SpsB3	5'-TAGAATTCTTAATTTTTAGTATTTTCAGG-3'	*Eco*RI
tr-SpsB5	5'-TACATATG*CACCATCACCATCACCAT*ATTGTTACACCATATA-3'	*Nde*I
pIsaA5	5'TACCATGG*CACATCACCATCACCATC*ACAAAAAGACAATTATGGC3'	*Nco*I
IsaA3Myc	5'TAGAATTCTTA**CAGATCCTCCTCTGAGATGAGCTTCTGCTC**GAATCCCCAAGCACCTAAACC3'	*Eco*RI

Restriction sites are underlined, hexa-histidine-encoding sequence is italicized and c-myc-encoding sequence is indicated in bold.

Chapter 3: Biochemical characterization of SpsB

In this chapter, the *in vitro* behaviour of the purified full-length SpsB with respect to its stability, pH requirement and enzymatic activity, is described. In order to obtain quantitative data on the SpsB activity and given that the preprotein assay is semi-quantitative at best, synthetic peptide substrates were tested and one of them was used to optimize another *in vitro* assay for SpsB. This assay was used to compare the activities of the full-length SpsB with its truncated derivatives.

3.1 Results

3.1.1 A continuous fluorometric assay for SpsB and measurement of its specific enzymatic activity

A FRET-based assay was designed for SpsB. The substrate used was an internally quenched peptide based on the signal peptide sequence of *S. epidermidis* SceD protein, coupled to a DABCYL/EDANS FRET-pair. SpsB was found to cleave this peptide efficiently in the presence of protease inhibitor cocktail, to which the bacterial type I SPases are resistant (Fig. 3.1). The hydrolysis of the peptide was measured by the increase in fluorescence on a microplate reader using excitation and emission wavelengths of 340 and 510 nm respectively. No increase in fluorescence was observed in the presence of the peptide or the enzyme only. The validation of this assay is described in chapter 4. The specificity of the proteolytic reaction of the SceD peptide

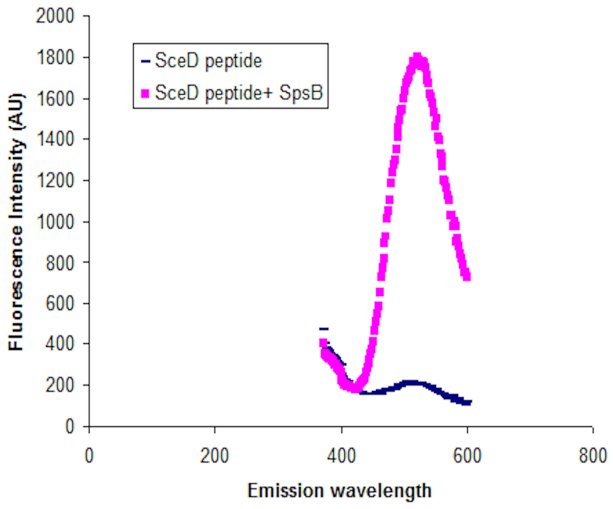

Figure 3.1: Emission scan of the reaction products containing SceD peptide with or without SpsB. The test reactions contained SpsB (1 μM) and the synthetic peptide SceD (10 μM), while the control reaction contained only the peptide substrate. The samples were incubated at 37 °C for 15 h followed by measurement of the fluorescence intensity as a function of wavelength (λ_{ex}= 340; λ_{em} = 510).

by SpsB was analysed by HPLC followed by electrospray ionization mass spectrometry (ESI-MS), (by Bockstael K as described in Bockstael *et al.*, 2009a). Cleavage of the fluorogenic synthetic SceD peptide by SpsB occurred specifically at the predicted site located at the A-S bond. The sequence and cleavage site of the SceD peptide in comparison with the SpsB cleavage site of the preprotein IsaA are indicated in Fig. 3.2.

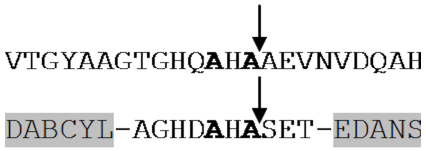

Figure 3.2: Signal peptidase recognition sequence and cleavage sites of the SpsB substrates used in this study. Part of the sequence of the IsaA precursor (upper row) and the sequence of the SceD peptide (lower row) with signal peptidase cleavage sites indicated. The signal peptidase recognition sequence which consists of small aliphatic residues at positions -1 and -3 relative to the cleavage sites, is indicated in bold.

It was observed that at high substrate concentrations (>20 μM), the linear correlation between the fluorescence and the substrate concentration is lost due to inner filter effect.

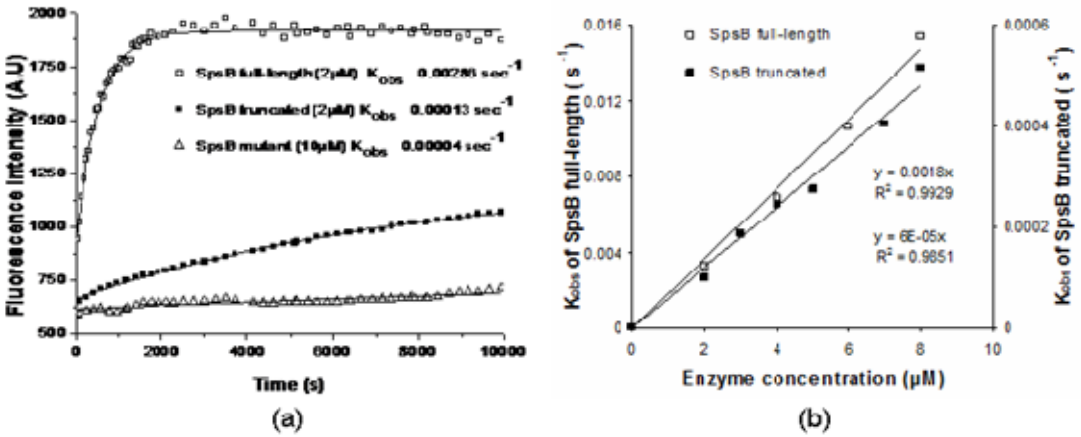

Figure 3.3: A comparison of the activities of the full-length and the truncated SpsB derivatives. (a) The enzyme assay was performed using 5 μM final concentration of the synthetic SceD peptide (where [S]<<K_m) in the presence of full-length SpsB (2 μM), truncated SpsB (2 μM) or an active-site mutant (10 μM) in a reaction buffer at 37 °C. Fluorescent intensity was measured as a function of time using a Tecan Infinite™ M200 microplate reader. (b) The specific enzymatic activity k_{cat}/K_m of full-length and truncated SpsB were compared using varying enzyme concentrations and a fixed concentration of the peptide substrate (5 μM for full-length and 2.5 μM for truncated SpsB). The pseudo-first order rate constant K_{obs} was plotted as a function of enzyme concentration.

Inner filter effect is the phenomenon observed when the fluorescent light is absorbed by quenching groups on neighbouring substrates or cleaved product molecules, allowing only a fraction of light to be detected by the instrument. Therefore, only k_{cat}/K_m could be

measured using the condition [S]<< K_m. Consistent with this condition, the time-course FRET assay with the enzyme followed simple first order kinetics. The pseudo-first order rate constant (k_{obs}) derived from these curves was directly proportional to the enzyme concentration throughout the experimentally accessible range of concentrations (0.1 to 10 μM). The apparent second order rate constant k_{cat}/K_m or specific enzymatic activity of the full-length SpsB was found to be $1.85 \pm 0.13 \cdot 10^3$ $M^{-1}s^{-1}$ (Fig. 3.3a,b).

The specific activity of the truncated derivative (tr-SpsB) was determined under the same conditions except that in order to achieve complete processing, the final substrate concentration used for the truncated enzyme was 2.5 μM. The apparent second order rate constant k_{cat}/K_m of the truncated enzyme was found to be 59.4 ± 6.4 $M^{-1}s^{-1}$ (Fig. 3.3a,b) in the presence of 0.5 % Triton X-100 (Fig. 3.3a). This 30-fold reduction in the specific activity of the truncated SpsB (tr-SpsB), compared to the full-length enzyme, confirms the importance of the transmembrane segment for optimum activity of the signal peptidases. Additionally, the truncated mutant (tr-mut-SpsB) in which the catalytic Ser is replaced by Ala was used as a control in the FRET assay. This mutant had a k_{cat}/K_m value of 4 ± 0.8 M^{-1} s^{-1} which is 14.8-fold lower than the active truncated (tr-SpsB) and 462-fold lower than the full-length enzyme (Fig. 3.3a). This also confirms that the *in vitro* activity is specifically due to the enzyme SpsB and not due to background activity of LepB of *E. coli* (which was used as the host for overproduction of SpsB).

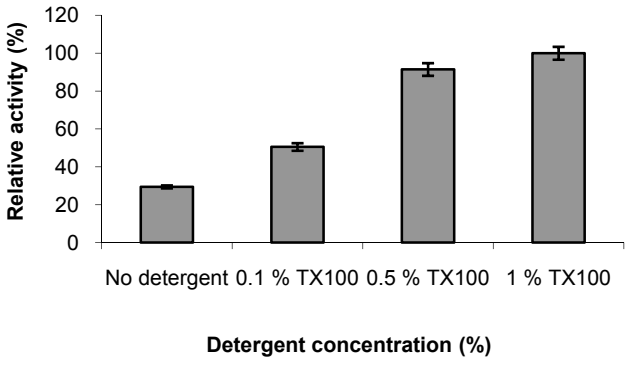

Figure 3.4: Effect of detergent (Triton X-100) on the activity of tr-SpsB. Specific enzymatic activity of tr-SpsB was determined in a FRET assay with SceD and tr-SpsB (at 2.5 μM and 5 μM final concentrations respectively) in the presence (at different concentrations) and absence of Triton X-100. The specific enzymatic activity of tr-SpsB at the highest detergent concentration (1 %) was fixed to 100 % and the remaining samples are represented against this value.

It was also observed that the non-ionic detergent Triton X-100 increases the activity of tr-SpsB, while the addition of sodium deoxycholate (ionic) or sulfobetain SB12 (zwitterionic) detergents render the enzyme inactive (data not shown). The effect on the activity of tr-SpsB in the presence or absence of Triton X-100 was studied in the FRET assay. Maximum activity of tr-SpsB was observed at 1 % Triton X-100, although the difference between 0.5 % and 1 % detergent is comparatively minor and the specific activity was halved in the absence of the detergent (Fig. 3.4).

3.1.2 Activity at varying pH and the pH-rate profile of SpsB

The pH-dependence of the SpsB activity was initially studied by monitoring the *in vitro* preprotein processing by SpsB in reaction buffers varying in pH from 2 to 12. The enzyme was found to be active at a wide pH range (pH 5 to 12) but not at or below pH 4, in three independent experiments (data not shown). An assessment of the amount of preprotein processed at varying pH did not yield sufficient quantitative data, and therefore the FRET-assay was used to study the effect of pH on enzyme activity. The stability of the synthetic SceD substrate was determined by incubating the peptide in

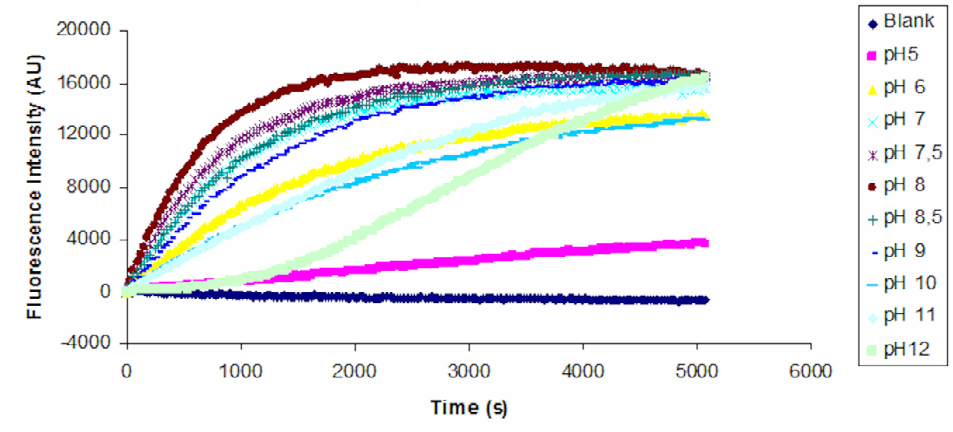

Figure 3.5: Effect of pH on the SpsB activity. SpsB (1 µM) was added to different buffers varying in pH from 5 to 12 and incubated for 5 min at 37 °C. The fluorogenic synthetic peptide SceD was added at a final concentration of 5 µM to start the reaction. Fluorescence intensity was measured as a function of time. The figure is a representative of three independent experiments.

different buffers in the absence of the enzyme. No increase in fluorescence was observed over the entire range of pH from 2 to 12 during the time-course assay (data not shown), confirming its suitability for this purpose. The enzyme reactions were carried out in different buffers from pH 5 to 12 and the increase in fluorescence was observed as a function of time (Fig. 3.5). The curve obtained for pH 12 could not be fitted to obtain

the exact k_{cat}/K_m value (Fig. 3.5). However, the activity at pH 12 appears to be lower in terms of the initial velocity and to plot the pH-rate profile, the approximate k_{cat}/K_m value obtained was used. The pH-rate profile obtained by plotting k_{cat}/K_m versus pH was fitted with the equation (Eqn.1) for a complex bell-shaped curve (Fig. 3.6). The activity of SpsB is maximum activity at pH 7.9 ± 0.2. The high pH optimum of SpsB *in vitro* is consistent with those reported for the other SPases and is in agreement with the catalytic mechanism.

$$k_{cat}/K_m = \frac{\left(\frac{k_{cat}}{K_m}\right)_1\left(\frac{H^{+2}}{K_{a3}K_{a2}}\right)+\left(\frac{k_{cat}}{K_m}\right)_2\left(\frac{H^{+}}{K_{a3}}\right)}{1+\frac{H^{+}}{K_{a3}}+\frac{H^{+2}}{K_{a3}K_{a2}}+\frac{H^{+3}}{K_{a3}K_{a2}K_{a1}}}$$

Equation 1

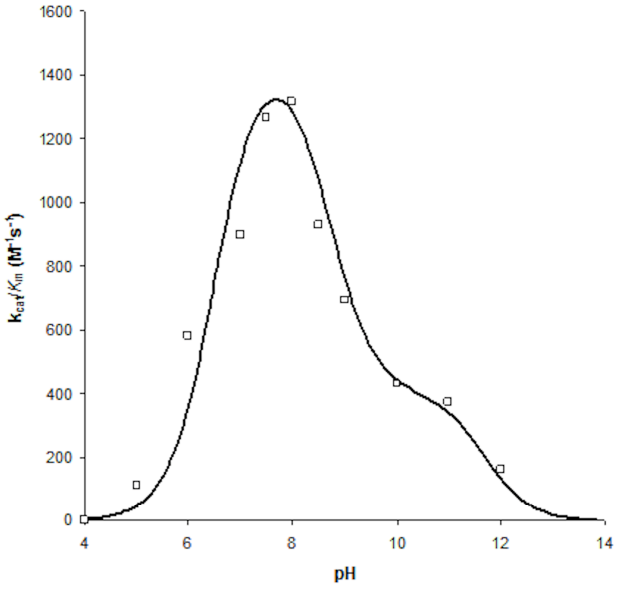

Figure 3.6: pH-rate profile of SpsB. The calculated specific enzymatic activities (k_{cat}/K_m) obtained after carrying out the reactions in buffers with varying pH from 4 to 12 were fitted using the equation for a complex bell-shaped curve. The results shown are an average of three independent experiments.

The curve obtained from the pH-rate profile (Fig. 3.6) was not a typical single bell-shaped curve as there appeared to be another smaller peak around pH 11. The apparent pK_a values for the free enzyme are approximately 6.6 and 8.7 with possibly another pK_a around 11.8. The presence of two peaks in the pH-dependence curve (Fig. 3.6) and the high pK_{a1} suggests that two acid groups can play the role of acid catalyst as represented in Scheme 1 (Brocklehurst & Dixon, 1976; Tipton & Dixon, 1979). Deprotonation of ESH_2^+ with a pK_{a2} of 8.7 decreases the rate of the catalyzed reaction. Further

deprotonation of ESH^+ with a pK_{a3} around 11.8 probably ends the catalytic reaction (Scheme 1). The k_{cat}/K_m values were calculated using Eqn 1.

$$\begin{array}{cccc} E+3H^+ \Leftrightarrow & EH^+ + 2H^+ \Leftrightarrow & EH_2^+ + H^+ \Leftrightarrow & EH_3^+ \\ + & + & + & + \\ S & S & S & S \\ \Updownarrow & \Updownarrow & \Updownarrow & \Updownarrow \\ ES & ESH^+ & ESH_2^+ & ESH_3^+ \\ & \downarrow & \downarrow & \\ & EH^+ + P & EH_2^+ + P & \end{array} \qquad \text{Scheme 1}$$

$$\text{For } ESH_2^+ \left(\frac{k_{cat}}{K_m}\right) \cong 1500 \quad \text{and} \quad ESH^+ \left(\frac{k_{cat}}{K_m}\right) \cong 400$$

3.1.3 Stability and the effect of temperature on the *in vitro* activity of SpsB

Since SPases are known to undergo degradation upon incubation or storage over time,

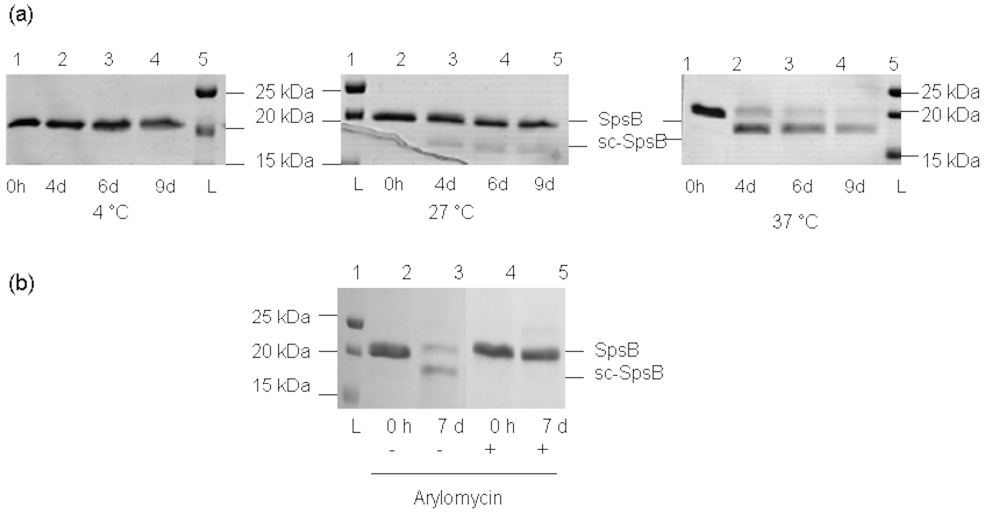

Figure 3.7: Stability of SpsB (a) at different temperatures and (b) in the presence of arylomycin A_2 (a) The stability of SpsB was tested by placing 20 µl aliquots of purified SpsB at different temperatures for up to 9 days. The proteins were analyzed by SDS-PAGE followed by staining with CBB. L, molecular weight marker; remaining lanes show the full-length SpsB and an additional band corresponding to the self-cleavage product (sc-SpsB) resulting from incubation for 4, 6 and 9 days respectively at 4 °C, 27 °C or 37 °C; SpsB stored at -80 °C represents the control reaction (0 h). (b) Purified full-length SpsB was incubated without and with arylomycin (200 µM final concentration) at 37 °C for 7 days and analyzed by SDS-PAGE. Lane 1, molecular weight marker; Lane 2, SpsB without arylomycin (time=0); Lane 3, SpsB without arylomycin incubated for 7 days; Lane 4, SpsB with arylomycin (time=0); Lane 5, SpsB with arylomycin incubated for 7 days.

we tested the stability of SpsB (full-length) by storing or incubating the enzyme at 4 °C, 27 °C or 37 °C for different lengths of time in the presence of general protease inhibitors. In the sample stored at 4 °C for 9 days, only one band corresponding to the native SpsB was observed (Fig. 3.7a). However, the k_{cat}/K_m of this sample was 70 $M^{-1}s^{-1}$ which was 18.5-fold lower compared to the enzyme stored at -80 °C for the same time period. After 4 days of incubation at 27 °C, apart from the band corresponding to the native SpsB, a smaller protein was found (MW~18 kDa) which we designated as sc-SpsB. The amount of sc-SpsB increased over time and with increasing temperature. The addition of the SPase inhibitor arylomycin A_2 blocked the appearance of sc-SpsB (Fig. 3.7b), suggesting that this protein fragment results from intermolecular self-cleavage.

3.1.4 *In vitro* self-cleavage

The N-terminal sequence analysis of the self-cleavage product sc-SpsB revealed that the enzyme was cleaved one amino acid before the catalytic serine (Fig. 3.8). The self-cleavage site resembles the signal peptide cleavage site following the (-1,-3) rule for SPase recognition, as seen in the case of LepB, SipS and Spi. A comparison of the SpsB and Spi self-cleavage sites shows that both proteins are cleaved at the same position, while in case of SipS from *B. subtilis*, the cleavage site is located immediately after the catalytic serine (Fig. 3.8).

It has been reported that the self-cleavage products of Spi and SipS have no SPase activity. The self-cleavage site in *E. coli* LepB is not in the vicinity of the catalytic Ser and the self-cleavage product had a 100-fold less specific activity compared to the native enzyme (Talarico *et al.*, 1991). We tested the self-cleavage product sc-SpsB and also found it to be inactive at the SPase concentration normally used in the FRET assay (1 μM).

SPase, Bacterial species	Alignment
SpsB, *S. aureus* (This chapter)	VTPYT**I**K**G**↓E*S*MDPTLKDGE
Spi, *S. pneumoniae* (Peng *et al.*, 2001a)	WSNVR**V**E**G**↓H*S*MDPTLADGE
SipS, *B.subtilis* (van Roosmalen *et al.*, 2000)	FAPYVVD**G**E***S***↓MEPTLHDRE

Figure 3.8: Site of self-cleavage of SpsB, in comparison with Spi and SipS. Alignment of SpsB with Spi and SipS sequences showing the sites of self-cleavage. The -1 and -3 positions relative to the cleavage sites are in bold, the catalytic serine is in italics and the site of self-cleavage is indicated with an arrow.

A very low residual activity of the self-cleavage product was found when the concentration of sc-SpsB was greatly increased (data not shown). Interestingly, the inability of sc-SpsB to cleave the substrate contrasts with the *in vitro* activity of tr-SpsB under standard conditions. Truncated SpsB has nine additional amino acids at the N-terminus compared to sc-SpsB and three of these residues are part of the conserved box B region (Fig. 3.9). The corresponding amino acids in this region preceding box B are a part of the substrate binding pocket in *E. coli* LepB as indicated by the crystal structure (Paetzel *et al.*, 1998) and modelling data (Choo *et al.*, 2008). Furthermore, NMR experiments on the truncated derivative of LepB also showed that five of these amino acids are perturbed by substrate binding (Musial-Siwek *et al.*, 2008b), confirming the interaction of these residues (in the proposed binding pockets of the enzyme) with the substrate. In SpsB, it is also likely that one or more of the amino acids immediately preceding the catalytic serine form a part of the substrate-binding pocket which can only

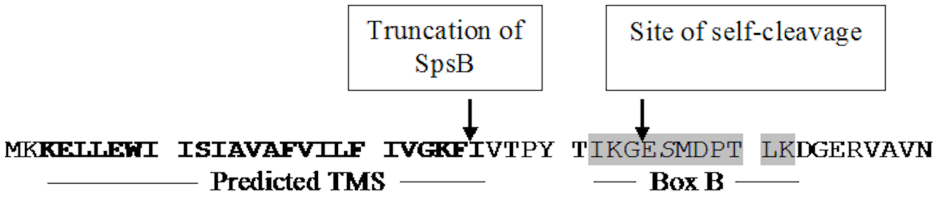

Figure 3.9: N-terminal region of the SpsB sequence showing the difference between the truncated SpsB (tr-SpsB) and the self-cleavage product (sc-SpsB). The starting points of the truncated SpsB and the self-cleavage product of SpsB are indicated in the SpsB sequence. The prediction of the transmembrane segment (TMS) was carried out using Porter server (Pollastri & McLysaght, 2005). The predicted TMS is in bold and the catalytic serine in italics. The conserved box B (Paetzel *et al.*, 2002b) is highlighted.

be confirmed when the crystal structure becomes available. These residues possibly also contribute to the correct folding and conformation of the enzyme.

3.2 Discussion

In this chapter, we have analyzed the activities of the full-length SpsB as well as the truncated derivatives using a synthetic peptide substrate which has enabled a quantitative comparison. Furthermore, we have studied the *in vitro* pH-requirement, stability and self-cleavage of the full-length enzyme and the effect of detergents on the truncated (tr-SpsB) derivative.

The specific enzymatic activity (k_{cat}/K_m) of the full-length SpsB on this internally quenched decapeptide, SceD is approximately 1850 $M^{-1}s^{-1}$ which is about a hundred-fold higher (Table 1.1) than the reported specific activity of the same enzyme with a fluorogenic hendeca peptide based on the signal peptide region of maltose-binding protein (Zhong & Benkovic, 1998). However, the specific enzymatic activity of SpsB on a 13-amino acid long synthetic peptide substrate with an N-terminal fatty acid (Bruton *et al.*, 2003) is over a thousand-fold (1240) higher compared the activity with the SceD peptide (Table 1.1). Although the length of the peptide substrate is known to influence activity (the longer the better), the presence of an N-terminal fatty acid in this case appears to contribute to the dramatic difference in specific activity. The above results further support the hypothesis of Brutton and co-workers (2003) on the beneficial role of N-terminal fatty acid in synthetic SPase substrates.

The *in vitro* activity of SpsB has been demonstrated using two different substrates: a preprotein (in chapter 2) and a synthetic peptide (this chapter). Interestingly, previous studies on the cleavage of peptide substrates by SpsB indicated that the enzyme prefers basic residues at the -2 position and tolerates hydrophobic residues as well (Bruton *et al.*, 2003). On the other hand an acidic residue at this position results in a significantly reduced rate of processing by SpsB (Bruton *et al.*, 2003). In agreement with this, both substrates pre-IsaA as well as the SceD peptide used in this work possess a basic residue (His) at the -2 position and have been processed efficiently by the enzyme. In parallel to this work, the -3 to +1 pattern for productive recognition and cleavage by SpsB was defined as (AVS)-(KHNDQSYEGLR)-A-(AESDIKL) by comparing the predicted SPase recognition and cleavage sites for signal peptides of proteomically identified extracellular proteins of *S. aureus* (Sibbald *et al.*, 2006). The residues in parenthesis are indicated in decreasing order of frequency of occurrence. The common residues in the two substrates used in this work at the -3 to -1 positions and the +1 residue (Ala in case of IsaA and Ser in case of SceD) are underlined. These experimental results are in favour of the above observations made *in silico*.

The optimum pH of SpsB (approximately pH 8) is comparable to that of Spi (*S. pneumoniae*), SipS (*B. subtilis*) and LepB (*E. coli*) which have optima of pH 8, pH 10 and pH 9, respectively (Paetzel *et al.*, 1997; Peng *et al.*, 2001a; van Roosmalen *et al.*, 2001), in agreement with the catalytic mechanism. Notably, SpsB is active at a broader range of pH

(5-12) compared to *E. coli* LepB which is active from pH 7-11 (Paetzel *et al.*, 1997). The pH-rate profile of SpsB did not result in a typical single bell-shaped curve which has been summarized in Scheme 1. Analysis of the pH-rate profile, suggests that the apparent pK_a value of 6.6 from the ascending limb could correspond to lysine which acts as a general base in this class of enzymes. It is interesting to note that this value is 2.1 pH units lower than that observed for LepB of *E. coli* (Paetzel *et al.*, 1997) and 4 pH units lower than the pK_a of lysine in solution. The reason for the decreased pK_a of the active-site Lys in the SPases is not known. It is also not clear whether the hydrophobic environment of the membrane contributes to this.

Full-length SpsB also appears to be comparatively stable *in vitro* as we can observe the protein on CBB-stained SDS-PAA gel after a minimum of 9 days (even up to 15 days, data not shown) storage at 4 °C. In contrast, 90 % of the full-length LepB of *E. coli*, is degraded in 11 days at 4 °C (Talarico *et al.*, 1991). Nevertheless, since self-cleavage is known to be a concentration-dependent event (as also observed during this work, data not shown), the self-cleavage event remains a hurdle in structure determination where highly pure and concentrated protein samples are required. For the *in vitro* assays, the purified enzyme was used within a couple of days or stored at -80 °C for subsequent use.

The self-cleavage of SpsB obeys the (-3,-1) rule of SPasesI as confirmed by N-terminal sequencing and is an intermolecular event as shown by the addition of the SPase inhibitor arylomycin which did inhibit autolysis. Self-cleavage of SpsB occurs in the region around the catalytic Ser, similar to that reported for Spi (*S. pneumoniae*) and SipS (*B. subtilis*). In contrast, self-cleavage in LepB (*E. coli*) occurs in the hydrophilic domain connecting the two transmembrane domains at the N-terminus (Talarico *et al.*, 1991). While the above observations of self-cleavage were made *in vitro*, self-cleavage has also been reported to occur *in vivo* in Spi. In the case of LepB, it is believed that the enzyme is protected from self-cleavage *in vivo* due to the fact that the autolysis site and the catalytic site are at the opposite sides of the membrane. This view has been supported by studies involving membrane-incorporated LepB where a dramatic decrease in self-cleavage was observed (Wang *et al.*, 2004).

The detergent requirement for the tr-SpsB is surprising as most of the predicted transmembrane residues have been removed. The detergent-dependent activity of

truncated SPase was first reported for *E. coli* LepB (Tschantz *et al.*, 1995). Among Gram-positive bacteria, a detergent-dependent activity of full-length signal peptidase has been reported in *S. pneumoniae* Spi (Peng *et al.*, 2001a), and in three of the four SPases (SipX, SipY and SipZ) of *S. lividans* (Geukens *et al.*, 2002). In *S. lividans,* a truncated SipY derivative devoid of the C-terminal anchor was shown to be stimulated by detergents, albeit to a lesser extent compared to the full-length (Geukens *et al.*, 2002). However, truncated SipS from *B. subtilis* was reported to have detergent-independent activity (van Roosmalen *et al.*, 2001). The effect of detergent on the truncated signal peptidase is most likely protein specific. Although it is not clear at this stage, the truncated SpsB probably has a better conformation in the presence of detergent which could partially make up for the lack of the hydrophobic membrane segment.

In chapter 2, we observed that the truncated derivative (tr-SpsB) lacking most of the transmembrane segment residues could process the preprotein substrate. In this chapter however, we show that despite no loss in cleavage fidelity is observed, the activity of this protein is 30-fold less compared to the full-length enzyme. The results highlight the importance of the transmembrane segment residues in the optimum activity of SpsB. Similar reduction in activity has been reported with truncated derivatives of LepB from *E. coli* and SipS from *B. subtilis* and it was also shown that these enzymes maintain their high *in vitro* cleavage fidelity (Carlos *et al.*, 2000b). Finally, we observed that the N-terminally truncated self-cleavage product of SpsB (sc-SpsB) is inactive, while tr-SpsB which has only 9 additional amino acids at the N-terminus remains active. These results indicate that some of the amino acid residues immediately preceding the catalytic Ser at the N-terminal part of SpsB sequence are essential for enzyme activity.

3.3 Experimental procedures

3.3.1 Specificity of the cleavage of the SceD peptide by SpsB

For the initial tests and validation of the FRET assay with SpsB, a small amount of the SceD peptide was obtained [synthesized by Bockstael K], while additional substrate for further work was procured from custom peptide synthesis (Peptide Protein Research Ltd). The specificity of cleavage was confirmed as described (Bockstael *et al.*, 2009a). In brief, SpsB and SceD peptide (at final concentrations of 1 μM and 500 μM, respectively) were incubated at 37 °C for 15 h in a total reaction volume of 40 μl. A negative control reaction without SpsB was included. The reactions were stopped by the addition of

trifluoroacetic acid. After centrifugation, supernatant from the samples were applied to a RP-HPLC column. The resulting fractions were collected, lyophilized and subsequently subjected to ESI-MS analysis.

3.3.2 FRET-based assay

The reaction mixtures in the FRET assay contained SpsB (pretreated with protease inhibitor cocktail - Complete, mini, EDTA-free, Roche Diagnostics) and SceD peptide (dissolved in DMF) at final concentrations of 1 and 10 μM, respectively, in the assay buffer (50 mM Tris-HCl, pH8 with 0.5 % Triton X-100) and the reactions were carried out in 96-well black, clear bottom microtitre plates (Greiner bio-one) at 37 °C in a total volume of 100 μl. The final concentration of DMF in the reaction mixtures was 1 %. The enzyme was initially pre-incubated in the buffer for 5 min at 37 °C and the reaction was started by the addition of the substrate. Fluorescence intensity measurements were taken as a function of time using an Infinite^{TM} M200 automated microplate reader (Tecan, Austria GmbH). The excitation and emission wavelengths used were 340 nm and 510 nm, respectively. The data obtained were fitted by non-linear curve fitting on Origin® Pro 7.5 (Microcal) using the equation $y = (A_0(1\text{-}e^{(-kt)})) + B0$, to get the first order rate constant $k = K_{obs.}$ The specific enzymatic activity was calculated using the equation $k_{cat}/K_m = k_{obs}/[Enz]$.

The specific enzymatic activity or apparent second order rate constant k_{cat}/K_m of the full-length and the truncated SpsB were measured using varying concentrations of the enzymes (freshly purified) and a fixed concentration of the peptide substrate, wherein $[S] << K_m$ (apparent). The final concentration of the substrate was 5 μM for the full-length and 2.5 μM for the truncated enzyme.

3.3.3 Activity at varying pH

For determination of optimum pH, the *in vitro* preprotein processing assay was carried out in the following buffers of varying pH: Glycine-HCl buffer pH 2; citric acid/sodium citrate buffer pH 3, 4 and 5; Clark and Lubs solutions-KH_2PO_4/NaOH pH 6 and 7; Tris-HCl buffer pH 7, 7.5, 8 and 8.5 and 9; glycine-NaOH buffer pH 9 and 10; carbonate buffer pH 10.9; phosphate buffer pH 11; hydroxide-chloride pH 12, prepared according to Dawson *et al.*, 1989.

The pH-rate profile using the synthetic SceD peptide was measured by calculating the k_{cat}/K_m values of the full-length enzyme incubated in buffers with varying pH. It should be noted that the freshly purified enzyme was stored at 4 °C for ~24 h prior to use. The reactions were carried out in a total volume of 100 µl with 1 µM final concentration of the enzyme. After pre-incubation of the reaction mixture for 5 min at 37 °C, the peptide substrate was added to obtain a final concentration of 5 µM ([S]<<Km). This was followed by measurement of fluorescence intensity as a function of time. The specific activity obtained was plotted as a function of pH using Eqn. 1 (see 3.1.2).

3.3.4 Stability at different temperatures

Purified SpsB (pre-treated with a general protease inhibitor) was aliquoted into polypropylene microfuge tubes (20 µl in each) and allowed to stand at different temperatures (27 °C, 37 °C or 4 °C) for a maximum of 9 days. All samples were initially stored at -80 °C and collected in the reverse order for incubation meaning that 9th day samples were incubated first followed by the 6th and the 4th and finally, 0 h sample was removed just before preparing the samples for loading on gel. For stability of SpsB in the presence of the inhibitor arylomycin A_2, 18 µl of purified full-length SpsB (31 µM stock concentration) was incubated with 2 µl arylomycin A_2 (2 mM stock concentration in DMSO) or DMSO (control) at 37 °C for 7 days. To these samples, 4 µl of 6x SDS-PAGE sample loading buffer was added and incubated for 10 min at 37 °C. The proteins were separated on 12.5 % w/v SDS-PAA gels followed by staining with CBB.

Chapter 4: Development and validation of *in vitro* inhibition assays for SpsB

In this chapter, we have focused on the standardization and evaluation of the SpsB-FRET assay described in chapter 3, as the primary assay for screening compounds that inhibit SpsB *in vitro*. Given the fact that the synthetic peptides are rather poor substrates for the SPases, we also set out to validate the preprotein processing assay, described in chapter 2. Although low-throughput this secondary assay is more relevant. It should be noted that for the inhibition assays, only full-length SpsB and not truncated derivative(s), was used.

4.1 Results

4.1.1 Set-up and validation of the SpsB-FRET (primary) assay for compound screening

4.1.1.1 SpsB activity as a function of time and enzyme concentration

Varying concentrations of the full-length SpsB (0.1 to 2 μM final concentration) and fixed concentrations of the SceD peptide substrate (5 and 10 μM final concentration) were tested in the FRET assay, described in chapter 3. A linear increase in signal was observed for all concentrations tested during the time-course of the assay (Figure 3.3, chapter 3). The linear regression analysis revealed R^2 values from 0.981 to 0.992 for the

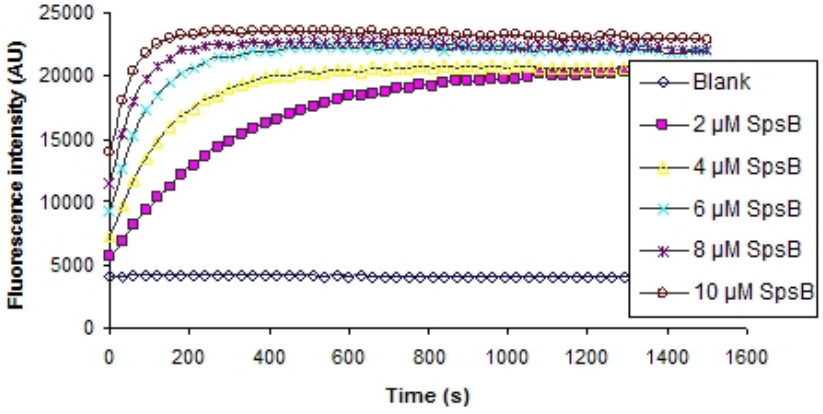

Figure 4.1: Time-course FRET assay with SpsB. Reaction mixtures containing different concentrations of SpsB (2 to 10 μM) in assay buffer were incubated for 5 min at 37 °C. Reactions were started by adding the synthetic SceD peptide (5 μM) and fluorescence intensity was measured as a function of time.

concentrations tested (0.2 to 1 μM) over a span of 870 seconds (data not shown). Complete processing as evidenced by no further increase in fluorescence intensity was achieved faster at higher enzyme concentrations. The complete processing of the substrate typically resulted in a 6-fold increase in signal from that of the initial value (Figure 4.1). Based on these results the enzyme concentration was fixed to a final concentration of 1 μM, while that of the substrate was fixed to 10 μM (where [S]<< K_m; predicted K_m value for the synthetic peptide is >100 μM) for initial studies. It should be noted that 5 or 2.5 μM (final concentration) of the substrate has also been used in some cases as indicated.

4.1.1.2 Initial velocity phase

It is important to ensure that the assays are conducted during the initial velocity phase in order to identify competitive inhibitors. The initial velocity is the best measure of enzyme reaction rate and this phase is most sensitive to reversible inhibitors (Copeland, 2005). The measurements were immediately stopped 30 minutes after the addition of the substrate and the data corresponding to the initial velocity phase were analyzed.

4.1.1.3 *In vitro* inhibition of SpsB in the presence of SPase inhibitor arylomycin A_2

As part of the validation of the FRET assay, the SPase inhibitor arylomycin A_2,was added to the reaction mixture. In the presence of the inhibitor, no increase in fluorescence intensity was observed during the time-course of assay (Fig. 4.2a), confirming that the peptide remains uncleaved, when the enzyme activity is inhibited. A dose-dependent response to arylomycin A_2 was plotted (Fig. 4.2b) and the IC_{50} of the inhibitor against SpsB was found to be 1 μM (0.82 μg/ml). Additionally, the protocol for this assay and the enzyme were used for testing a set of rationally designed lipopeptides of which the best compound, a peptide aldehyde inhibitor was shown to have an IC_{50} of 0.09 μM against SpsB (Buzder-Lantos *et al.*, 2009).

4.1.1.4 Microplate uniformity test

Prior to compound screening, it is important to test plate uniformity or signal variability between individual wells of a microplate. For this purpose, positive controls (with enzyme, substrate and DMSO in assay buffer) giving the maximum signal and negative controls (with substrate and DMSO in assay buffer but not the enzyme) giving minimum or the background signal were set up in a 96-well plate. The final concentrations were 1 μM of the enzyme and 2.5 μM of the substrate in a total volume of 100 μl. DMSO was

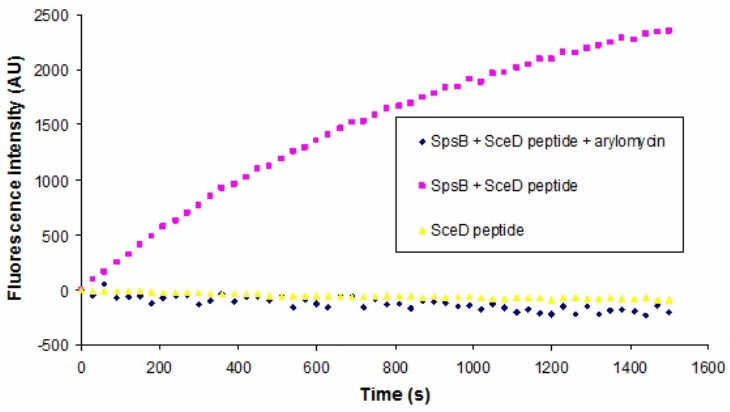

(a)

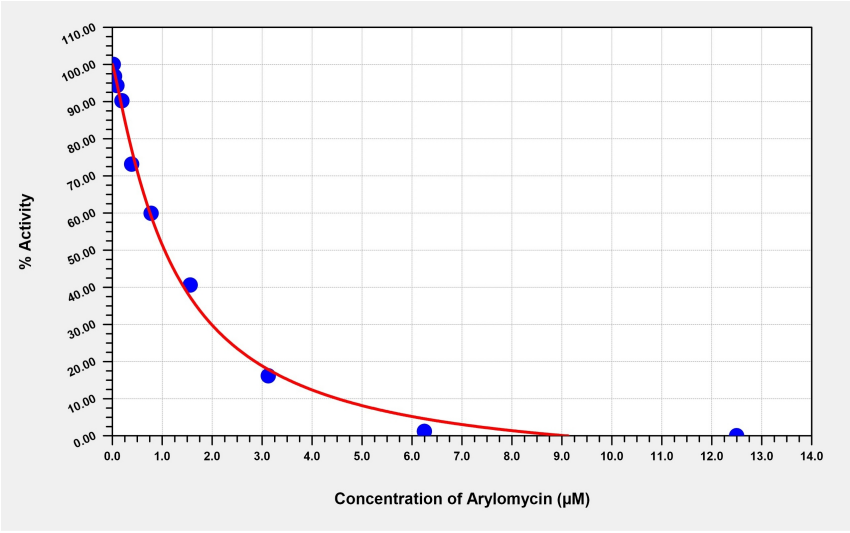

(b)

Figure 4.2: Inhibition of SpsB activity by arylomycin A_2 in the FRET assay. (a) Time-based scan: SpsB (1 μM final concentration) was incubated without or with arylomycin A_2 (10 μM final concentration) for 15 minutes at 37 °C followed by the addition of SceD peptide (5 μM final concentration). Fluorescence intensity was measured as a function of time. **(b) Dose-dependent response**: The assay was carried out with SpsB (1 μM final concentration) incubated with different concentrations of arylomycin A_2 (from 20 μM to 0.0244 μM) followed by the addition of the peptide (10 μM final concentration). Percent SpsB activity was plotted as a function of inhibitor concentration (using curve expert 1.3: http://userpages.xfoneusa.net/~dhyams/cmain.htm) to obtain the IC_{50} value arylomycin A_2 against SpsB.

present at a final concentration of 10 %. All additions were done manually using single channel pipettes and the readings were taken immediately after the addition of the peptide substrate. Upon data analysis it was confirmed that the readings are consistent throughout the plate, with a minor but negligible difference between the ends and center of the plate (Figure 4.3; Table 4.1). Subsequently, multichannel and repeat pipettes were used for preparing reaction mixtures which minimizes the handling times and improved the uniformity of the signals (data not shown).

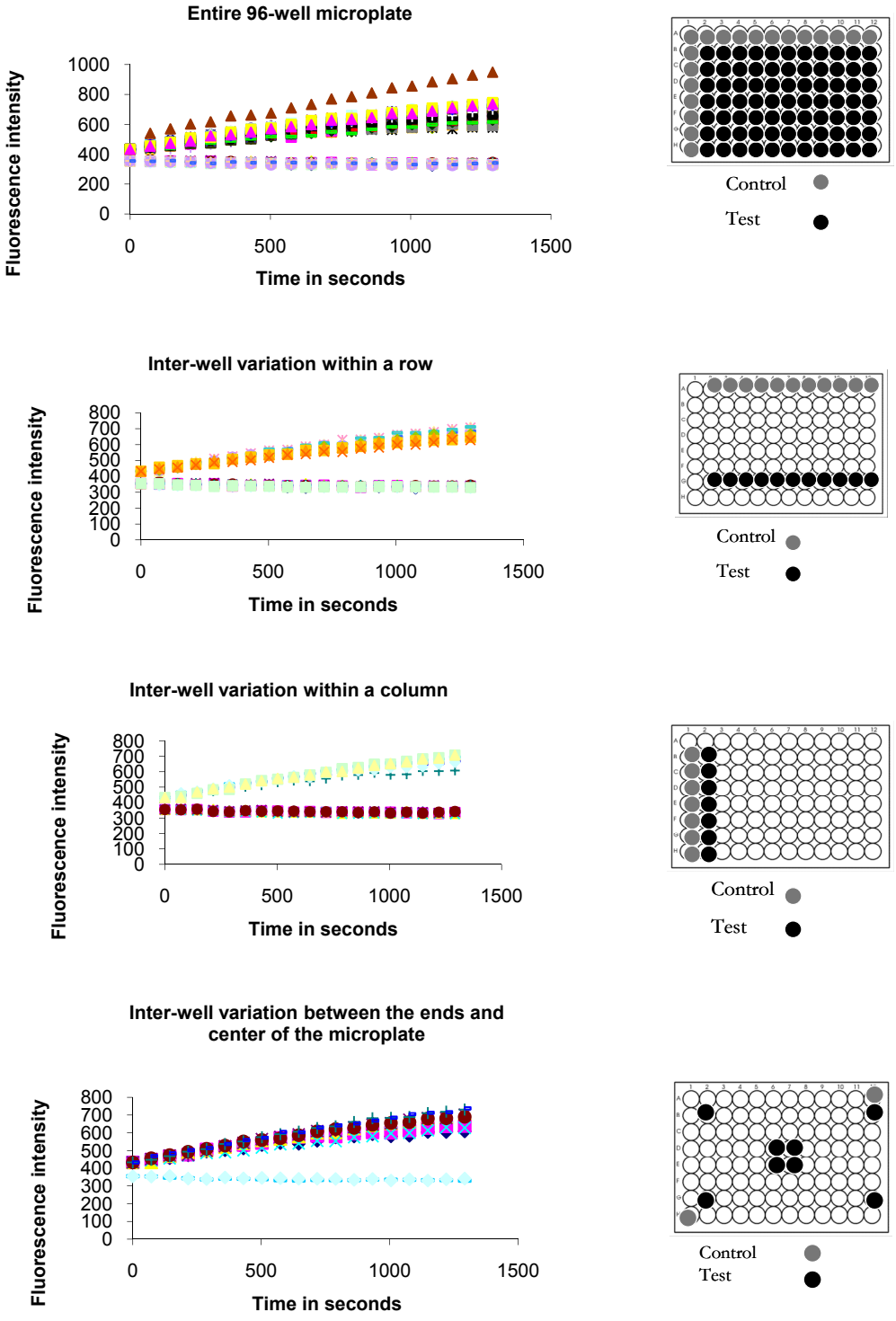

Figure 4.3: Plate uniformity test. The positive and negative control reactions (with and without the enzyme, respectively) were set up in a single microtitre plate in the format indicated. The data corresponding different parts of the plate are indicated. The colour lines indicate samples from different wells. The signal remains constant over time in control reactions compared to a progressive increase in signal intensity in the test samples.

Table 4.1: Signal variation within a microtitre plate

Area in the microplate	***Slope (average)***	***Standard deviation***	***Slope (average)***	**Standard deviation**
	Negative control	Negative control	Positive control	Positive control
Rows	-0.01396	0.001111	0.191033	0.020282
Columns	-0.01684	0.002516	0.208807	0.064613
Ends	-0.01409	0.00055	0.164554	0.02845
Center	N/A	N/A	0.218694	0.014791
Entire plate	-0.01497	0.002221	0.195133	0.037028

4.1.1.5 DMSO compatibility

Since compounds to be tested are routinely dissolved in DMSO, solvent compatibility in the assay was also tested. It was observed that the assay is compatible with DMSO up to 10 % (v/v) (data not shown) and therefore the reactions were carried out at a maximum of this concentration of the solvent.

4.1.1.6 Inter-plate and inter-day variation

The assays were carried out for three consecutive days to check for inter-plate as well as for inter-day and intra-day variation. The analysis showed that the variations between these data sets were negligible and the assay quality was satisfactory (data not shown). The quality of the enzyme (temperature and duration of storage) is important for maintaining the assay quality. As discussed in chapter 3, even storage for a long period at 4 °C decreased the activity of the enzyme. Freshly purified enzyme was stored at 4 °C and used within a period of three days.

4.1.2 Set-up and validation of the SpsB-preprotein processing (confirmatory) assay for testing positive compounds

The SPase inhibitor arylomycin A_2 was also tested in the preprotein processing assay, discussed in chapter 2. In the presence of the SPase inhibitor, the substrate pre-IsaA remained unprocessed by SpsB (Figure 4.4). Similarly, another SPaseI inhibitor (5*S*,6*S*)-6-[(*R*)-acetoxyethyl]-penem-3-carboxylate (a kind gift from Glaxo Smith Kline, Harlow,

UK) could inhibit preprotein processing by SpsB (data not shown). These observations confirmed the suitability of the *in vitro* assay for confirming hits obtained from the primary assay. Additionally, the presence of DMSO up to 10 % (v/v) or the presence of a non-SPase inhibitor (up to 5 mM final concentrations) did not affect preprotein processing by SpsB (data not shown).

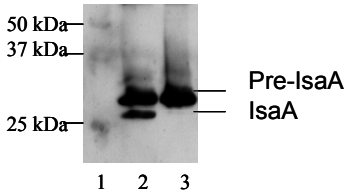

Figure 4.4: Preprotein processing by SpsB blocked by arylomycin A_2 SpsB and pre-IsaA (1 and 10 μM final concentrations, respectively) were incubated without and with arylomycin A_2 (200 μM final concentration) for 15 h at 37 °C. The proteins were separated on 12.5 % (w/v) SDS-PAA gels and analyzed by Western blotting and chemiluminescent detection. Lane 1, molecular weight marker; Lane 2, pre-IsaA processing by SpsB; Lane 3, pre-IsaA processing blocked by arylomycin A_2.

4.1.3 Manual screening and further analysis of compounds

Manual screening was carried out in 96-well plates with at least two positive and negative controls. The standard protocol involved the addition of enzyme and the compounds (at 1 μM and 200 μM final concentrations respectiveley) to the assay buffer followed by a brief incubation and the addition of the SceD peptide substrate (10 μM final concentration). The fluorescence intensity was measured over a period of 30 min. The reactions were carried out in a total volume of 100 μl at 37 °C. The percent activities relative to the positive control reactions were calculated. The threshold for hit calling was set to 60 % inhibition of the enzyme activity. Around 6,200 compounds obtained from different sources were screened manually in the FRET assay against SpsB. The compounds tested consisted of synthetic compounds (received from the lab of Prof. Dr. Erik Van der Eycken, K.U.Leuven), small molecules from the chemical compound libraries of the Rega Institute and Center for Drug Design and Discovery (CD3), rationally designed peptides based on modeling into the active site of LepB (received from Prof. Dr. Joost Schymkowitz, VUB, Brussels) and small molecules based on virtual screening using the crystal structure of LepB [received from Center for Innovation and Stimulation of Drug Discovery (CISTIM), Leuven].

The primary screen with the FRET assay did not result in any compound reaching the set threshold (>60 % inhibition of SpsB activity). The compounds obtained from virtual screening also did not significantly inhibit SpsB or *E. coli* LepB in the FRET assay. Nevertheless, we observed that most of the compounds from *in silico* screening were able to inhibit *E. coli* LepB *in vitro* to a greater extent in comparison with SpsB. We found that a number of compounds interfered with fluorescence. Approximately 1 % of the total number of compounds screened could not be interpreted correctly due to this reason, and hence, were tested in the preprotein processing assay. None of these compounds did inhibit preprotein processing by SpsB. They were also subsequently ruled out as potential inhibitors after confirmation of their interference in the assay by testing them in the absence of the enzyme but in the presence of the peptide substrate.

In order to possibly minimize the interference of the test compounds in the FRET assay, a new peptide with an identical sequence as the SceD peptide, except for an additional C-terminal Lys and with a new FRET pair (5-FAM/5-TAMRA), was procured. The additional Lys at the C-terminus of the peptide was required to attach the 5-TAMRA to the side chain amine. Unfortunately, the peptide was not recognized and cleaved by SpsB in the FRET assay using excitation and emission wavelengths of 485 and 520 nm, respectively. However, the peptide could be non-specifically cleaved by proteinase K as evidenced by a significant increase in fluorescence intensity compared to a control without the peptide.

4.2 Discussion

For a biochemical assay with a potential high-throughput screening application it is necessary to ensure reproducibility and reliability of the output data. This chapter focuses on the pre-screen and in-screen evaluation of the SpsB-FRET assay. The initial conditions for the FRET assay were standardized and the *in vitro* inhibition of SpsB in this assay was first demonstrated using the known SPase inhibitor arylomycin A_2. Pre-screen evaluation included the study of signal variation within a microplate, storage and compatibility of the assay components and comparison of inter-day and intra-day data.

After the initial tests were positive, manual screening was commenced with compounds (small molecules/peptides) from different groups. The criterion for selecting a compound from the primary screen was set initially to 60 % inhibition of SpsB in the *in*

vitro assay. The maximum inhibition that could be achieved was 40 % and given the high concentration of the inhibitor used in the assay, this activity was not considered significant. One of the shortcomings of the FRET assay is its incompatibility with compounds that are autofluorescent or those that interfere with fluorescence. Many such compounds were observed and those that could not be clearly distinguished (61 compounds i.e., 1 % of the total compounds tested) were analyzed in the preprotein assay but none of these compounds were inhibitory. However, it should be noted that the preprotein assay is much more stringent than the FRET assay as the affinity of the enzyme for the preprotein is much higher than for a short peptide. A much higher inhibitor concentration (at least a 100-fold higher concentration compared to that used in the FRET assay) is required for inhibition of preprotein processing by SpsB. Although it is possible to distinguish a potent inhibitor from a non-inhibitor in the preprotein assay, it is difficult to analyze weak inhibitors in this assay, since the assay is semi-quantitative at best. The FRET assay can potentially identify weak inhibitors as long as they do not interfere with fluorescence. To find out if the problem of fluorescence interference by the compounds could be lowered, a peptide substrate with a new FRET pair was obtained. Although theoretically this should not affect the behaviour of the substrate, it could not be processed by SpsB. The reason for the inability of SpsB to process this new peptide remains unclear. It might be a result of steric hindrance caused by the dye which is attached to the side chain of Lys. In contrast, the EDANS/DABCYL peptide substrate has the FRET pair in the main chain of the peptide.

Given that the crystal structure of SpsB is not available, rational approaches for designing/finding effective inhibitors are pretty limited. There is less than 30 % sequence identity among SpsB and *E. coli* LepB which makes it difficult to come up with a homology model of SpsB based on the known crystal structure of LepB. Among the compounds screened against SpsB, a set of 124 compounds were based on *in silico* screening of compounds in the active site of *E. coli* LepB. With the limited number of such compounds tested in the FRET assay, we did not see significant inhibition of SpsB or LepB *in vitro*, although we observed that most compounds were comparatively better against *E. coli* LepB. This again implies that there are subtle differences among the two signal peptidases. Nevertheless, this approach holds potential in finding a broad spectrum inhibitor.

Despite screening over 6,000 compounds we could not come up with a single potent inhibitor. This in fact is not very surprising as we can see from the literature that SPasesI have been difficult targets as far as finding effective inhibitors are concerned. As already mentioned, the type I signal peptidases are resistant to the general protease inhibitors against the four different classes of proteases. Ever since the SPasesI were proposed as targets more than a decade back, efforts from different groups resulted in only the few potent inhibitors that have been described (chapter 1; Table 1.2). These inhibitors were obtained using two different approaches, one of which is the classical approach by rational modification of lipopeptides based on preprotein sequence data. The second is the screening approach to possibly obtain new classes of inhibitors, which is also the focus of this and the preceding chapter. A fluorimetric assay (similar to the one described in this chapter) was used by a group at Eli Lilly and company for high-throughput screening of 50,000 pre-fractionated natural samples against signal peptidase *S. pneumoniae*, Spi (Kulanthaivel *et al.*, 2004). This work by Kulanthaivel and co-workers led to the identification of a single sample with reproducible activity – the lipoglycopeptide inhibitors (see chaper 1). There is no literature available on how the inhibitory activity of arylomycins against the SPases was found as the first report on this inhibitor was the crystal structure of Δ2-75 SPase in complex with the arylomycin A_2 (Paetzel *et al.*, 2004). It is not clear whether the structural similarities between lipoglycopeptides and arylomycins subsequently led to the antibacterial activity of arylomycins being attributed to their inhibition of SPases. Another pharmaceutical company where extensive studies on SPase inhibitors were undertaken is SmithKline Beecham Pharmaceuticals (now GSK) (Harlow, Essex, UK). Their work started when very little was known about the catalytic centre of SPasesI and later when evidence started accumulating in favour of SPasesI being a serine protease utilizing a Ser/Lys catalytic dyad mechanism (around 1992-1993), they began screening a range of compounds from a large in-house collection of beta-lactam containing compounds (Allsop *et al.*, 1995). Their compound collection is said to have consisted of inhibitors developed against bacterial beta-lactamases, transpeptidases and carboxypeptidases; enzyme families that are also based on a serine/lysine catalytic dyad (Allsop *et al.*, 1995). This led to the discovery of the 5S penems inhibitors and their optimization work culminated in the identification of the compound allyl (5*S*,6*S*)-6-[(*R*)-acetoxyethyl]-penem-3-carboxylate (Black and Bruton, 1998).

Comparatively, the number of compounds screened here (this chapter) and random screening is indisputably a matter of chance. However, we ruled also out the possibility that the low success rate might just be a reflection of the assay quality by assessing the reliability of the FRET assay based on the method described by Zhang and co-workers (Zhang et al., 1999). In addition, we have demonstrated *in vitro* inhibition of SpsB in the FRET assay using two different inhibitors under the same conditions described in this chapter. Apart from the random screening approach it was also our intent to try and obtain structural data on SpsB to be able to carry out virtual screening and subsequently test the interesting compounds *in vitro*. The purified full-length SpsB and the truncated active and inactive SpsB were provided for crystallization trials to Prof. Dr. R. Loris (VUB, Brussels), under a collaborative project. The crystallization trials so far have been unsuccessful due to problems of instability of the active forms and aggregation observed in the truncated inactive mutant of SpsB.

4.3 Experimental procedures

4.3.1 *In vitro* inhibition of pre-IsaA processing by SpsB

For the preprotein assay in the presence of inhibitor, arylomycin A_2 (200 μM final concentration) was added to a reaction mixture containing SpsB (1 μM final) in the assay buffer and the samples were incubated for 5 minutes at 37 °C followed by the addition of pre-IsaA (10 μM). After incubation for 15 h at 37 °C, the reactions were stopped by addition of 4 μl of 6 x SDS-PAGE sample loading buffer. The proteins were separated by SDS-PAGE using 12.5 % (w/v). Western blotting and immunodetection were carried out as described in chapter 2, section 2.3.7.

4.3.2 FRET assay with the inhibitor arylomycin A_2:

The inhibitor arylomycin A_2 (Baselia Pharmaceutica) was dissolved in DMSO and diluted to obtain different stock concentrations. For the *in vitr*o assay, the reaction mixtures containing SpsB (1 μM final concentration) with different concentrations of arylomycin A_2, were incubated in the assay buffer for 15 minutes. The final concentration of DMSO in each reaction mixture was 2 %. The fluorogenic synthetic peptide SceD (5 or 10 μM) was added and fluorescence intensity was measured (using excitation and emission wavelengths of 340 and 510 nm, respectively) as a function of time. For dose-dependent response and determination of IC_{50}, ten different concentrations of arylomycin A_2 were used (two-fold serial dilutions starting from 12.5 to 0.0244 μM final concentration) and

the substrate concentration was 10 μM (final). Percent inhibition was calculated using the equation $[(1-(v_i/v_0)] \times 100$, where v_i is the initial velocity in the presence of inhibitor, v_0 is the initial velocity in the absence of inhibitor. The IC_{50} value was determined by fitting the percentage inhibition versus inhibitor concentration using the MMF model for sigmoidal curve (see following equation).

$$y = \frac{ab + cx^d}{b + x^d} \qquad \text{Equation 2}$$

4.3.3 SpsB-FRET assay for compound screening

The assay was carried out in black transparent bottom 96-well microplates (Greiner) in a total volume of 100 μl. The full-length SpsB premixed in the assay buffer was dispensed (90 μl of 1.1 μM stock of the enzyme) in each well (except for the negative control) followed by the addition of 10 μl of the test compound (or DMSO in case of the positive control). To the negative control reactions, 90 μl of buffer without the enzyme was added, followed by the addition of DMSO. The reactions were incubated for 5 minutes at 37 °C followed by the addition of 1 μl of the SceD peptide (1 mM stock in DMF) and fluorescence intensity measurement (using excitation and emission wavelengths of 340 and 510 nm, respectively; time interval of 30 sec for a total number of 65 cycles). The fluorescence intensities obtained were first scaled to zero. Next, the end values (final measurement at 30 min minus the initial measurement) for each compound was converted to percent activity with respect to the positive control (without the inhibitor).

Chapter 5: High-throughput screening of compounds against SpsB and analysis of possible hits

In this chapter, the transfer of the SpsB-FRET assay from the research lab to a high-throughput screening center is described. The assay transer was carried out from the laboratory of Bacteriology, Rega Institute, K.U.Leuven to CISTIM, Leuven, in close collaboration with CD3, K.U.Leuven. The process of assay transfer towards automation requires a pre-assessment of the consistency and quality of data that can be obtained. To this end, possible modifications were made to the existing protocol and the assay was fine-tuned with the input from ing. Hugo Klaassen (Director, high-throughput screening facility, CISTIM).

5.1 Results

5.1.1 Assay transfer

Inter-day as well as intra-day data were obtained from the FRET assay carried out during a two-day period. The assays were carried out in 384-well plates in the same format as that used for the final screening (described in 5.1.3), except that it was done manually. Analysis of data indicated that the assay was reproducible and consistent (data not shown). The process of automation was carried out in steps starting with four 384-well plates per day till up to twenty four 384-well plates per day.

5.1.2 SpsB purification for HTS

For high-throughput screening of the compounds, SpsB was purified in large quantities (to cover for 50,000 data points), pooled, aliquoted and stored at -80 °C until use. The enzyme was not subjected to freeze and thaw cycles and aliquots once drawn from -80 °C were maintained at 4 °C until its use on the same day. The purity of SpsB was assessed by SDS/PAGE followed by CBB staining. On an average, the concentration amounted to approximately 13 μM or 0.3 mg/ml which was statisfactory for the *in vitro* assay.

5.1.3 Set-up of compound library screening

The full-length SpsB (0.25 μM), the test compound (10 μM) and lastly the substrate (5 μM) at the final concentrations indicated were added to the assay buffer. The total volume of each reaction mixture was 50 μl and the final concentration of DMSO was 2

% (v/v). Fluorescence intensity was measured at a single, fixed time point, 45 min after the addition of the substrate. Fixed-time point measurements also significantly increased the number of compounds that could be tested in comparison with the time-course assays. Attempts to stop the reactions after 45 minutes for end-point measurements did not prove to be successful (data not shown). The reactions were carried out at RT (22 °C). We did not observe significant difference resulting from running the assay at either 37 °C (previously used) or at 22 °C (data not shown). Reactions containing DMSO but without the test compounds served as negative controls while those containing the peptide aldehyde inhibitor (Buzder-Lantos *et al.*, 2009) served as positive controls in the assay. Raw data were converted into percent inhibition (PIN), which is given by (1-(sample-μ_{C+})/(μ_{C-}- μ_{C+}))*100, where μ_{C+} and μ_{C-} are the means of positive and negative controls, respectively. Inter-day data were obtained from independent experiments carried out on two days using this adapted protocol and analyzed before assay transfer. Analysis and final validation of the assay quality is described below.

5.1.4 Quality of the screen

The assay was calibrated using the peptide aldehyde inhibitor. Each 384-well plate contained 32 positive controls with the SPase inhibitor and 32 negative controls without

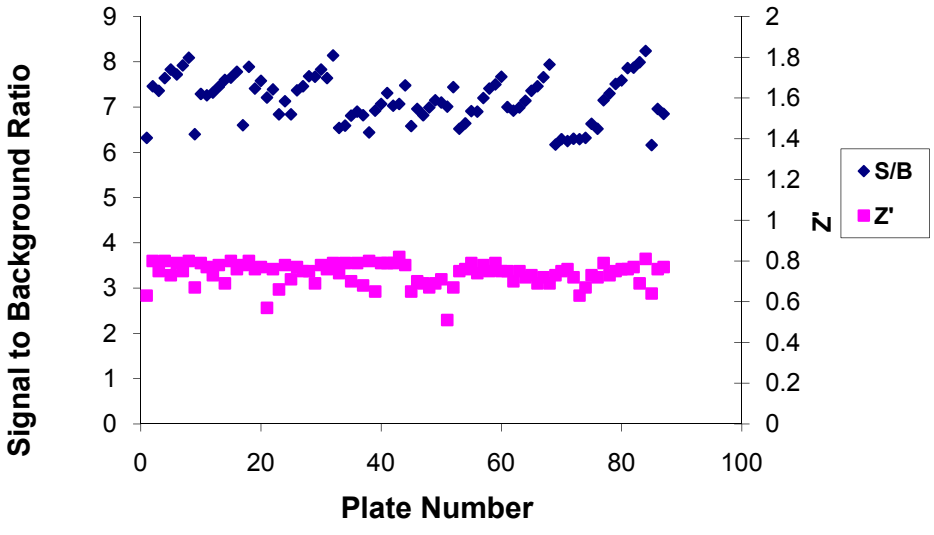

Figure 5.1: Assessment of assay quality. Each microplate for compound screening contained 38 positive controls (SPase inhibitor) and 38 negative control (DMSO) reactions. Z' value and signal-to-background ratio for each plate was obtained as described (see text)

compound but with DMSO. The quality of data obtained from screening was assessed by calculating the Z' factor (Zhang *et al.*, 1999) using the formula

$$\text{Z Prime or Z'} = \quad 1 - \frac{(3\sigma_{c+} + 3\sigma_{c-})}{|\mu_{c+} - \mu_{c-}|}$$

Where, σ_{C+} and σ_{C-} are standard deviations of positive and negative controls, respectively while μ_{C+} and μ_{C-} are the means of positive and negative controls respectively. According to Zhang and co-workers, for an assay to be considered good for high-throughput screening the Z' factor has to be ≥0.5. Prior to assay transfer, manual testing using the 384-well format resulted in an average Z' factor of 0.65. The analysis of the data quality from the SpsB inhibitor screening is summarized in (Fig. 5.1). Also indicated in Fig. 5.1 is the signal-to-background ratio denoted as S/B (=mean signal/mean background) which is another expression that is also used to indicate the quality of an assay. As seen in the figure, the Z' factor during screening remained ≥0.5 with an average Z' factor of 0.73 for the entire screen, indicating that the assay is robust.

5.1.5 Screening results and follow-up tests

An entire library of compounds from the Centre for Drug Design and Discovery (CD3) library compounds (25,621 in total) was screened. This library contains a wide variety of compounds, selected from an original 5 million compounds. Molecules were obtained from various sources worldwide after applying various filters including the Lipinski rule and some filters used by pharmaceutical companies to eliminate compounds that are toxic or poorly absorbed. The compounds from CD3 that were screened manually (from the compound library and those based on *in silico* screening data) were re-screened along with the rest of the compounds. Apart from the CD3 library, a set of 182 compounds were also screened from the chemical compound library of the Rega institute. The compounds that interfered with fluorescence (approximately 1 %) were not considered in the test. The final threshold for hit calling was set to >25 % inhibition. The three most active compounds were re-confirmed in an independent experiment and analyzed further.

5.1.5.1 Dose-response for active compounds

Dose-dependent response was observed against *S. aureus* SpsB with IC_{50} of 36 μM (JRD2191), 51 μM (JRD2189), 34 μM (CL018090) for the active compounds (codes mentioned in brackets) and IC_{50} of 0.23 μM for the positive control (peptide aldehyde).

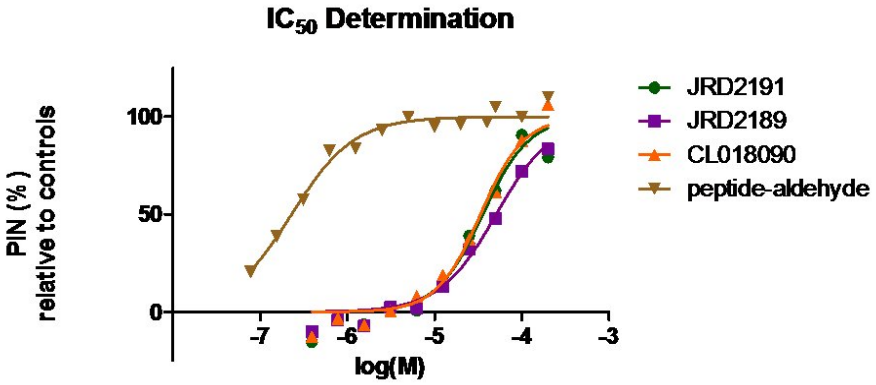

Figure 5.2: Dose-response curves for selected active compounds in the SpsB-FRET assay. The SpsB-FRET assay was repeated with the selected active compounds at varying concentrations from 200 µM (diluted two-fold) to 0.39 µM. Percent inhibition was plotted in function of compound concentration. Peptide aldehyde inhibitor was used as the positive control.

5.1.5.2 Preprotein-processing assay

The preprotein processing assay was carried out using different concentrations of the test

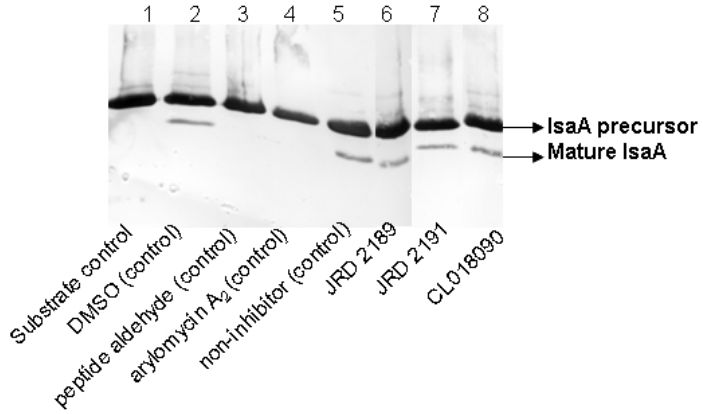

Figure 5.3: Analysis of the hits in the preprotein processing assay. The preprotein assay was set up with the following components at final concentrations indicated between brackets: pre-IsaA (5 µM), SpsB (0.25 µM), test compounds or known inhibitor (500 µM) and incubated for 15 h at 37 °C. The proteins were separated on SDS/PAA gels and analyzed by western blot followed by chemiluminiscent detection. Two negative controls (DMSO and a compound that does not inhibit SpsB activity) and two positive controls (peptide aldehyde and arylomycin A_2) were included.

compounds (100 µM, 200 µM, 500 µM, 1 mM and 5 mM) and with appropriate controls. The concentration of the enzyme and the substrate were the same as those used in the SpsB-FRET assay. Unfortunately, the selected active compounds did not inhibit preprotein processing (see Fig. 5.3) and hence cannot be regarded as potent inhibitors as such.

5.1.5.3 FRET assay with *E. coli* lepB

The three active compounds (JRD 2189, JRD 2191 and CL018090) behaved similarly showing a dose-dependent inhibition of *E. coli* SPase activity *in vitro* (data not shown). The slope values obtained from the progress curves of the reaction, correlated directly with the concentration of the active compounds. An increase in concentration of the compound resulted in lower slope values.

5.1.5.4 Interference with fluorescence

During further analysis, it was observed that two of the active compounds, when present at high concentrations, (>100 μM) actually quenched fluorescence to a certain extent (Fig. 5.4). This was confirmed by running the assay in the presence of the peptide

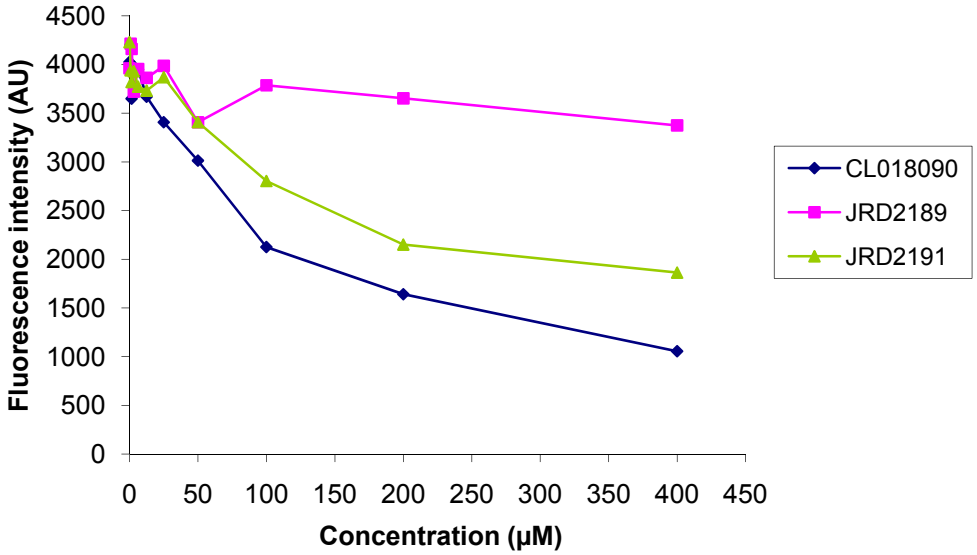

Figure 5.4: Test compounds with the peptide substrate - The compounds that were active in the SpsB-FRET assay were retested in the absence of the enzyme. Fluorescence intensity was measured for each of the compound wells containing a different concentration of the test compounds.

substrate alone without the SPases (SpsB or lepB). JRD 2189 was the only compound that was effective against *E. coli* SPase and did not interfere with fluorescence.

5.1.5.5 Antibacterial activity test

Antibacterial susceptibility tests against *S. aureus* and *E. coli* were not positive (up to 500 μg/ml) for these selected compounds.

5.2 Discussion

In this chapter, we have optimized the SpsB-FRET assay for automated high-throughput screening of potential SpsB inhibitors. The screening protocol was modified to improve efficiency and make it economically feasible. The changes include a decrease in the concentration of the assay components, a reduction in the total reaction volume, a change in the microplate format, the use of a SPase inhibitor as positive control, a change in assay temperature (RT) and finally a fixed time-point measurement. Peptide aldehyde inhibitor was preferred over arylomycin as positive control as the former does not interfere with fluorescence. Arylomycin A_2 interferes with fluorescence in the SpsB-FRET assay to a certain extent, especially at higher concentrations. Nevertheless, its inhibitory activity against SpsB is very clear as the fluorescence intensity of the reaction mixture remains largely unchanged during the time-course of the FRET assay. We have shown that the assay is robust (Z' value of 0.73) and suitable for screening chemical compound libraries. It is now possible to screen more than 10,000 compounds per day. About 27,000 compounds were screened which include the entire CD3 library and a few others (~260 compounds from Rega library and a few compounds selected based on virtual screening data). None of the hit compounds analyzed so far were good enough to be used directly. The hit compound JRD2189 could be further analysed by computational docking of the molecule into the active site of *E. coli* SPase. Although this compound is not very potent, it could serve as a starting point for further modifications.

Compounds interfering with fluorescence are not compatible for high-throughput screening using the FRET assay since the assay is based on fixed time-point measurements which are compared with controls. Such compounds were treated as outliers and eliminated from further analysis. At the moment, it is difficult to test such compounds rapidly. In future, it might be interesting to run a parallel screen on a Biacore 3000 instrument (or higher). This approach of parallel testing for inhibitory activity in the FRET assay as well as analysis of the affinity of the compounds for the immobilized enzyme on a Biacore system could possibly increase the number of compounds that can be tested. If any of the autofluorescent compounds show good *in vitro* affinity for the enzyme, they can be tested in the preprotein processing assay. In addition, the dual approach could facilitate better interpretation of low-affinity inhibitors. In the present set-up, although the FRET assay can fish out low-affinity inhibitors (as long as they do not interfere with fluorescence) the preprotein assay might possibly eliminate these. We

also analyzed the selected active compounds against *E. coli* LepB in the FRET assay to partly address the problem of validating these inhibitors. For this, however, the inhibitor has to have a broad specificity to be able to inhibit both enzymes. The active compound JRD2189 could inhibit both the SPases to a limited extent *in vitro*. However, it remains to be seen whether the compound could be modified further based on modelling data.

The hit rate in the FRET assay has been disappointingly low with the small molecule screening, although it might be too early to conclude that small molecules are not ideal candidates for this target. However, the prospects for pursuing this line of work remains, with several interesting possibilities. For example, it might be interesting to test natural compounds produced by certain micro-organisms in order to survive in their natural environment (secondary metabolites). Such compounds have been indispensable in the area of antibacterial drug discovery. Arylomycins and lipoglycopeptide inhibitors of signal peptidases are examples of this type of molecules. Natural products are proposed as optimal candidates for antibacterial drug screening as they have optimal cellular penetration and privileged structures to interact with finite structural spaces in protein folds (Devasahayam *et al.*, 2010). In recent years, another school of screening that has been pursued in target-based drug discovery process is the fragment-based method for identifying lead compound(s). This involves screening fragments or scaffolds which are of lower molecular weight (MW < 200 Da) than the molecules that are typically found in high-throughput compound collections. Once fragment hits are found to act against a target protein, they are then grown, linked or decorated to larger, drug-sized compounds often using structure-guided medicinal chemistry (Jhoti, 2005). The fragments often exhibit lower affinities (μM to mM) but then fragment-to-lead activity typically allows the affinity to be increased by 3-5 orders of magnitude after synthesis of less than 100 compounds (Jhoti, 2005). The assays developed in this work should enable further screening with different kinds of compound libraries. Additionally, if and when the crystal structural of SpsB becomes available, *in vitro* screening could be complemented with virtual screening to improve the chances of obtaining hit compounds.

5.3 Experimental procedures

5.3.1 Assay components (Preparation and storage)

Assay buffer (50 mM Tris HCl pH8 with 0.5 % Triton X-100) was prepared fresh for every batch of screening and kept at RT. Compounds from the CD3 library were

dissolved in 100 % DMSO to a 5 mM concentration using an automated liquid handling system (Evo-200, Tecan) and diluted (1:25) in assay buffer (to obtain a 200 μM working solution of the compound) for immediate use while the rest was stored at -20 °C. The compounds from Rega Library were prepared as 10 mM stocks in DMSO, dispensed manually into 96-well storage plates and stored at -20 °C O/N. The subsequent dilution in assay buffer (to obtain 200 μM) was carried out at CISTIM prior to screening. The stock solution (1 mM) of SceD peptide substrate was prepared in DMF starting from the lyophilized powder stored at -20 °C, or prepared a day in advance and stored as aliquots at -20 °C. The SPase inhibitor peptide aldehyde was obtained commercially (PeptideSynthetics, Peptide Protein Research Limited, UK). SpsB was purified as indicated in 2.3.4 (chapter 2) in large batches. After analysis by SDS/PAGE followed by CBB staining the purified fractions were pooled, quantified, aliquoted and stored at -80 °C.

5.3.2 Compound screening (standardized protocol)

The standardized tests were carried out in 384-well full black plates (Greiner). The enzyme was pre-mixed in the assay buffer and 42.5 μl of this solution was dispensed in each well using a plate dispenser (Xrd- 384, fluidx). The first and last two rows in the 384-well plate were used for control reactions. To the top half of the first and last two rows, 2.5 μl of DMSO was added. To the bottom half of the first and last two rows 2.5 μl of peptide aldehyde inhibitor (200 μM stock in assay buffer) were added manually. Next, 2.5 μl of the test compounds (200 μM in assay buffer) was added to each well and mixed using a liquid handling robot. Finally, 5 μl of the substrate, freshly diluted in assay buffer (50 μM working solution), was added to each well. The plates were centrifuged at 314 x g for 1 minute followed by incubation in dark (as the substrate is photosensitive) for 45 minutes at 22 °C. Fluorescence intensity was measured (during the initial velocity phase) 45 minutes after the addition of the substrate, using a microplate reader (Envision 2104, Perkin Elmer). The raw data obtained from screening was converted to percent inhibition using Pipeline Pilot software (Accelrys).

5.3.3 Dose-response

The stock solutions of selected compounds were prepared freshly and diluted (two-fold) in 100 % DMSO. The concentrations of the stock solutions ranged from 10 mM to 0.0195 mM for the compounds and 1 mM to 0.00195 mM for the peptide aldehyde

inhibitor. The assay was carried out as indicated above with positive controls in the first and last two columns. The data analysis was carried out using Graphpad prism software.

5.3.4 Additional tests

5.3.4.1 FRET assay with *E. coli* lepB

The plasmid carrying *E. coli* SPase encoding gene was obtained and LepB was overproduced and purified as described (Bockstael *et al.*, 2009a). The purification protocol was essentially the same as that for the full-length SpsB except that the Ni^{2+}-NTA column was washed twice with buffer containing 20 mM imidazole prior to elution with a buffer containing 250 mM imidazole (omitting the previous step of elution with buffer containing 100 mM imidazole). The FRET assay was set up and dose-response studies with the compounds of interest were carried out as described for SpsB.

5.3.4.2 Preprotein assay

The assay was carried out as described in chapter 4 except that for each compound multiple concentrations were used.

5.3.4.3 Antibacterial activity tests

Antimicrobial susceptibility testing against *E. coli* DH5 alpha and *S. aureus* ATCC 65388, was carried out according to standard procedures using the broth microdilution method in LB medium (NCCLS, 2003).

Chapter 6: General discussion and future perspectives

S. aureus may occur as a commensal, but is also a pathogen responsible for a wide array of infections. The problem of multi-drug resistance in *S. aureus* is a reason for the growing concern in the medical community. Given the emergence of resistant strains in community and hospital environments, an urgent need for new classes of antibiotics has surfaced. This has led to an interest in new antibiotic target sites in the bacteria for possibly minimizing cross-resistance to any new drug. The type I signal peptidases are considered attractive targets thanks to their good accessibility and prokaryotic exclusivity. The *S. aureus*, genome encodes two SPaseI homologues namely SpsA and SpsB. It appears that SpsA is inactive as it lacks the catalytic Ser and Lys residues (replaced by Asp and Ser, respectively). It is believed that SpsA has probably persisted as a non-hydrolyzing enzyme already for a considerable period of time in *S. aureus*, as the active-site mutations each necessarily involve changes to at least two nucleotides of the codon, and transitional forms of inactive enzyme must have preceded the formation of SpsA with a non-aspartyl replacement for the active-site Ser and a non-seryl replacement of the active site Lys (Cregg *et al.*, 1996). The presence of an apparently catalytically inactive SpsA homologue is a conserved feature of all staphylococci with sequenced genomes (Sibbald *et al.*, 2006). To date, it is not known whether the inactive SPase homologues contribute somehow to protein secretion in these organisms. The catalytically active SPase is SpsB which was shown to be essential for growth and viability of *S. aureus* (Cregg *et al.*, 1996). Although the enzyme remains to be structurally characterized, a set of lipopeptide inhibitors were developed using the classical approach and were shown to inhibit the enzyme (Bruton *et al.*, 2003).

The objectives of this project were (i) to analyze the *in vitro* biochemical properties of the SPaseI of *S. aureus*, SpsB; (ii) to develop and validate an *in vitro* assay for high-throughput screening of potential inhibitors of SpsB and (iii) finally to screen small molecule compound libraries against this target, in the search for new classes of antibiotics.

In this work, we purified SpsB and confirmed its *in vitro* activity on two selected substrates. The first was the native preprotein substrate IsaA precursor that is known to play a role in the virulence of *S. aureus*. The second was a synthetic decapeptide based on the signal peptide sequence of *S. epidermidis* preprotein (SceD precursor) with quencher

Dabcyl and fluorophore EDANS at its N- and C-terminus respectively. We confirmed that the substrates are cleaved at the predicted site following the "Ala-X-Ala" rule of SPase recognition and cleavage. We also designed and purified two truncated SpsB derivatives lacking most of the hydrophobic transmembrane residues. The truncated SpsB derivatives were identical in sequence except for the catalytic Ser replaced by an Ala in one of the truncated derivatives which we designated the truncated mutant (tr-mut-SpsB). The other truncated derivative, in which catalytic Ser remained as such, was designated as tr-SpsB. We showed that tr-SpsB retained SPaseI activity as evidenced by processing of both the preprotein as well as the synthetic peptide substrate. These results demonstrated that the transmembrane anchor is not required for enzymatic activity of SpsB.

The specific enzymatic activity (k_{cat}/K_m) of the full-length SpsB was found to be approximately 1850 $M^{-1}s^{-1}$ in the FRET assay using the synthetic SceD peptide. The k_{cat}/K_m value of SpsB obtained in this work using the SceD peptide (10-mer) is intermediate when compared to its specific enzymatic activity reported in literature using two other synthetic peptide substrates. Of the two synthetic peptide substrates described, one is an 11-mer based on the signal peptide region of maltose binding protein of *E. coli* (Zhong & Benkovic, 1998) and the other is a 13-mer based on the preprotein sequence data in *S. aureus* (Bruton *et al.*, 2003). The k_{cat}/K_m values obtained for SpsB were 18.4 and $4.2x10^5$ $M^{-1}s^{-1}$ using the former and latter peptide, respectively (Bruton *et al.*, 2003). To the latter synthetic peptide a fatty acid tail was added to mimic the hydrophobic signal peptide region of a natural SPaseI substrate which resulted in a better substrate for SpsB.

The FRET assay with the synthetic peptide was used to compare the catalytic efficiencies of the full-length and the truncated derivative of SpsB while the truncated mutant served as a control. Notably, in this work we have shown that the specific enzymatic activity of the full-length SpsB is 30-fold higher, compared to tr-SpsB which has a k_{cat}/K_m value of 59.4 ± 6.4 $M^{-1}s^{-1}$. This highlights the importance of the transmembrane segment residues for optimum activity of SpsB. Importantly we also showed that the presence of the non-ionic detergent Triton X-100 is required for optimum *in vitro* activity of tr-SpsB, although it lacks most of the hydrophobic residues in the transmembrane segment. Additionally, the specific enzymatic activity of tr-mut-SpsB was determined to be 4 ± 0.8 M^{-1} s^{-1}, which is not significant. The full-length SpsB has a 462-fold higher activity compared to the tr-

mut-SpsB which confirms that the activity observed in the *in vitro* assay is specifically due to SpsB and not due to the background activity of LepB of *E. coli* (which was used as the host for overproduction of SpsB).

We analyzed the *in vitro* behaviour of the full-length SpsB in terms of its pH requirement and stability. Compared to *E. coli* LepB which is active from pH 7 to 11, SpsB is capable of functioning at a wider pH range *i.e.,* from pH 5 to 12. The optimum pH of SpsB was shown to be approximately 8, which is basic, as is the case for other SPases characterized *in vitro* and which is also in agreement with the catalytic mechanism. The specific enzymatic activity of SpsB was plotted as a function of pH to obtain the pH-rate profile. Interestingly, the pH-rate profile of the enzyme did not result in a typical bell shaped curve as we observed also another, smaller peak around pH 11. Hence, the pH-rate profile was fitted with the equation for a complex bell-shaped curve. The apparent pK_a values for the free enzyme was determined to be approximately 6.6 and 8.7 with possibly another pK_a around 11.8. The two shoulders in the pH-rate profile are a signature of the fact that there are three acid groups that are important and therefore four species: E, EH^+, EH_2^+, EH_3^+, of which E and EH_3^+ are inactive. EH_3^+ is probably the enzyme with the catalytic Lys protonated (with a very abnormal low pK_a); EH^+ and EH_2^+ may be involved in the stabilisation of the active conformation. However, without the crystal structures of the extreme forms E and EH_3^+, one cannot say much more. So when the pH is raised to create E the enzyme is no longer active.

We studied the effect of temperature (4 °C, 27 °C and 37 °C) on the stability of SpsB during storage for varying periods of time in the presence of a general protease inhibitor cocktail. SpsB was observed to be generally more stable in comparison with *E. coli* LepB stored under similar conditions (Talarico *et al.*, 1991). However, upon prolonged storage, we observed the appearance of a smaller band, apart from that corresponding to the full-length SpsB. We confirmed that this smaller band is the result of intermolecular self-cleavage of SpsB as it did not appear when the SPase inhibitor arylomycin A_2 was added to the purified protein sample. We also showed that self-cleavage of SpsB occurs following the "Ala-X-Ala" rule for SPase cleavage based on the N-terminal sequencing data of the self-cleavage product obtained. The self-cleavage product of SpsB still contains the catalytic Ser although it is at the penultimate end on the N-terminus of the protein. We then analyzed the activity of the self-cleavage product of SpsB in the FRET

assay but could not observe processing of the synthetic peptide under the standardized conditions *in vitro*.

These results led to the interesting observation that the difference of only nine amino acids between the self-cleavage product of SpsB and the N-terminally truncated derivative (tr-SpsB) influenced their ability to be active or not. While the former was unable to process the synthetic peptide substrate in the FRET assay, the latter retained a significant activity. We believe that this difference is due to the lack of residues which are part of the conserved box B region of the signal peptidases in the self-cleavage product of SpsB. Many of these residues most likely reside in the substrate binding site of SpsB analogous to LepB. The nine additional residues preceding the catalytic Ser are probably required for the proper conformation of the enzyme.

We then validated the FRET assay for screening compounds against SpsB. Initially, different conditions in the FRET assay were studied such as the concentration and compatibility of the different components of the reaction mixture, signal uniformity within a microplate and variations between intra-day and inter-day data. Based on these data the assay was standardized and *in vitro* inhibition of SpsB was demonstrated using the SPase inhibitor arylomycin A_2. The SpsB-FRET assay was subsequently used to also demonstrate the suitability of a rationally designed peptide (Buzder-Lantos *et al.*, 2009) for SPaseI-cleavage inhibition testing. We further showed that the preprotein processing of SpsB is blocked in the presence of SPase inhibitors such as arylomycin A_2 and (5*S*,6*S*)-6-[(*R*)-acetoxyethyl]-penem-3-carboxylate. The preprotein processing assay could be adapted for use as a confirmative assay in the search for SpsB inhibitors.

Approximately 6,200 compounds were screened manually in the SpsB-FRET assay. The compounds were mostly small molecules from the chemical compound libraries belonging to CD3 and the Rega Institute and a few peptides based on *in silico* data. None of the compounds could inhibit SpsB to a considerable extent. Compounds that could not be analyzed properly due to interference with fluorescence (approximately 1 % of the total) in the FRET assay were analyzed in the preprotein processing assay. Again, none of these were found to be active against SpsB. The quality of the assay was assessed as previously described (Zhang *et al.*, 1999) and was found to be reliable for screening. We also observed that the compounds selected from an *in silico* screen against the *E. coli*

SPase structure were able to inhibit this particular enzyme better than *S. aureus* SpsB, highlighting the subtle differences between the two enzymes but also emphasizing the need for the crystal structure of SpsB.

Based on the above results, one obvious question that comes to mind is why was the success rate so low? This is in part due to the nature of the enzyme. SPasesI are regarded as difficult targets when it comes to finding effective inhibitors (Black & Bruton, 1998). There are very few good SPaseI inhibitors available as of now; this is in spite of the efforts of various groups including pharmaceutical giants who have worked in this area like Merck, GlaxoSmithKline, Procter and Gamble and Lilly laboratories. Secondly, the lack of structural information leaves us with not too many options but random screening for inhibitors against SpsB. The homology modelling of SpsB based on the structure of LepB is not reliable as there is less than 30 % sequence identity between the two enzymes. In addition, the basic properties of the enzyme (SpsB) such as the requirement for detergent (even for the truncated derivative) and self-cleavage activity makes it a difficult candidate for crystal structure determination. The group of Prof. Dr. Remy Loris (VUB, Brussels) set-up crystallization trials on SpsB and its derivatives obtained in this work using different conditions and also attempting several different approaches in pursuance of the structural information on SpsB. Unfortunately, none of the conditions or approaches resulted in obtaining crystals suitable for X-ray diffraction. Another possible reason for lack of hits could be due to the common selection criteria/filters applied while building the compound library. The rules for selection normally focus on drug-like properties of the compounds and therefore a particular compound library might or might not work on different targets. On the other hand the number of compounds screened in this work is limited to ~27,000 and it might be too early to conclude anything about the suitability of a particular compound library. Whether natural compounds like secondary metabolites from microbial sources would be better candidates for screening remains to be seen.

The next step was to increase the throughput of the assay to be able to screen chemical compound libraries. Where possible, necessary changes were made in the protocol and a complete library of small molecules belonging to CD3 was screened. The assessment of assay quality based on the screening data reflected the robustness of the assay (Z' of each plate screened ≥ 0.5; average Z' = 0.73). Further analysis of the most active compounds

identified in the HTS resulted in the identification of at least one compound (JRD 2189) which could inhibit SpsB in the *in vitro* FRET assay (IC_{50}= 51 μM). However, the compound was not active in the preprotein processing assay which confirms its low potency against the enzyme. We also showed that JRD 2189 inhibits *E. coli* LepB in the FRET assay. Weak inhibitors do not make good starting points as drug leads and are usually only pursued if they indicate a new mode of inhibition that can be exploited by other means. An example for a weak inhibitor of SPase that has been shown to have such a potential is the β-sultam inhibitor BAL0019193 (Luo *et al.*, 2009). It therefore remains to be seen if molecular modelling in the active site of LepB looks positive or not. If the modelling data looks encouraging, only then would it be interesting to study structure activity relationship and possibly optimize the compound for better efficiency.

Currently, CD3/Rega library compounds have not been tested by us directly on bacterial cells in phenotypic assays. Both whole cell approach and target based approach have advantages and disadvantages. In the first place, we have focused on the latter approach so that we do not miss out the compounds that are effective inhibitors but are not effective on whole cells due to their physicochemical properties or are prone to enzymatic modifications. The idea is to improve the solubility and drug-like properties of such hits to obtain useful antibiotics. Although there are no data from whole cell assays, we agree that it is interesting to test antibacterial activity of these compounds and this would be feasible when this test is automated as well.

In essence, in this work, *S. aureus* SpsB was studied to gain a better understanding of its properties in particular and that of SPaseI in general. In light of its potential use as a non-conventional antibiotic target, *in vitro* inhibition assays were developed. High-throughput screening of a chemical compound library against SpsB yielded data of good quality confirming its suitability for this purpose, but unfortunately did not result in finding effective inhibitors.

Nevertheless, SpsB remains an attractive target for deriving novel antibacterials, given the need for new drugs to combat multi-drug resistant strains. In the absence of structural data for SpsB, random screening continues to be an attractive approach for deriving novel antibacterials against *S. aureus*. In addition, virtual screening using the structure of LepB could possibly aid in finding certain broad spectrum inhibitors. Finally, when the

crystal structure of SpsB is solved the data could help significantly in the drug discovery process and the *in vitro* assays developed in this work will continue to play an important part.

Among the questions that will need to be addressed in future are:

- How different is the 3D structure of the active site of SpsB in comparison with LepB?
- What could be the possible role of signal peptidase like-protein SpsA in *S. aureus*?
- Finally, it remains to be seen whether *S. aureus* will continue to emerge stronger and persist by developing resistance to SPase inhibitors as well?

References

Allsop, A., Ashby, M., Brooks, G. & other authors (1997). Inhibition of protein export in bacteria: the signaling of a new role for β-lactams. In *2nd International Symposium on Recent Advances in Chemistry of Anti-infective Agents*, pp. 61-72. Edited by P. Bentley & P. O'Hanlon. Churchill College, Cambridge, England: The Royal Society of Chemistry.

Allsop, A. E., Brooks, G., Bruton, G. & other authors (1995). Penem inhibitors of bacterial signal peptidase. *Bioorganic & Medicinal Chemistry Letters* 5, 443-448.

Ashman, S., Black, M. T., Bruton, G., Humphries, A. J. & Moore, K. J. M. (2000). Bacterial signal peptidase inhibitors and uses thereof: PCT Int. Appl. WO 0046250

Barkocy-Gallagher, G. A. & Bassford, P. J., Jr. (1992). Synthesis of precursor maltose-binding protein with proline in the +1 position of the cleavage site interferes with the activity of *Escherichia coli* signal peptidase I in vivo. *J Biol Chem* 267, 1231-1238.

Bendtsen, J. D., Nielsen, H., von Heijne, G. & Brunak, S. (2004). Improved prediction of signal peptides: SignalP 3.0. *J Mol Biol* 340, 783-795.

Bitter, W., Houben, E. N., Luirink, J. & Appelmelk, B. J. (2009). Type VII secretion in mycobacteria: classification in line with cell envelope structure. *Trends Microbiol* 17, 337-338.

Black, M. T., Munn, J. G. & Allsop, A. E. (1992). On the catalytic mechanism of prokaryotic leader peptidase 1. *Biochem J* 282, 539-543.

Black, M. T. (1993). Evidence that the catalytic activity of prokaryote leader peptidase depends upon the operation of a serine-lysine catalytic dyad. *J Bacteriol* 175, 4957-4961.

Black, M. T. & Bruton, G. (1998). Inhibitors of bacterial signal peptidases. *Curr Pharm Des* 4, 133-154.

Bockstael, K., Geukens, N., Rao, C. V., Herdewijn, P., Anne, J. & Van Aerschot, A. (2009a). An easy and fast method for the evaluation of *Staphylococcus epidermidis* type I signal peptidase inhibitors. *J Microbiol Methods* 78, 231-237.

Bockstael, K., Geukens, N., Van Mellaert, L., Herdewijn, P., Anne, J. & Van Aerschot, A. (2009b). Evaluation of the type I signal peptidase as antibacterial target for biofilm-associated infections of *Staphylococcus epidermidis*. *Microbiology* 155, 3719-3729.

Bonnemain, C., Raynaud, C., Reglier-Poupet, H., Dubail, I., Frehel, C., Lety, M. A., Berche, P. & Charbit, A. (2004). Differential roles of multiple signal peptidases in the virulence of *Listeria monocytogenes*. *Mol Microbiol* 51, 1251-1266.

Brocklehurst, K. & Dixon, H. B. (1976). pH-dependence of the steady-state rate of a two-step enzymic reaction. *Biochem J* 155, 61-70.

Bruton, G., Huxley, A., O'Hanlon, P. & other authors (2003). Lipopeptide substrates for SpsB, the *Staphylococcus aureus* type I signal peptidase: design, conformation and conversion to alpha-ketoamide inhibitors. *Eur J Med Chem* 38, 351-356.

Buzder-Lantos, P., Bockstael, K., Anne, J. & Herdewijn, P. (2009). Substrate based peptide aldehyde inhibits bacterial type I signal peptidase. *Bioorg Med Chem Lett* 19, 2880-2883.

Carlos, J. L., Klenotic, P. A., Paetzel, M., Strynadka, N. C. & Dalbey, R. E. (2000a). Mutational evidence of transition state stabilization by serine 88 in *Escherichia coli* type I signal peptidase. *Biochemistry* 39, 7276-7283.

Carlos, J. L., Paetzel, M., Brubaker, G., Karla, A., Ashwell, C. M., Lively, M. O., Cao, G., Bullinger, P. & Dalbey, R. E. (2000b). The role of the membrane-spanning domain of type I signal peptidases in substrate cleavage site selection. *J Biol Chem* 275, 38813-38822.

Casey, A. L., Lambert, P. A. & Elliott, T. S. (2007). Staphylococci. *Int J Antimicrob Agents* 29, S23-32.

Catrein, I., Herrmann, R., Bosserhoff, A. & Ruppert, T. (2005). Experimental proof for a signal peptidase I like activity in *Mycoplasma pneumoniae*, but absence of a gene encoding a conserved bacterial type I SPase. *Febs J* 272, 2892-2900.

Chambers, H. F. & Deleo, F. R. (2009). Waves of resistance: *Staphylococcus aureus* in the antibiotic era. *Nat Rev Microbiol* 7, 629-641.

Chatterjee, S., Suciu, D., Dalbey, R. E., Kahn, P. C. & Inouye, M. (1995). Determination of K_m and k_{cat} for signal peptidase I using a full length secretory precursor, pro-OmpA-nuclease A. *J Mol Biol* 245, 311-314.

Chaudhuri, R. R., Allen, A. G., Owen, P. J. & other authors (2009). Comprehensive identification of essential *Staphylococcus aureus* genes using Transposon-Mediated Differential Hybridisation (TMDH). *BMC Genomics* **10**, 291.

Choo, K. H., Tong, J. C. & Ranganathan, S. (2008). Modeling *Escherichia coli* signal peptidase complex with bound substrate: determinants in the mature peptide influencing signal peptide cleavage. *BMC Bioinformatics* 9, S15.

Copeland, R. (2005). Evaluation of Enzyme Inhibitors in Drug Discovery: A Guide for Medicinal Chemists and Pharmacologists.

Cregg, K. M., Wilding, I. & Black, M. T. (1996). Molecular cloning and expression of the *spsB* gene encoding an essential type I signal peptidase from *Staphylococcus aureus*. *J Bacteriol* 178, 5712-5718.

Dalbey, R. E. & Wickner, W. (1985). Leader peptidase catalyzes the release of exported proteins from the outer surface of the *Escherichia coli* plasma membrane. *J Biol Chem* 260, 15925-15931.36

Dalbey, R. E. (1990). Positively charged residues are important determinants of membrane protein topology. *Trends Biochem Sci* 15, 253-257.

Dalbey, R. E., Lively, M. O., Bron, S. & van Dijl, J. M. (1997). The chemistry and enzymology of the type I signal peptidases. *Protein Sci* 6, 1129-1138.

Date, T. (1983). Demonstration by a novel genetic technique that leader peptidase is an essential enzyme of *Escherichia coli*. *J Bacteriol* 154, 76-83.39BDawson, R., Elliott, D., Elliott, W. & Jones, K. (1989). *pH, buffers and physiological media.*, 3rd edition edn: Oxford University Press, London.

de Vrije, G. J., Batenburg, A. M., Killian, J. A. & de Kruijff, B. (1990). Lipid involvement in protein translocation in *Escherichia coli*. *Mol Microbiol* 4, 143-150.

Devasahayam, G., Scheld, W. M. & Hoffman, P. S. (2010). Newer antibacterial drugs for a new century. *Expert Opinion on Investigational Drugs* 19, 215-234.

Economou, A., Christie, P., Fernandez, R., Palmer, T., Plano, G. & Pugsley, A. (2006). Secretion by numbers: protein traffic in prokaryotes. *Molecular Microbiology* 62, 308-319.

Ekici, O. D., Karla, A., Paetzel, M., Lively, M. O., Pei, D. & Dalbey, R. E. (2007). Altered -3 substrate specificity of *Escherichia coli* signal peptidase 1 mutants as revealed by screening a combinatorial peptide library. *J Biol Chem* 282, 417-425.

Fischbach, M. A. & Walsh, C. T. (2009). Antibiotics for emerging pathogens. *Science* 325, 1089-1093.

Fitzpatrick, F., Humphreys, H. & O'Gara, J. P. (2005). The genetics of staphylococcal biofilm formation--will a greater understanding of pathogenesis lead to better management of device-related infection? *Clin Microbiol Infect* 11, 967-973.

Foster, T. J. (2004). The *Staphylococcus aureus* "superbug". *J Clin Invest* 114, 1693-1696.

Foster, T. J. (2005). Immune evasion by staphylococci. *Nat Rev Microbiol* 3, 948-958.

Forsyth, R. A., Haselbeck, R. J., Ohlsen, K. L. & other authors (2002). A genome-wide strategy for the identification of essential genes in *Staphylococcus aureus*. *Mol Microbiol* **43**, 1387-1400.

Fraser, C. M., Gocayne, J. D., White, O. & other authors (1995). The minimal gene complement of *Mycoplasma genitalium*. *Science* 270, 397-403.

Garcia-Lara, J., Masalha, M. & Foster, S. J. (2005). *Staphylococcus aureus*: the search for novel targets. *Drug Discov Today* 10, 643-651.

Geukens, N., Lammertyn, E., Van Mellaert, L., Engelborghs, Y., Mellado, R. P. & Anne, J. (2002). Physical requirements for *in vitro* processing of the *Streptomyces lividans* signal peptidases. *J Biotechnol* 96, 79-91.

Geukens, N., Frederix, F., Reekmans, G., Lammertyn, E., Van Mellaert, L., Dehaen, W., Maes, G. & Anne, J. (2004). Analysis of type I signal peptidase affinity and specificity for preprotein substrates. *Biochem Biophys Res Commun* 314, 459-467.

Harris, D. A., Powers, M. E. & Romesberg, F. E. (2009). Synthesis and biological evaluation of penem inhibitors of bacterial signal peptidase. *Bioorg Med Chem Lett* 19, 3787-3790.

Holden, M. T., Feil, E. J., Lindsay, J. A. & other authors (2004). Complete genomes of two clinical *Staphylococcus aureus* strains: evidence for the rapid evolution of virulence and drug resistance. *Proc Natl Acad Sci U S A* 101, 9786-9791.

Holtzel, A., Schmid, D. G., Nicholson, G. J., Stevanovic, S., Schimana, J., Gebhardt, K., Fiedler, H. P. & Jung, G. (2002). Arylomycins A and B, new biaryl-bridged lipopeptide antibiotics produced by *Streptomyces* sp. Tu 6075. II. Structure elucidation. *J Antibiot (Tokyo)* 55, 571-577.

Hu, X. E., Kim, N. K., Grinius, L., Morris, C. M., Wallace, C. D., Mieling, G. E. & Demuth, T. P. (2003). Synthesis of (5S)-Tricyclic Penems as Novel and Potent Inhibitors of Bacterial Signal Peptidases. *Synthesis* 2003, 1732-1738.

Inada, T., Court, D. L., Ito, K. & Nakamura, Y. (1989). Conditionally lethal amber mutations in the leader peptidase gene of *Escherichia coli*. *J Bacteriol* 171, 585-587.

Ito, K. & Mori, H. (2009). *The Sec Protein Secretion System*: Caister Academic Press.58BJhoti, H. (2005). A new school for screening. *Nat Biotechnol* 23, 184-186.

Ji, Y., Zhang, B., Van, S. F., Horn, Warren, P., Woodnutt, G., Burnham, M. K. & Rosenberg, M. (2001). Identification of critical staphylococcal genes using conditional phenotypes generated by antisense RNA. *Science* **293**, 2266 - 2269.

Kaderbhai, N., Khan, T. & Kaderbhai, M. (2008). An Anti-microbial Peptide Derivative of Flesh Fruit Fly Mimics Secretory Signal Sequence and Inhibits Signal Peptidase-I in the Export Pathway. *International Journal of Peptide Research and Therapeutics* 14, 173-181.

Karla, A., Lively, M. O., Paetzel, M. & Dalbey, R. (2005). The identification of residues that control signal peptidase cleavage fidelity and substrate specificity. *J Biol Chem* 280, 6731-6741.

Kavanaugh, J. S., Thoendel, M. & Horswill, A. R. (2007). A role for type I signal peptidase in *Staphylococcus aureus* quorum sensing. *Mol Microbiol* 65, 780-798.

Kim, Y. T., Muramatsu, T. & Takahashi, K. (1995). Identification of Trp300 as an important residue for *Escherichia coli* leader peptidase activity. *Eur J Biochem* 234, 358-362.

Kluytmans, J., van Belkum, A. & Verbrugh, H. (1997). Nasal carriage of *Staphylococcus aureus*: epidemiology, underlying mechanisms, and associated risks. *Clin Microbiol Rev* 10, 505-520.

Koshland, D., Sauer, R. T. & Botstein, D. (1982). Diverse effects of mutations in the signal sequence on the secretion of beta-lactamase in *Salmonella* Typhimurium. *Cell* 30, 903-914.

Krogh, A., Larsson, B., von Heijne, G. & Sonnhammer, E. L. (2001). Predicting transmembrane protein topology with a hidden Markov model: application to complete genomes. *J Mol Biol* 305, 567-580.

Kulanthaivel, P., Kreuzman, A. J., Strege, M. A. & other authors (2004). Novel lipoglycopeptides as inhibitors of bacterial signal peptidase I. *J Biol Chem* 279, 36250-36258.

Kuo, D. W., Chan, H. K., Wilson, C. J., Griffin, P. R., Williams, H. & Knight, W. B. (1993). *Escherichia coli* leader peptidase: production of an active form lacking a requirement for detergent and development of peptide substrates. *Arch Biochem Biophys* 303, 274-280.

Lammertyn, E., Van Mellaert, L., Meyen, E., Lebeau, I., De Buck, E., Anne, J. & Geukens, N. (2004). Molecular and functional characterization of type I signal peptidase from *Legionella pneumophila*. *Microbiology* 150, 1475-1483.

Lasa, I. & Penades, J. R. (2006). Bap: a family of surface proteins involved in biofilm formation. *Res Microbiol* 157, 99-107.

Lorenz, U., Ohlsen, K., Karch, H., Hecker, M., Thiede, A. & Hacker, J. (2000). Human antibody response during sepsis against targets expressed by methicillin resistant *Staphylococcus aureus*. *FEMS Immunol Med Microbiol* 29, 145-153.

Luo, C., Roussel, P., Dreier, J., Page, M. G. & Paetzel, M. (2009). Crystallographic analysis of bacterial signal peptidase in ternary complex with arylomycin A_2 and a beta-sultam inhibitor. *Biochemistry* 48, 8976-8984.

Menard, R. & Storer, A. C. (1992). Oxyanion hole interactions in serine and cysteine proteases. *Biol Chem Hoppe Seyler* 373, 393-400.

Musial-Siwek, M., Kendall, D. A. & Yeagle, P. L. (2008a). Solution NMR of signal peptidase, a membrane protein. *Biochim Biophys Acta* 1778, 937-944.

Musial-Siwek, M., Yeagle, P. L. & Kendall, D. A. (2008b). A small subset of signal peptidase residues are perturbed by signal peptide binding. *Chem Biol Drug Des* 72, 140-146.

Natale, P., Bruser, T. & Driessen, A. J. (2008). Sec- and Tat-mediated protein secretion across the bacterial cytoplasmic membrane--distinct translocases and mechanisms. *Biochim Biophys Acta* 1778, 1735-1756.

NCCLS (2003).Methods for dilution antimicrobial susceptibility test for bacteria that grow aerobically. Wayne, Pa.: Approved standard M7-A6, 6 ed. National Committee for Clinical Laboratory Standards.

Nielsen, H., Engelbrecht, J., Brunak, S. & von Heijne, G. (1997). Identification of prokaryotic and eukaryotic signal peptides and prediction of their cleavage sites. *Protein Eng* 10, 1-6.

Nilsson, I. & von Heijne, G. (1992). A signal peptide with a proline next to the cleavage site inhibits leader peptidase when present in a sec-independent protein. *FEBS Lett* 299, 243-246.

Ohlsen, K. & Lorenz, U. (2007). Novel targets for antibiotics in *Staphylococcus aureus*. *Future Microbiol* 2, 655-666.

Paetzel, M., Chernaia, M., Strynadka, N., Tschantz, W., Cao, G., Dalbey, R. E. & James, M. N. (1995). Crystallization of a soluble, catalytically active form of *Escherichia coli* leader peptidase. *Proteins* 23, 122-125.

Paetzel, M., Strynadka, N. C., Tschantz, W. R., Casareno, R., Bullinger, P. R. & Dalbey, R. E. (1997). Use of site-directed chemical modification to study an essential lysine in *Escherichia coli* leader peptidase. *J Biol Chem* 272, 9994-10003.

Paetzel, M., Dalbey, R. E. & Strynadka, N. C. (1998). Crystal structure of a bacterial signal peptidase in complex with a beta-lactam inhibitor. *Nature* 396, 186-190.

Paetzel, M., Dalbey, R. E. & Strynadka, N. C. (2000). The structure and mechanism of bacterial type I signal peptidases. A novel antibiotic target. *Pharmacol Ther* 87, 27-49.

Paetzel, M., Dalbey, R. E. & Strynadka, N. C. (2002a). Crystal structure of a bacterial signal peptidase apoenzyme: implications for signal peptide binding and the Ser-Lys dyad mechanism. *J Biol Chem* 277, 9512-9519.

Paetzel, M., Karla, A., Strynadka, N. C. & Dalbey, R. E. (2002b). Signal peptidases. *Chem Rev* 102, 4549-4580.

Paetzel, M., Goodall, J. J., Kania, M., Dalbey, R. E. & Page, M. G. (2004). Crystallographic and biophysical analysis of a bacterial signal peptidase in complex with a lipopeptide-based inhibitor. *J Biol Chem* 279, 30781-30790.

Page, M. I. (2004). Beta-sultams-mechanism of reactions and use as inhibitors of serine proteases. *Acc Chem Res* 37, 297-303.

Panahandeh, S., Holzapfel, E. & Müller, M. (2009). *The Twin-arginine Translocation pathway*: Caister Academic Press.

Payne, D. J. (2008). MICROBIOLOGY: Desperately Seeking New Antibiotics. *Science* 321, 1644-1645.

Peng, S. B., Wang, L., Moomaw, J. & other authors (2001a). Biochemical characterization of signal peptidase I from gram-positive *Streptococcus pneumoniae*. *J Bacteriol* 183, 621-627.

Peng, S. B., Zheng, F., Angleton, E. L., Smiley, D., Carpenter, J. & Scott, J. E. (2001b). Development of an internally quenched fluorescent substrate and a continuous fluorimetric assay for *Streptococcus pneumoniae* signal peptidase I. *Anal Biochem* 293, 88-95.

Plata, K., Rosato, A. E. & Wegrzyn, G. (2009). *Staphylococcus aureus* as an infectious agent: overview of biochemistry and molecular genetics of its pathogenicity. *Acta Biochim Pol* 56, 597-612.

Pollastri, G. & McLysaght, A. (2005). Porter: a new, accurate server for protein secondary structure prediction. *Bioinformatics* 21, 1719-1720.

Rahman, M. S., Simser, J. A., Macaluso, K. R. & Azad, A. F. (2003). Molecular and functional analysis of the lepB gene, encoding a type I signal peptidase from *Rickettsia rickettsii* and *Rickettsia typhi*. *J Bacteriol* 185, 4578-4584.

Roberts, T. C., Smith, P. A., Cirz, R. T. & Romesberg, F. E. (2007). Structural and initial biological analysis of synthetic arylomycin A_2. *J Am Chem Soc* 129, 15830-15838.

Sambrook, J., Fritsch, E. & Maniatis, T. (1989). *Molecular Cloning: A laboratory manual*, 2nd Edition edn. Cold Spring Harbor, New York: Cold Spring Harbor Laboratory Press.

Schimana, J., Gebhardt, K., Holtzel, A., Schmid, D. G., Sussmuth, R., Muller, J., Pukall, R. & Fiedler, H. P. (2002). Arylomycins A and B, new biaryl-bridged lipopeptide antibiotics produced by *Streptomyces sp.* Tu 6075. I. Taxonomy, fermentation, isolation and biological activities. *J Antibiot (Tokyo)* 55, 565-570.

Sibbald, M. J., Ziebandt, A. K., Engelmann, S. & other authors (2006). Mapping the pathways to staphylococcal pathogenesis by comparative secretomics. *Microbiol Mol Biol Rev* 70, 755-788.

Stapleton, M. R., Horsburgh, M. J., Hayhurst, E. J., Wright, L., Jonsson, I. M., Tarkowski, A., Kokai-Kun, J. F., Mond, J. J. & Foster, S. J. (2007). Characterization of IsaA and SceD, two putative lytic transglycosylases of *Staphylococcus aureus*. *J Bacteriol* 189, 7316-7325.

Stein, R. L., Barbosa, M. D. & Bruckner, R. (2000). Kinetic and mechanistic studies of signal peptidase I from *Escherichia coli*. *Biochemistry* 39, 7973-7983.

Stephens, C. & Shapiro, L. (1997). Bacterial protein secretion--a target for new antibiotics? *Chem Biol* 4, 637-641.

Studier, F. W. & Moffatt, B. A. (1986). Use of bacteriophage T7 RNA polymerase to direct selective high-level expression of cloned genes. *J Mol Biol* 189, 113-130.

Suciu, D., Chatterjee, S. & Inouye, M. (1997). Catalytic efficiency of signal peptidase I of *Escherichia coli* is comparable to that of members of the serine protease family. *Protein Eng* 10, 1057-1060.

Sung, M. & Dalbey, R. E. (1992). Identification of potential active-site residues in the *Escherichia coli* leader peptidase. *J Biol Chem* 267, 13154-13159.

Talarico, T. L., Dev, I. K., Bassford, P. J., Jr. & Ray, P. H. (1991). Inter-molecular degradation of signal peptidase I *in vitro*. *Biochem Biophys Res Commun* 181, 650-656.

Talarico, T. L., Barkocy-Gallagher, G. A., Ray, P. H. & Bassford, P. J., Jr. (1993). *In vitro* processing by signal peptidase I of precursor maltose-binding protein species with alterations in and around the signal peptide. *Biochem Biophys Res Commun* 197, 1154-1166.

Thanassi, D. G. & Hultgren, S. J. (2000). Multiple pathways allow protein secretion across the bacterial outer membrane. *Curr Opin Cell Biol* 12, 420-430.

Tipton, K. & Dixon, H. (1979). Effect of pH on enzymes. *Methods in Enzymology* 63, 183-234.

Tschantz, W. R., Sung, M., Delgado-Partin, V. M. & Dalbey, R. E. (1993). A serine and a lysine residue implicated in the catalytic mechanism of the *Escherichia coli* leader peptidase. *J Biol Chem* 268, 27349-27354.

Tschantz, W. R., Paetzel, M., Cao, G., Suciu, D., Inouye, M. & Dalbey, R. E. (1995). Characterization of a soluble, catalytically active form of *Escherichia coli* leader peptidase: requirement of detergent or phospholipid for optimal activity. *Biochemistry* 34, 3935-3941.

van Dijl, J. M., van den Bergh, R., Reversma, T., Smith, H., Bron, S. & Venema, G. (1990). Molecular cloning of the *Salmonella* Typhimurium *lep* gene in *Escherichia coli*. *Mol Gen Genet* 223, 233-240.

van Dijl, J. M., de Jong, A., Venema, G. & Bron, S. (1995). Identification of the potential active site of the signal peptidase SipS of *Bacillus subtilis*. Structural and functional similarities with LexA-like proteases. *J Biol Chem* 270, 3611-3618.

van Roosmalen, M. L., Jongbloed, J. D., Kuipers, A., Venema, G., Bron, S. & van Dij, L. J. (2000). A truncated soluble Bacillus signal peptidase produced in *Escherichia coli* is subject to self-cleavage at its active site. *J Bacteriol* 182, 5765-5770.

van Roosmalen, M. L., Jongbloed, J. D., de Jonf, A., van Eerden, J., Venema, G., Bron, S. & van Dijl, J. M. (2001). Detergent-independent *in vitro* activity of a truncated *Bacillus* signal peptidase. *Microbiology* 147, 909-917.

van Roosmalen, M. L., Geukens, N., Jongbloed, J. D., Tjalsma, H., Dubois, J. Y., Bron, S., van Dijl, J. M. & Anne, J. (2004). Type I signal peptidases of Gram-positive bacteria. *Biochim Biophys Acta* 1694, 279-297.

von Heijne, G. (1992). Membrane protein structure prediction. Hydrophobicity analysis and the positive-inside rule. *J Mol Biol* 225, 487-494.

von Heijne, G. (1998). Life and death of a signal peptide. *Nature* 396, 111-113.

Wang, Y., Bruckner, R. & Stein, R. L. (2004). Regulation of signal peptidase by phospholipids in membrane: characterization of phospholipid bilayer incorporated *Escherichia coli* signal peptidase. *Biochemistry* 43, 265-270.

Wickner, W., Moore, K., Dibb, N., Geissert, D. & Rice, M. (1987). Inhibition of purified *Escherichia coli* leader peptidase by the leader (signal) peptide of bacteriophage M13 procoat. *J Bacteriol* 169, 3821-3822.

Xia, M., Lunsford, R. D., McDevitt, D. & Iordanescu, S. (1999). Rapid method for the identification of essential genes in *Staphylococcus aureus*. *Plasmid* **42**, 144-149.

Zhang, J. H., Chung, T. D. & Oldenburg, K. R. (1999). A Simple Statistical Parameter for Use in Evaluation and Validation of High Throughput Screening Assays. *J Biomol Screen* 4, 67-73.

Yin, D. & Ji, Y. (2002). Genomic analysis using conditional phenotypes generated by antisense RNA. *Curr Opin Microbiol* **5**, 330-333.

Zhang, L., Fan, F., Palmer, L. M. & other authors (2000). Regulated gene expression in *Staphylococcus aureus* for identifying conditional lethal phenotypes and antibiotic mode of action. *Gene* 255, 297-305.

Zhang, Y. B., Greenberg, B. & Lacks, S. A. (1997). Analysis of a *Streptococcus pneumoniae* gene encoding signal peptidase I and overproduction of the enzyme. *Gene* 194, 249-255.

Zhong, W. & Benkovic, S. J. (1998). Development of an internally quenched fluorescent substrate for *Escherichia coli* leader peptidase. *Anal Biochem* 255, 66-73.

Zwizinski, C., Date, T. & Wickner, W. (1981). Leader peptidase is found in both the inner and outer membranes of *Escherichia coli. J Biol Chem* 256, 3593-3597.

Professional career: Smitha Rao C.V.

Born on 20th October 1976, in Bangalore, India, Smitha Rao C.V., completed her Bachelor's degree (Microbiology, Biochemistry and Botany) in 1997 from the University of Mysore, Mysore, India. She graduated as Master of Science (Microbiology) from the University of Mysore in 1999 and started her career as a project assistant at the Department of Food Microbiology, Central Food Technological Research Institute, Mysore. She then worked as a Research officer for Virtue Biotech Labs Pvt. Ltd., Mysore from 2000 to 2002. Subsequently, she worked as a research fellow at the Department of Microbiology, Kidwai Memorial Institute for Oncology, Bangalore, India from 2003 to 2004. In 2004, she joined as a pre-doctoral student at the Lab of Bacteriology, Rega Institute, Katholieke Universiteit Leuven, obtained the Certificate of Medical Sciences in 2006 and continued her doctoral studies in the same laboratory. Since 2006, she has been a recipient of the IRO scholarship of KULeuven. The results of her research are reported in this doctoral thesis and in the publications as listed on the previous pages.